THE ROLE OF PKS1-MEDIATED SECONDARY METABOLISM IN HOST PENETRATION AND COLONIZATION DURING RICE BLAST DISEASE

QU ZIWEI

A THESIS SUBMITTED

FOR THE DEGREE OF DOCTOR OF PHILOSOPHY

DEPARTMENT OF BIOLOCAL SCIENCES

NATIONAL UNIVERSITY OF SINGAPORE

2016

Declaration

"I hereby declare that this thesis is my original work and it has been written by me in its entirety. I have duly acknowledged all the sources of information,which has been used in the thesis.

This thesis has not been submitted for any degree in any university previously."

Qu Ziwei

18 Jan 2016

Acknowledgements

I wish to express my appreciation to my supervisor, Dr. NAQVI Naweed at Temasek Life Sciences Laboratory, for his excellent supervision, suggestions and helpful discussions in this project. I would also thank my Thesis Advisory Committee, Dr. YEW Joanne and Dr. JEDD Gregory, for their suggestions and criticism.

I would also like to thank Dr. PATKAR Rajesh for his suggestion and assistance on the biochemistry work, and I would like to thank all my present and past lab members for their useful discussion and support.

I thank Dr. OUYANG Xuezhi for preparing the samples for transmission electron microscopy, and Dr. BENKE Peter for his assistance in the mass spectrometry work.

I would thank the TLL community, especially the Facilities/Support staff, the Sequencing Lab and the Microscopy Unit. I would also thank TLL and the National Research Foundation, Singapore for providing the funding support.

Table of contents

Summary

In Chapter I, a brief literature review about *Magnaporthe oryzae* and polyketide synthases (PKS) is presented. *M. oryzae* is the causal agent of the devastating rice blast disease, which is one of the most significant constraints on global food production. Hence, detailed molecular analyses of fungal pathogenesis using Rice Blast/*M. oryzae* as a model system, is critical for sustainable agriculture and food security. An abundance of genes encoding polyketide synthases (PKSs) have been predicted in *M. oryzae* genome, but the function of PKSs and polyketides during pathogenesis still remains elusive. This research work addressed whether secondary metabolism plays a key role in pathogenic development of rice blast and/or Magnaporthe-Rice interaction. I focused on the functional analysis of a *PKS1* containing gene cluster, which is essential for the appressorial function of host penetration by *M. oryzae*.

In Chapter III, I describe that the *PKS1*-deletion mutant generates non-functional appressoria, which fail to elaborate a proper penetration pore and are unable to enter the host plant. The *pks1*Δ mutant also showed defects in melanin deposition, pore wall overlay formation and septin assembly. Melanin synthesis and Pks1-mediated biosynthesis are thus metabolically related during appressorium formation.

I found that the *ABC3* transporter and an esterase *FSH1* share the

aforementioned gene cluster with *PKS1*. These genes are co-regulated with *PKS1* and are required for the penetration step of *Magnaporthe* pathogenesis. This suggests that *ABC3* and *FSH1* might be involved in Pks1-mediated secondary metabolism.

Cellular localization of Pks1-GFP and Fsh1-mCherry was also analyzed as part of this graduate research. Pks1 is expressed as early as 4 hpi in the appressoria, and is cytosolic at first, and then transfers to the vacuoles in the mature appressoria. Fsh1 is expressed after 10 hpi in the appressoria and only accumulates in the vacuoles. The cellular localization of Pks1 and Fsh1 indicates that the Pks1-associated polyketide synthesis begins in the cytosol and is shifted to vacuoles during the later stages of appressorial development. Interestingly, deletion of *PKS1* or *FSH1* is able to affect the vacuolar morphology and assembly in the mature appressoria.

Lastly, we compared the appressorial metabolomics of wild type and *pks1*Δ mutant. The global metabolomics profiling in the mutant appressoria showed a significant variation compared to the wild type, which suggests that Pks1 mediated secondary metabolite biosynthesis plays an important role in the appressorial metabolism.

List of Tables

Table **Page**

List of Figures

List of Abbreviations

aa	Amino acid
ACP	Acyl carrier protein
ACS	Acetosyringone
AT	Malonyl-CoA:ACP transacylase
ATS	Abc3 transporter efflux substrate
BM	Basal medium
cAMP	Cyclic adenosine monophosphate
cDNA	Complementary DNA
CM	Complete medium
CMAC	7-amino-4-chloromethylcoumarin
CoA	Coenzyme A
DAPI	4',6-diamidino-2-phenylindole
DH	Enoyl reductase
DMATS	Dimethylallyltryptophan synthetase
ECL	Enhanced chemiluminescence
EDTA	Ethylenediaminetetraacetic acid
ER	Dehydratase
FSH	Family of Serine Hydrolases
GFP	Green fluorescent protein
HPH	Hygromycin phosphotransferase

hpi	Hour post inoculation
HRP	Horseradish peroxidase
HR-PKS	Highly reducing polyketide synthase
h or hr	Hour
IM	Induction medium
KR	β-keto reductase
KS	β-ketoacyl synthase
MAPK	Mitogen-activated protein kinase
MT	Methyltransferase
NADPH	Reduced form of nicotinamide adenine dinucleotide phosphate
NRPS	Non-ribosomal peptide synthetase
ORF	Open reading frame
PA	Prune agar
PAGE	Polyacrylamide gel electrophoresis
PBS	Phosphate-buffered saline
PCR	Polymerase chain reaction
PKS	Polyketide synthase
PPTase	4′-phosphopantetheinyl transferase
PVDF	Polyvinylidene fluoride
RFP	Red fluorescent protein
SDS	Sodium dodecyl sulfate

SSC	Saline-Sodium Citrate buffer
Tc	Tricyclazole
TE	Thioesterase
TEM	Transmission election microscopy
TS	Terpene synthase
UTR	Untranslated region
WT	Wild type

Chapter I Literature Review

Rice blast is the most serious fungal disease that can reduce rice production by 10-30% worldwide (Dean et al., 2012). It is known that some of the secondary metabolites have important functions during pathogenesis by the rice blast fungus. In this chapter, we review previous work on rice blast disease, secondary metabolism, and how secondary metabolism contributes to fungal pathogenesis.

1.1 General introduction to Magnaporthe oryzae and the rice blast disease

Magnaporthe oryzae (or *Pyricularia oryzae*) is the causal agent of blast, one of the most serious crop diseases worldwide (Ou, 1980). *M. oryzae* is a filamentous ascomycete, which infects all the developmental stages of the rice plant including foliage, roots and panicles. *M. oryzae* also causes blast disease in a variety of grasses including cereal crops like barley, wheat and millet (Couch et al., 2005). *M. oryzae* genome was fully sequenced and annotated in 2005 (Dean et al., 2005), and in the following years, genomic resources of different strains of *M. oryzae* or related species have been emerging fast, with genome sequence available for more than 30 strains of *M. oryzae*, and various transcriptome datasets and proteomic analyses are also available (Gowda et al., 2006; Nunes et al., 2011; Oh et al., 2008). Given its economic importance and the ease of genetic manipulations and

experimental tractability (Jeon et al., 2007; Valent and Chumley, 1991), *M. oryzae* has become a top model organism to study plant pathogen interactions (Dean et al., 2012). Although the blast-resistant rice cultivars are available and viable, the fungus easily overcomes the host resistance within 2-3 years (Ou, 1980; Zeigler et al., 1994). Therefore the rice blast disease control requires further research and deeper understanding of the blast fungus and the host species.

1.1.1 Life cycle of *M. oryzae*

The life cycle of *M. oryzae*, especially the early infection stages, is very well studied. The foliar infection starts with the attachment of the three-celled conidia to the hydrophobic plant surface. The conidia adhere to the plant surface tightly by producing adhesive mucilage from the spore tip (Hamer et al., 1988). As shown in Figure 1, the conidia germinate once they attach to the plant. Upon sensing cues from the plant surface, the germ tube differentiates into a dome shaped structure, the appressorium, which is necessary for invading the host. Appressorium formation requires a hydrophobic, hard surface and cAMP signaling (Liu et al., 2007). Enormous turgor is generated within the appressorium via accumulation of a high concentration of glycerol, and is used to forcibly rupture the plant surface and gain entry into the host (de Jong et al., 1997; Howard et al., 1991). The blast fungus then grows invasively in the plant cells and colonizes the host.

After a few days of infection, the fungus sporulates from the disease lesions, and a next generation of infection begins by spreading conidia to the adjacent plant tissues.

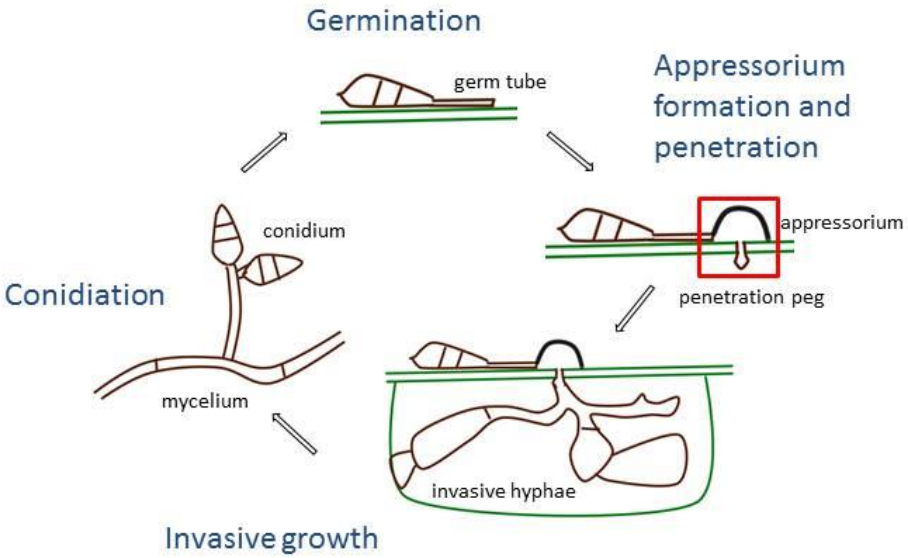

Figure 1 Pathogenic life cycle of *M. oryzae*. The asexual spores, conidia, are produced at the tip of aerial hyphae. Once the conidia attach to the host surface, they germinate and respond to host cues to form the appressoria (highlighted in red). Appressorium adheres to the host surface and functions in direct penetration of the host cell. Mature appressorium contains a thick melanin layer (black line) outside the plasma membrane. Following the penetration, the blast fungus ramifies the susceptible host tissue. The rapid proliferation results in lesion formation around 4 to 5 days after infection. Subsequent rounds of conidiation occur within the lesions and lead to further manifestation and spread of the blast disease symptoms.

1.1.2 Appressorium Formation and Host Penetration

Forming a functional appressorium is the key step for the successful infection cycle. Appressorium is formed in response to external cues like hard, hydrophobic surface, cutin monomers (cis-9,10-epoxy-18-hydroxyoctadecanoic acid) and lipid monomers (1,16-hexadecanediol) from the plant (Ebbole, 2007; Jelitto et al., 1994; Lee and Dean, 1993; Talbot, 2003; Xiao et al., 1994). The initiation of the appressorium development requires G-protein signaling, the Pmk1 mitogen-activated protein kinase (MAPK) signaling and the cyclic AMP (cAMP) response pathway (Choi and Dean, 1997; Mitchell and Dean, 1995; Nishimura et al., 2003; Ramanujam and Naqvi, 2010; Xu and Hamer, 1996). The G protein-coupled receptor Pth11 has been shown to be the bona fide receptor for the G protein signaling pathway as is essential for appressorium formation on the hydrophobic surface (DeZwaan et al., 1999; Ramanujam et al., 2013). In response to the surface cues, the G proteins activate the cAMP signaling pathway and the Pmk1 MAP kinase to initiate the appressorium formation.

After the appressorium matures, the high internal turgor within the appressoria, which can be as high as 8.0 MPa, is translated into physical force to breach the host leaf surface (de Jong et al., 1997; Howard et al., 1991). The high turgor in the appressorium is generated by hyperaccumulation of glycerol (de Jong et al., 1997). Glycerol is produced

from the storage products in conidia. Detailed analysis showed that the conidia are rich in lipids, glycogen and trehalose, but once the conidia start to germinate, the lipids, glycogen and trehalose are metabolized rapidly (Foster et al., 2003; Thines et al., 2000). Therefore the lipids, glycogen and trehalose are proposed to be the most important sources of glycerol generation in the appressorium. The fast catabolism of lipids also yields acetyl-CoA by beta-oxidation in peroxisomes, which is essential for the appressorium development (Ramos‐Pamplona and Naqvi, 2006). Such acetyl-CoA is used for the synthesis of secondary metabolites like melanin and polyketides (Wang et al., 2007). Deletion of *PEX6* produces non-functional appressoria that are defective in melanin synthesis and host penetration (Ramos‐Pamplona and Naqvi, 2006).

To maintain the high turgor by preventing the effusion of high concentration of glycerol, a thick melanin layer is deposited between the cell wall and plasma membrane and functions as a semi-permeable barrier during appressorium development. The melanin synthesis deficient mutants *alb1*Δ, *rsy1*Δ and *buf1*Δ are unable to generate sufficient turgor, and fail to penetrate and infect the plant (Chumley and Valent, 1990; Howard and Valent, 1996). The melanin layer is absent from the zone of attachment (or Appressorial pore), where the appressorium is in contact with the surface (Fig. 1). A new layer of cell wall (pore wall overlay) is deposited on the appressorium pore after the melanin layer formation (Bourett and Howard, 1990) and the

penetration peg forms and penetrates through this pore wall overlay into the host cell wall.

It has been reported that a septin ring is assembled at the base of the appressorium to facilitate the penetration (Dagdas et al., 2012). Septins including Sep3, Sep5 and Sep6, scaffold a toroidal F-actin network to restrict the Bin-Amphiphysin-Rvs (BAR)-domain proteins, which are required for curving the membrane and generating the penetration peg (Dagdas et al., 2012). The septin ring formation is regulated by reactive oxygen species generated by NADPH oxidases (Nox) in the appressoria (Ryder et al., 2013), which suggests that the septin assembly is highly related to the appressorial metabolism and subsequent function.

1.2 General introduction to secondary metabolism in fungi

Fungi produce a wide variety of secondary metabolites, which are small molecules that are not directly required for the basic growth or cell processes. The secondary metabolites are considered crucial to fungal ecological functions such as environmental sensing or microbial interaction, and some of the compounds are essential for fungal development or pathogenesis (Spatafora and Bushley, 2015). Secondary metabolites produced by fungi mainly include polyketides, terpenes, peptides and alkaloids, and they are synthesized by complex pathways. The core enzymes involved in these

pathways are polyketide synthases (PKS), terpene synthases (TS), dimethylallyltryptophan synthetase/CymD prenyl transferase family (DMATS), and non-ribosomal peptide synthetases (NRPS) respectively (Keller et al., 2005). Such core coding sequences always locate in gene clusters which include genes involved in metabolite synthesis, regulation and transport (Andersen et al., 2013). Although a huge number of secondary metabolites have been identified from the fungal species, many secondary metabolism gene clusters are known to be silent under laboratory conditions (Brakhage and Schroeckh, 2011). Therefore, the blast fungus still has great potential for mining more of such elusive secondary metabolites therein.

Secondary metabolites function during the pathogenesis in several plant pathogenic fungi. For example, the trichothecene deoxynivalenol (DON), which belongs to the terpene family, is produced by *Fusarium graminearum*, the causal agent of head blight (Fig. 2). This mycotoxin helps the fungus to colonize the barley or wheat heads (Arunachalam and Doohan, 2013). Some secondary metabolites produced during pathogenesis, for example, fumonisins (polyketide, Fig. 2) synthesized by *Fusarium verticillioides*, still have unclear functions (Proctor et al., 2003). In this project, I mainly worked on a novel *PKS* in the rice blast fungus *M. oryzae*. In the next section, PKS and polyketides will be reviewed.

1.3 Polyketides and PKS

1.3.1 Cellular functions of polyketides and PKSs

Polyketides are the major secondary metabolites with various biological functions in fungi. They include mycotoxins, such as aflatoxins and trichothecenes produced by *Aspergillus* spp. and *Fusarium* spp. respectively, or virulence factors, such as the host selective toxin (HST) T-toxin produced by *Cochliobolus heterostrophus* (Fig. 2) (Collemare et al., 2008a). Polyketides synthesized by fungi are also the source of clinically important drugs, which include the heart disease prevention drug lovastatin and the immunosuppressive mycophenolic acid (Fig. 2) (Chooi and Tang, 2012a). However, the biological functions of a vast majority of polyketides in fungi are still poorly understood.

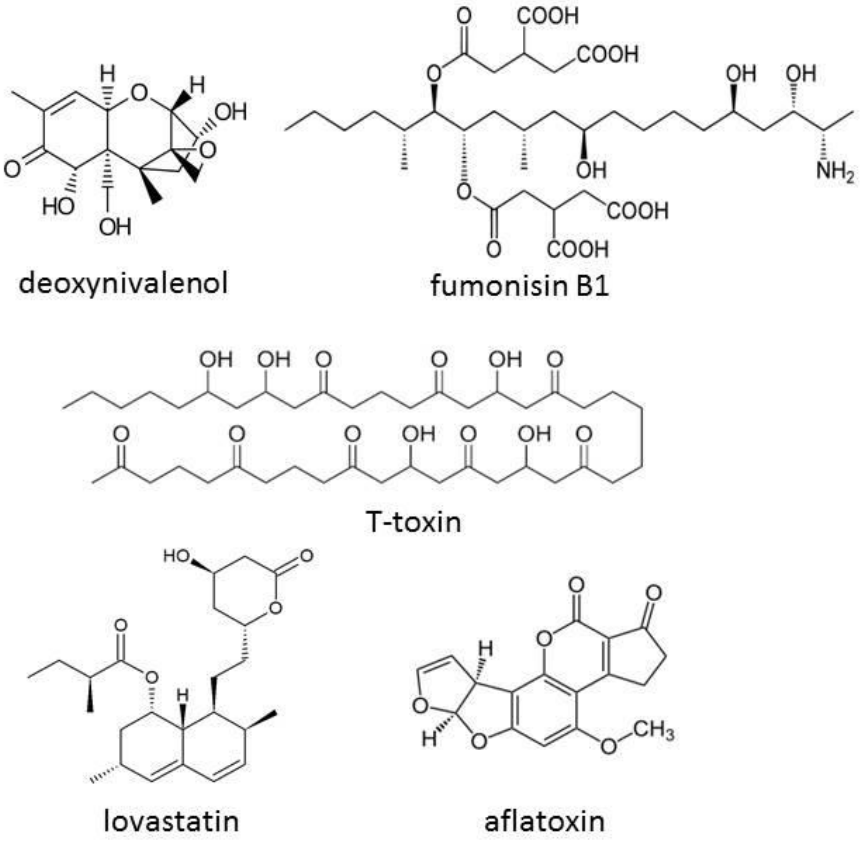

Figure 2 Examples of secondary metabolites produced by fungi.

Since the identification of the first polyketide by Collie and Myers in 1893, only chemists worked in this field (Collie, 1893). But with the development of genetic sciences, the genes that are responsible for polyketide synthesis were first discovered in 1979 by Rudd and Hopwood (RUDD and HOPWOOD, 1979). Later such genes were classified as *PKS*.

PKSs are multi-domain megasynthases, Three domains are essential to form a minimal functional PKS: the β-ketoacyl synthase (KS), the malonyl-CoA:ACP transacylase (AT), and the acyl carrier protein (ACP). These domains are responsible for the chain extension reaction. The synthesis usually starts with loading of the starter unit, acetyl, into the KS mediated by ACP domain. Then the extender unit, malonyl, is loaded to AT mediated by CoA. The KS domain then catalyzes the starter and extender unit by Claisen condensation reaction to extend the carbon backbone. The product could be transported back to KS for another round of extension by loading another extender unit or gets released from the enzyme by the releasing enzyme or domain once the correct chain length is reached (Hendrickson et al., 1999; Proctor et al., 1999; Staunton and Weissman, 2001). Apart from the three key domains, additional domains like β-keto reduction motifs (β-keto reductase KR, Dehydratase DH, and Enoyl reductase ER), the releasing domain Thioesterase (TE) and Methyltransferase (MT) domain are also present in some of the PKSs to

modify the polyketide products. Polyketide synthesis is similar to the fatty acid metabolism, since the enzymology of PKSs parallels that of the fatty acid synthases (FAS): they both use the repetitive Claisen condensation to form β-ketoacetyl polymers (Birch and Donovan, 1953). However, compared to fatty acid synthesis, the polyketide synthesis is more complex and biosynthetically programmed. For example, PKSs could use substrates other than malonyl-CoA and acetyl-CoA to produce a much wider range of products (Monaghan and Tkacz, 1990), and some PKSs also contain additional domains to modify the products via cyclization, methylation or amidation (Cox, 2007).

PKSs can be divided into three groups (Hertweck, 2009; Shen, 2003; Weissman, 2009):

- Type I PKSs contain multiple domains and the proteins are usually very large;
- Type II PKSs are large protein complexes, each protein has different catalytic domains;
- Type III PKSs do not use the acyl carrier protein domains (Meier and Burkart, 2009).

Most of the fungal PKSs are mainly classified as iterative type I PKSs, which contain monomodular multi domains and use these domains iteratively to elongate the polyketide backbone. Type I and type II PKSs require a

4′-phosphopantetheinyl transferase (PPTase) to activate a specific Ser residue in the acyl carrier proteins (ACP) (Lai et al., 2006). PPTase catalyzes the transfer of the 4'-phosphopantetheinyl group derived from coenzyme A, and changes the apo-ACP into holo-ACP (Lai et al., 2006). In *M. oryzae*, a single copy of PPTase is highly expressed during all stages of the life cycle (Horbach et al., 2009). Deletion of this PPTase leads to a nonpathogenic *Magnaporthe* mutant (Horbach et al., 2009), which suggested active PKSs are essential virulence factors. In the next section, a sub group of iterative type I PKS, HR-IPKS, will be discussed.

1.3.2 HR-IPKS

If the PKS contains all the three reduction domains, KR, DH, and ER, it is classified into a poorly characterized PKS subgroup called the Highly-Reducing Iterative PKS (HR-IPKS), which could produce a large diversity of linear and cyclic nonaromatic compounds (Chooi and Tang, 2012a). The HR-IPKS could selectively use the three β-keto reduction domains to catalyze the β-keto to different reduction levels in each cycle. This makes the prediction of the HR-IPKS products even harder. Most HR-IPKSs lack a releasing domain, *e.g.* TE (thioesterase) domain (Cox et al., 2004). Therefore, an additional releasing enzyme is needed for the HR-IPKS function. In our study, an HR-IPKS was characterized in detail in the rice blast fungus

M. oryzae. Function and subcellular localization of the protein was examined in Chapter III.

1.3.3 PKS gene clusters

With the exception of all the functional domains in the PKSs, additional enzymes are required to modify the intermediate compounds synthesized by PKSs. The genes encoding the modifying enzymes and the PKSs are always closely localized and co-regulated in the genome, thus defining a typical gene cluster (Keller and Hohn, 1997). Typically a transcription factor that regulates the gene cluster transcription is present in the PKS gene cluster (Wu et al., 2012). For example, *aurR1*, *aurR2* and *aurJ* are the transcription regulators in the aurofusarin gene cluster (Malz et al., 2005) and *ZEB2* (ZEB2L and ZEB2S) regulates the zearalenone gene cluster (Kim et al., 2005; Park et al., 2015). It is also known that the PKS gene cluster sometimes encodes a transporter, such as the gene encoding ATP-binding cassette (ABC) in the nystatin biosynthesis gene cluster in *Streptomyces noursei* ATCC 11455, but the function of the transporter during the synthesis is still unknown (Wu et al., 2012). Therefore, to understand the polyketide synthesis pathway, it is important to study the genes surrounding the *PKS* locus of interest.

Our group previously reported that the Abc3 transporter plays an essential

role in host penetration and *in planta* growth of *M. oryzae* (Sun et al., 2006a). Abc3 mediates the efflux of a digoxin-like endogenous steroidal glycoside which is important for proper appressorial function (Patkar et al., 2012). The genomic neighborhood of the *ABC3* locus contains several genes encoding metabolic enzymes including a putative *PKS* (*MGG_04775*; which we designated as *PKS1*). The transcription of *PKS1* is highly upregulated during appressorium formation similar to *ABC3* (Soanes et al., 2012; Sun et al., 2006a). This suggests that Pks1 may be involved in synthesizing an important secondary metabolite required for appressorium development and/or function. It is also likely that Pks1 synthesizes one (or more) of the efflux targets of the Abc3 pump in *Magnaporthe.*

1.3.4 Regulation of PKS gene clusters

As mentioned in the previous section, secondary metabolism gene clusters are always co-regulated similar to the bacterial operon system. However, unlike the bacterial operons, the genes in the biosynthesis clusters have their own promoters. The regulation of the PKS gene clusters is usually controlled by a transcription factor contained therein, and the transcription factor is under the control of upstream regulators to fit into the different environment and fungal development stages (Calvo et al., 2002).

Studies on secondary metabolism in *Aspergillus* species have revealed a

number of important transcriptional regulation pathways (Bhatnagar et al., 2006). For example, the sterigmatocystin (ST) biosynthesis is linked with fungal development. The *A. nidulans* mutant that failed to produce ST is also defective in conidiation (Kale et al., 2003; Kale et al., 1996). This finding led to the discovery that conidiation and ST biosynthesis are both regulated by a G-protein/cAMP/protein kinase A pathway (Bok and Keller, 2004; Hicks et al., 1997; Roze et al., 2004; Shimizu et al., 2003). A global secondary metabolism regulator, VeA, which controls sexual development was also identified in *A. nidulans* (Kato et al., 2003; Kim et al., 2002). VeA is essential for biosynthesis of several toxins including aflatoxin or ST (Kato et al., 2003). VeA regulates secondary metabolism biosynthesis in many fungi and is conserved in ascomycetes (Myung et al., 2012). The nuclear protein LaeA is also a global secondary metabolism regulator in several aspergilli (Bok et al., 2006; Bok and Keller, 2004). LaeA is a putative methyltransferase, which interacts with the VeA complex and is involved in chromatin conformation (Bayram et al., 2008; Reyes‐Dominguez et al., 2010). In addition, epigenetic factors also affect the secondary metabolism, e.g. the biosynthesis of aflatoxin/ST is regulated by histone modifications including acetylation and methylation (Reyes‐Dominguez et al., 2010; Roze et al., 2007; Shwab et al., 2007). Post-translational modifications and ribosomal engineering could alter secondary metabolism in microbes (Hosaka et al., 2009; Ochi et al., 2004; Scherlach et al., 2011). Inhibition of

the ubiquitin-mediated protein degradation by deleting the subunits of the COP9 signalosome activates secondary metabolism gene clusters in *A. nidulans* (Wei et al., 2008). A secondary metabolism gene cluster which contains a PKS gene, *dbaI* is silent in normal conditions but is activated upon loss of COP9 deneddylase subunit *CSN5*, thus leading to the production of the polyketide antibiotics, 2,4-dihydroxy-3-methyl-6-(2-oxopropyl) benzaldehyde (DHMBA) (Gerke et al., 2012).

Studies on regulation of secondary metabolism in *M. oryzae* are limited. A homolog of VeA in *M. oryzae* has been studied recently (Kim et al., 2014). Deletion of *MoVEA* led to defects in conidiation and appressorium formation. *MoVEA* is also involved in ROS (reactive oxygen species) responses, but whether *MoVEA* regulates secondary metabolism in *M. oryzae* is still unknown.

1.4 Polyketide synthases characterized in M. oryzae

The *Magnaporthe* genome contains 22 PKS genes and 10 PKS-NRPS (non-ribosomal peptide synthetase) hybrid genes, and 1 newly found NRPS-PKS gene *TAS1*, which indicates an overall abundance of secondary metabolite production therein (Collemare et al., 2008a; Yun et al., 2015). Tas1 is a unique NRPS–PKS hybrid enzyme and is responsible for the Tenuazonic acid (TeA) production (Yun et al., 2015). The product of *ACE1*

serves as an avirulence factor and is expressed exclusively during the host penetration phase of blast infection. *M. oryzae* strains that express *ACE1* are unable to infect rice varieties that contain a functional Pi33 resistance locus (Böhnert et al., 2004). However *ace1*Δ, *syn2*Δ, *syn6*Δ and *tas1*Δ mutants do not have any pathogenic defects on susceptible rice cultivars (Böhnert et al., 2004; Collemare et al., 2008a; Yun et al., 2015). Among these PKSs and PKS-NRPSs, only the melanin synthase Alb1 is known to be essential for virulence in the rice blast fungus (Chumley and Valent, 1990). *ALB1*-mediated melanin synthesis and the function of Ace1 and Tas1 will be discussed in the next section.

1.4.1 Melanin synthesis

Melanin is a dark pigment/polymer that is usually insoluble, and shows resistance to hot concentrated acid or alkaline treatment and can be bleached by oxidizing agents (Nicolaus et al., 1964). Due to the complexity and insolubility of melanin, the exact structure of melanin remains elusive (Prota et al., 1998). There are mainly two types of melanin, the DHN melanin and the DOPA melanin (Langfelder et al., 2003). DHN (1,8-dihydroxynaphthalene) is an intermediate product of the DHN melanin synthesis pathway, and DOPA ($_{L}$-3,4-dihydroxyphenylalanine) is one of the precursors of DOPA melanin.

The DHN pathway is the best characterized melanin synthesis pathway (Bell and Wheeler, 1986), and follows a pentaketide route which starts with type I PKS catalysis. The requisite PKS produces 1,3,6,8-tetrahydroxynapthalene (1,3,6,8-THN) by utilizing five malonyl-CoA as the starter and extender units (Fujii et al., 2000). Then the 1,3,6,8-THN is reduced to scytalone by a reductase activity (Thompson et al., 2000; Tokousbalides and Sisler, 1979; Wheeler and Bell, 1988), such as *arp2* in *A. fumigatus* (Tsai et al., 1997) and *BRM2* in *A. alternata* (Kawamura et al., 1999). In the next step, scytalone is dehydrated to 1,3,8-trihydoxynaphthalene and reduced to vermelone (Alspaugh et al., 1998). Tricyclazole is able to inhibit the two reduction steps (Tokousbalides and Sisler, 1979). If tricyclazole is added, the fungus produces shunt products and resembles the defect of the reductase deletion mutant. Next, vermelone is dehydrated to 1,8-DHN, the precursor of DHN melanin (Butler and Day, 1998). How the 1,8-DHN polymerizes to melanin is still unclear, but a laccase or DHN oxidase is to catalyze this step (Geis et al., 1984; Tsai et al., 1999).

M. oryzae produces DHN melanin but not DOPA melanin. Three genes have been found in the DHN synthesis pathway in *M. oryzae*: *ALB1* (encoding the PKS), *RSY1* (encoding the dehydratase) and a reductase encoding gene *BUF1* (Chumley and Valent, 1990). A second reductase gene, *4HNR,* has been predicted in the *M. oryzae* genome, although its involvement in the DHN melanin synthesis remains unclear (Thompson et al., 2000). The *alb1*Δ,

*rsy1*Δ and *buf1*Δ mutants show melanin synthesis defects and produce non-melanized appressoria that are incapable of penetrating the host surface (Chumley and Valent, 1990). The melanization of *M. oryzae* vegetative hyphae is regulated by a transcriptional regulator Pig1, but Pig1 does not regulate the appressorial melanization (Tsuji et al., 2000). This suggests that appressorial melanization is transcriptionally controlled by a Pig1-independent pathway. Interestingly, *PIG1, ALB1* and *4HNR* are closely located in the genome, indicating that they may function together as a gene cluster.

1.4.2 Function of other PKSs in *M. oryzae*

Ace1 is a PKS-NRPS hybrid synthase which synthesizes a secondary metabolite that can be recognized by the cognate R-protein Pi33 in specific rice cultivars (Böhnert et al., 2004). *ACE1* is only expressed in the appressorium during the initiation of host penetration (Fudal et al., 2007). *ACE1* belongs to a secondary metabolism gene cluster which contains 15 genes (Collemare et al., 2008c). *SYN2*, another PKS-NRPS is also involved in this gene cluster, but it is not required for the avirulence function. The 15 genes in the cluster are expressed specifically in the appressorium, but function of the other 14 genes is still unclear (Collemare et al., 2008c). Heterologous expression of *ACE1* and an enoyl reductase encoding gene

RAP1 (located next to ACE1 in the gene cluster) in *A. oryzae* and *M. oryzae* results in production of novel metabolites such as 12,13-dihydroxy magnaporthepyrone and 10,11-dihydroxy magnaporthepyrone (Song et al., 2015). However these metabolites could not induce avirulence or hypersensitive reaction on the Pi33 rice cultivars, which suggests that these metabolites are not the avirulence signals and are likely different from the natural compounds synthesized by the *ACE1* gene cluster (Song et al., 2015).

TAS1 encodes an NRPS-PKS and synthesizes the mycotoxin TeA (Yun et al., 2015). It only contains a KS domain for the PKS portion. Although TeA has been reported to be toxic for the rice plant (Umetsu et al., 1972), not all *M. oryzae* strains produce TeA. Therefore, whether *TAS1* is required for *M. oryzae* virulence has not been determined yet.

1.5 Purpose and significance of the study

In this study, I aimed at:

- Characterizing the function of *PKS1* gene in *M. oryzae*;
- Discovering the possible modification enzymes in the *PKS1* gene cluster;
- Studying the function and regulation of the *PKS1* gene cluster;
- Identifying the substrate and product of Pks1.

This study was aimed at improving our understanding of the pathogenesis mechanism of *M. oryzae.* It was also aimed at providing clear evidence that *PKS1* mediated secondary metabolism does play an important role in infection-related development in the rice blast fungus. Furthermore, this study would also be important in the light of recent trends in the fungal PKS studies and be beneficial to the PKS research field.

1.6 Scope and limitations

Given the complexity in secondary metabolite identification and due to time constraints, only *PKS1* containing gene cluster has been studied in detail in this thesis. The high transcriptional levels of *PKS1* during the pathogenesis phase suggested that it would be important for the establishment and/or spread of rice blast. Therefore, we mainly focused on the functional study of *PKS1* during pathogenesis. We investigated the relationship between *PKS1* and other factors which are important for pathogenesis including melanin synthesis and septin assembly. We also studied the PKS1 gene cluster and the regulation of the cluster. Although we made significant progresses in understanding the PKS1 containing gene cluster, there was limited success of identifying the biosynthesis products of Pks1. It is mainly because of the complexity of the PKS pathway and secondary metabolism in the blast fungus. Future studies are still needed to identify the products.

Chapter II Materials and Methods

2.1 Fungal strains and growth conditions

The *M. oryzae* wild-type strains B157 (Field isolate) was obtained from the Directorate of Rice Research (Hyderabad, India) and the Sep5-GFP Guy11 strain was a kind gift from the Talbot lab (Exeter, UK). All the blast strains used in this study are listed in Table 1. For normal growth, *M. oryzae* was cultured on Prune-agar (PA) medium (Prune Juice 40 mL/L, Lactose 5 g/L, Yeast Extract 1 g/L, Agar 20 g/L), and was incubated at 28 ℃. For conidiation, *M. oryzae* was grown in dark for 3 days and then under constant light for 5 days at room temperature. Conidia and mycelia were harvested by scraping the colonies with inoculation loops in the presence of water. The mycelia were removed by filtering the total suspension through two layers of Miracloth (Calbiochem, CA), and then the conidia were centrifuged and washed with sterile water.

Table 1 *M. oryzae* strains used in this study.

Name	Genotype	Source
B157	Wild type	this study
*pks1*Δ	*pks1*Δ::*hph*$^+$	this study
*pks1*C	*PKS1-bar*$^+$ / *pks1*Δ::*hph*$^+$	this study
Pks1-GFP	Pks1-GFP-*hph*$^+$	this study
Pks1-GFP;hH1-RFP	Pks1-GFP-*hph*$^+$ / hH1-RFP-*ilv2*$^+$	this study
Pks1-GFP;*alb1*Δ	Pks1-GFP-*hph*$^+$ / *alb1*Δ::*bar*$^+$	this study
Pks1-GFP;*buf1*Δ	Pks1-GFP-*hph*$^+$ / *buf1*Δ::*bar*$^+$	this study
Pks1-GFP;*fsh1*Δ	Pks1-GFP-*hph*$^+$ / *fsh1*Δ::*ilv2*$^+$	this study
Pks1-GFP;*abc3*Δ	Pks1-GFP-*hph*$^+$ / *abc3*Δ::*ilv2*$^+$	this study
Fsh1-mCherry	Fsh1-mCherry-*ilv2*$^+$	this study
Pks1-GFP;FSH1-mCherry	Pks1-GFP-*hph*$^+$ / *ilv2*$^+$	this study
DH-ERΔ	DH/ERΔ::*ilv2*$^+$	this study
KRmut	KRmut::*ilv2*$^+$	this study
pTrpC::Pks1-GFP	pTrpC::Pks1-GFP-*bar*$^+$	this study
pTrpC::Fsh1-mCherry	pTrpC::Fsh1-mCherry-*ivl2*$^+$	this study
Pks1-GFP;*gk1*Δ	Pks1-GFP-*hph*$^+$ / *gk1*Δ::*bar*$^+$	this study
Sep5-GFP (Guy11)	Sep5-GFP-*bar*$^+$	(Dagdas et al., 2012)
Sep5-GFP;*pks1*Δ (Guy11)	Sep5-GFP-*bar*$^+$ / *pks1*Δ::*hph*+	this study

Sep5-GFP;*fsh1*Δ (Guy11)	Sep5-GFP-*bar*$^{+}$ / *fsh1*Δ::*hph*$^{+}$	this study
Pks1-GFP;*stu1*Δ	Pks1-GFP-*hph*$^{+}$/ *stu1*Δ::*bar*$^{+}$	this study
Pks1-GFP;*mst12*Δ	Pks1-GFP-*hph*$^{+}$/ *mst12*Δ::*bar*$^{+}$	this study
Pks1-GFP;*MoveA*Δ	Pks1-GFP-*hph*$^{+}$/ *MoveA*Δ::*bar*$^{+}$	this study
Pks1-GFP;*csn7*Δ	Pks1-GFP-*hph*$^{+}$/*csn7*Δ::*ivl2*$^{+}$	this study

M. oryzae mutant generated by *Agrobacterium tumefaciens* mediated transformation was first selected and cultured in different mediums based on the selection marker. For hygromycin (250 μg/ml) selection, CM (complete medium, Yeast Extract 6 g/L, Casein Hydrolysate 6 g/L, Sucrose 10g/L, Agar 20 g/L) medium was used. For basta (ammonium glufosinate, 50 μg/ml) and sulfonylurea (chlorimuron-ethyl, 50 μg/ml) selection, BM (basal medium, Yeast Nitrogen Base 1.6 g/L, Asparagine 2.0 g/L, NH_4NO_3 1.0 g/L, Glucose 10 g/L, Agar 20g/L, pH 6.0) was used. To extract genomic DNA or total protein from the mycelia, fungus agar plugs were cultured in the liquid CM for 3-4 days in 28 ℃ shaker.

2.2 Agrobacterium tumefaciens mediated Transformation

In our study, all the deletion mutants and gene-tagging strains were generated by *Agrobacterium tumefaciens* mediated Transformation (ATMT) method. *A. tumefaciens* strain AGL-1 was used to do the transformation, and it was cultured by LB medium (Tryptone 10 g/L, Yeast Extract 5 g/L, NaCl 5 g/L) at 28 ^{o}C.

2.2.1 Electroporation of *A. tumefaciens*

Plasmid constructs were transformed into AGL-1 competent cells by electroporation. Frozen AGL1 competent cells (50 μL per tube) were first

thawed on ice and mixed with 100 ng of plasmid DNA. The cells were transferred to the electroporation cuvette (gap 0.1 cm) (Bio-rad, USA) and were electroporated by Bio-Rad MicroPulser (USA) at 1.8 KV for 5 msec. Then the cells were recovered in 1 mL LB liquid medium in 28^{o}C for 45 min. Recovered 100 μL cell suspensions were plated on LB agar medium with kanamycin selection (100 μg/mL). AGL1 transformants were grown at 28^{o}C for 2-3 days.

2.2.2 Fungal transformation

1. Fresh AGL1 was grown overnight in liquid LB medium at 28 ^{o}C

2. Diluted to OD_{600} = 0.15 with IM medium (induction medium, K salts 10 mL/L, M salts 20 mL/L, NH_4NO_3 (20%) 2.5 mL/L, $CaCl_2$ (1%) 1 mL/L, Glucose 5 mM, MES 40 mM, Glycerol 0.5% w/v; K salts: K_2HPO_4, 20.5%, KH_2PO_4 14.5%; M salts: $MgSO_4$ ·7H2O 3%, NaCl 1.5%, $(NH_4)_2SO_4$ 2.5%). Kanamycin (100 μg/mL) and 200 μg/mL ACS (acetosyringone) were added to the IM medium before culturing.

3. Cultured at 28 ^{o}C for 6 h, and 100 μL culture mixed with 100 μL conidial suspension (~10^6/mL). The mixture was placed and air-dried on to 0.45 μm nitrocellulose film (Merck Millipore, Germany) placed on IM agar containing 200 μg/mL ACS, 60 μg/mL streptomycin and 100 μg/mL ampicillin.

4. The AGL1/conidia mixture was grown at 28 ^{o}C for 2 days and was scraped from the nitrocellulose film into 1 mL sterile water.

5. Vortexed mixture was then plated on selection medium containing 200 μM Cefotaxime (to kill the agrobacteria).

6. The culture was incubated at 28 ^{o}C for 4-5 days. The colonies were subcultured on PA medium or liquid CM for further genotyping and confirmation.

2.3 Molecular methods

2.3.1 DNA manipulation, gene tagging and deletion

2.3.1.1 PCR

Different PCR polymerases were used in this study. A homemade Taq polymerase was used for routine PCR tests. KAPA HiFi DNA polymerase (Kapa Biosystem Inc**,** USA) was commonly used for amplifying fragments for use in constructs. Expand Long Template PCR System (Roche Diagnostics, Germany) was only used for amplifying DNA fragments larger than 4 KB. All PCR were carried out followed by the manufacturer's instructions.

Fusion PCR was done by KAPA HiFi polymerase. The first round of the

PCR followed the manufacturer’s instructions. Two DNA fragments were amplified and gel purified. The second round of the PCR used the products of the first round PCR as DNA templates. The DNA template concentration was used according to the instructions, and a pair of primers was used for normal PCR.

Table 2 Oligonucleotide primers used in this study

Descriptions	Primers (5’ - 3’)	
PKS1 deletion	Pks1-5UTR-F-KpnI	GTGTGGTACCCTAAAGATAGCTCAGCTCAG
	Pks1-5UTR-R-XbaI	GTGTTCTAGAGATCTACTGGGCAGGTTCGG
	Pks1-3UTR-F-HindIII	GTGTAAGCTTGCCGTCATAGTATTTCCTTTG
	Pks1-3UTR-R-HindIII	GTGTAAGCTTTGTCTGTGGACGTAAATGATC
CSN5 deletion	Csn5-5UTRf-EcoRI	GTGTGAATTCATGAGCCGCAGTCATAGTAG
	Csn5-5UTRr-SpeI	GTGTACTAGTGGCTGGCTGACTTATGCTTG
	Csn5-3UTRf-PstI	GTGTCTGCAGTGGGCAAACAGAACATCAAG
	Csn5-3UTRr-PstI	GTGTCTGCAGTAACATGGAAATCCCGGAAC
Pks1-GFP	Pks1orf-F-EcoRI	GTGTGAATTCACGAGCTGTTCAAGGGACTG
	Pks1orf-R-KpnI	GTGTGGTACCGCTCAACCCAACACAAAGC
PKS1 complementation	4775UPcomp-F-EcoRI	GTGTGAATTCCTCCGCTTCTGCATGCCCAAAC

	4775ORFcomp-R-EcoRI	GTGTGAATTCGCTCAACCC AACACAAAGCTTGCTC
FSH1 deletion	4774-5UTR-F-XhoI	GAGAGTGTTCTGCAGCTTG CTTCTTTCTTAATTC
	4774-5UTR-R-EcoRI	GAGAGTGTTCGATCGGCCA CAAACAATACGGAC
	4774 3'UTR-f-SalI	GTGTCGACCTTGCTTCTTTC TTAATTCTGC
	4774 3'UTR-r-SalI	GTGTCGACCCACAAACAAT ACGGACTGG
Fsh1-mCherry and complementation	4774-5UTR-F-XhoI	GAGAGTGTTCTGCAGCTTG CTTCTTTCTTAATTC
	4774orf-R-EcoRI	GTGTGAATTCCTACAGTAG ACCATCCTCCC
ALB1 deletion	Alb1 5'UTR-f-EcoRI	GTGAATTCTGCAGAGGGCG GCACATCAC
	Alb1 5'UTR-r-SacI	GTGAGCTCGATGGTTGTCA GCATGTATTCC
	Alb1 3'UTR-f- PstI	GTCTGCAGATCATTAGAAG CCTTGATGG
	Alb1 3'UTR-r- HindIII	GTAAGCTTGCAAAGACCGT GTCAGAAACC
BUF1 deletion	Bufl 5'F-EcoRI	GTGTGAATTCGCCACTGAC TATATCACGTGC
	Bufl 5'R-BamHI	GTGTGGATCCAATTGATGG ATCGTCCTGTG

	Bufl 3’F-SalI	GTGTGTCGACACGTACTTG AAACAATGGAG
	Bufl 3’R-HindIII	GTGTAAGCTTGATCGGGTA AAGTAAATACG
GK1 deletion	GK1 5’F-XhoI	GTGTCTCGAGATTCGGGCC AGGTCCTGTAC
	GK1 5’R-BamHI	GTGTGGATCCCTTTCTCTC GATCGGGCTTG
	GK1 3’F-HindIII	GTGTAAGCTTTACTGGTTA TGGGTGGTAGG
	GK1 3’R-HindIII	GTGTAAGCTTAGGATTCCA GGGGCACAAAG
MoVEA deletion	Vel3F-PstI	gtgtctgcagCGGTGTTTCTTCC ATGTTAGC
	Vel3R-HindIII	gtgtaagcttGGGCGATGGGTAG AAGAATTG
	Vel5F-KpnI	gtgtggtaccGCTGCATGAATCT TGGCTAGG
	Vel5R-BamHI	gtgtggatccGTGAATCGCCAAT CCTGCAAC
DH-ER domain deletion	ATf-EcoRI	GTGTGAATTCTCCCTCGCC GGTGTCATGAAG
	ATr-XmaI	GTGTCCCGGGGTTGCGCGG GAACTTGCGGAAC
	KR-PPf-XmaI	GTGTCCCGGGCGCAGCATG GCCAAGTGGATG

	KR-PPr-SpeI	GTGTACTAGTCTAGCTCAACCCAACACAAAGCTTG
	4775TermF-H3	gtgtAAGCTTGCCGTCATAGTATTTCCTTTG
	4775TermR-H3	gtgtAAGCTTTGTCTGTGGACGTAAATGATC
KR domain mutation	4775KR-F-KpnI	gtgtGGTACCGGCTGTCTTGTCAACGTCTCTG
	4775KR-R-SpeI	gtgtACTAGTctaGCTCAACCCAACACAAAGC
	KRmut-F	CAGGCCGCATtaGCGGCCGCCgcCACGTTCCTC
	KRmut-R	GAGGAACGTGgcGGCGGCCGCtaATGCGGCCTG
MST12 deletion	Mst5f-SacI	gtgtgagctcAAATGATTCCCACCCAGCTAC
	Mst5r-BamHI	gtgtggatccGTGAGGGACGACTCTATGGA
	Mst3f-SalI	gtgtgtcgacCTTCTATCATTGCCTGGTGG
	Mst3r-PstI	gtgtctgcagCGTGACCAAGTCAAACAAAG
STU1 deletion	stu5f-EcoRI	gtgtgaattcACCCACACAGGTCCAAGATC
	stu5r-SpeI	gtgtactagtGCTGTTGTATGCAGGAATGGC

	stu3f-SalI	gtgtgtcgacTACGAGGCTCGCTGTATATTG
	stu3r-PstI	gtgtctgcagCATATCGTCTCAAATTGCCCAC
Reverse Transcript PCR	Alb1-RTf	AGCTGGCTTTCCTCCTCTTC
	Alb1-RTr	TGTGACTCGTGGAATCCAGC
	Buf1-RTf	AGCTCGACATCGTTTGCTCC
	Buf1-RTr	GATCACTTTCCCAGTGACCC
Real Time PCR	Alb1-qPf	GACGGCCACCATCTACAAG
	Alb1-qPr	GGTCTTGTGGCTACCATGC
	Buf1-qPf	AGGAGGTTGACGAGTATGCC
	Buf1-qPr	TACCGATCACTTTCCCAGTG
	Tub-qPf	GAGTCCAACATGAACGATCT
	Tub-qPr	GTACTCCTCTTCCTCCTCGT

2.3.1.2 Gel electrophoresis and DNA purification

DNA gel electrophoresis was performed using 1% agarose gels in 1X TAE buffer (89 mM Tris base, 89 mM boric acid, 2.6 mM EDTA, pH8.3). 1X SYBR green (Sigma-Aldrich, USA) was used for detection. DNA samples were loaded to the gel with 10 × DNA loading dye (40% glycerol, 0.5% SDS, 10 mM EDTA, 2.5 mg/mL bromophenol blue). The 1 KB ladder (NEB, USA) was used for DNA size estimates.

DNA fragments either from PCR amplification or enzyme digestion were purified using NucleoSpin Gel and PCR Clean-up kit (Macherey Nagel, Germany) following the manufacturer's instructions.

2.3.1.3 Plasmid manipulation

DNA digestion and ligation were executed using restriction enzymes and T4 ligase from Thermos Scientific (USA), and were carried out according to the manufacturer's instructions. Plasmid DNA was purified by the High-Speed Plasmid Mini Kit (Geneaid Biotech, Taiwan). The correct cloning was confirmed by PCR and restriction digestion. Nucleotide sequence analysis was employed to check the reliability of the recombinant DNA by using the Applied Biosystems Prism 377 DNA sequencer (Forster, USA).

2.3.1.3 Southern blot

Standard protocal was followed to perform the southern blotting (Sambrook et al., 1989).

Genomic DNA was digested with FastDigest (Thermos Scientific, USA) restriction enzyme following the manufacturer's instruction. Hybond-N+ (Amersham, USA) nylon membrane was used for the blotting and UV stratalinker 2400 (Stratagene, USA) was used for DNA cross-linking. DNA probe labeling and hybridization process used the kit from Amersham Pharmacia Biotech (USA)

2.3.2 RNA techniques

2.3.2.1 RNA extraction

1. Extraction from mycelia: *M. oryzae* mycelia were culture in liquid CM for 3 days. Mycelia were harvested by filtering through Mirocloth, washed with water and were dried by tissue paper. Then the mycelia were grounded into powder in liquid nitrogen immediately. The total RNA was extracted by RNeasy mini kit (Qiagen, Netherlands) following the manufacturer's instructions.

2. Extraction from appressoria: *M. oryzae* conidia were harvested from the PA medium and were suspended in water. At least 5×10^6 conidia were needed for the RNA extraction. Adjust the conidia concentration to 1×10^5 /mL with sterile water. Then the conidia suspension was placed on the hydrophobic glass sheathes. At the dedicated time point, water was removed from the lass sheathes. Filter paper could be used to remove the excess water.

0.5 mL of the RTL buffer from RNeasy mini kit (Qiagen, Netherlands) was added to the glass sheathes directly. Scrape the appressoria off from the glass sheets with RTL buffer carefully. Then the suspension was grounded with the presence of a little liquid nitrogen. Collect as much RTL buffer suspension as possible. The following steps were the same as the manufacturer's instructions of the RNeasy mini kit.

3. Extraction from conidia: Conidial RNA extraction was similar with appressorium RNA extraction. Only the conidia were not placed on the glass sheathes, but were grounded in the RTL buffer with the presence of a little liquid nitrogen directly after harvest.

2.3.2.2 Reverse transcriptase PCR

1. Total RNA was treated with DNase I from Thermo Scientific followed the manufacturer's instructions.

2. RevertAid First Strand cDNA Synthesis Kit from Thermo Scientific was used to synthesize cDNA from 1 μg of total RNA.

3. DNA fragment was amplified by designed primers for RT-PCR.

4. *Tubulin* (*MGG_00604.6*) was used as a loading control.

2.3.2.3 Quantitative Real-time PCR

1. Total RNA was treated with DNase I from Thermo Scientific (USA) followed the manufacturer's instructions.

2. RevertAid First Strand cDNA Synthesis Kit from Thermo Scientific (USA) was used to synthesize cDNA from 1 μg of total RNA.

3. qRT-PCR was performed by using the KAPA SYBR FAST qPCR Kits (KAPA Biosystems, USA). The PCR reaction mixture was prepared with: 5 μl 2×iQ SYBR green, 0.5 μl Forward Primer (10 μM), 0.5 μl Reverse Primer (10 μM), 1 μl cDNA (20 ng) and 3 μl H2O.

4. Real-time PCR was run by ABI Prism SDS 7900HT (USA) machine. PCR program was set according to the instructions of KAPA SYBR FAST qPCR Kits. The relative changes of the mRNA levels were assessed by the comparative CT (cycle threshold) method (ddCT method).

2.3.3 Protein related methods

2.3.3.1 Preparation of total protein lysates (denatured)

1. *M. oryzae* mycelia were cultured in liquid CM at 28 ^{o}C for 2-3 days.

2. Mycelia were harvested by filtering through Mirocloth and washed with chilled sterile water and dried by blotting with tissue paper. Mycelia were ground into a powder in liquid nitrogen immediately.

3. About 300 μl of SDS lysis buffer (10 mM Na_3PO_4, 0.5% SDS, 1 mM DTT, 1 mM EDTA, pH 7.0) was added to 100 mg mycelial powder and incubated on ice for 10 min, then boiled with 5x SDS loading buffer (working concentration: 50 mM Tris-HCl, pH 6.6, 2% SDS, 10% glycerol, 1%

2-mercaptoethanol, 12.5 mM EDTA, 0.02% bromophenol blue) at 100 ℃ for 10 min.

5. The boiled mixture was centrifuged at 14,000 rpm at room temperature for 10 min. The supernatant was then collected and stored at 4 ℃ for subsequent experiments.

2.3.3.2 RFP-Trap assay

M. oryzae mycelia were prepared as the steps 1-2 in section 2.3.3.1. Then the mycelia powder was added to lysis buffer provided in the RFP-Trap kit (Chromo Tek GmbH, Germany) with additional 1x protease inhibitor cocktail (Roche Diagnostics, Germany). RFP-Trap assay was performed according to the manufacturer's instructions. The trapped proteins were analyzed by western blotting described in section 2.3.3.3.

2.3.3.3 Western blot

Standard western blotting method was performed (Sambrook et al., 1989). Proteins were transferred onto the PVDF membrane (Millipore, USA). The enhanced chemiluminescence system (ECL, Amersham) was conducted to detect the signal from the membrane.

2.3 Staining methods

2.3.1 CMAC staining

CellTracker™ Blue CMAC Dye (Thermo Fisher Scientific Inc., USA) was dissolved in DMSO to a concentration of 10 mM. The working concentration of 5 μM was added to the conidial suspension. Then the conidial suspension was placed on the coverslip to develop appressoria for 20-30 hrs. CMAC-stained vacuoles were imaged using 405nm excitation laser and the DAPI filter for CMAC dye.

2.3.2 Aniline blue staining

Barley leaves were inoculated with conidia for 28-30 h. The infected leaf area was cut and incubated overnight in the fixing solution at room temperature (acetic acid: ethanol = 1: 3, v/v). The fixing solution was replaced with 1M NaOH and incubated for 1 h. The stained tissue was washed several times with water until the pH stabilized. Fresh 0.1% (w/v) aniline blue working solution was prepared in 100 mM K_3PO_4 (pH ~11). The treated leaf tissue was incubated in the aniline blue working solution in dark for at last 2 h at room temperature. Stained samples were observed using the DAPI filter under epifluorescent microscope.

2.4 Blast infection assays

2.4.1 Barley leaf infection

Barley seeds were planted in soil in a growth chamber at 16 ^{o}C (16 h illumination/d) for two weeks. Barley leaves were cut and sterilized with 40% ethanol for a few second and quickly washed with sterile water containing 100 μg/ml streptomycin and 100 μg/ml ampicillin. The leaves were placed on kinetin agar medium (100 μg/ml streptomycin, 100 μg/ml ampicillin and 2 μg/ml kinetin). To keep the leaves fresh, the cut ends were covered with wet sterilized filter paper. Then droplets (20 μL each) of required concentration of the conidial suspension were inoculated on the leaf surface. The leaves were kept in the 22^{o}C incubator with 16 h light per day for 7 days.

2.4.2 Wounding assay

Similar method was performed as 2.4.1 for the wounding assay, but the barley leaves were wounded/abraded with a sharp needle tip prior to conidial inoculation.

2.4.3 Rice seedling infection

The blast susceptible CO39 rice seeds were soaked in water at 37 ^{o}C for 3 days for germination. Then the germinated seeds were planted in soil in

green house for 4 weeks. Conidial suspension (1×10^6 conidia/mL, with 0.01% gelatin) was evenly sprayed onto the rice seedlings. The inoculated rice seedlings were covered by transparent plastic film and grown in a 22 ^{o}C growth chamber (80-95% humidity, 16 h illumination per day) for 7 days.

2.4.4 Rice sheath infection

Rice seedlings were grown as described in section 2.4.3. Rice sheath was separated carefully from a one to two month old seedling. The sheath was cut into 3 cm pieces and stuck on wet filter paper. Conidia suspension (20,000 conidia per mL) was inoculated on the sheath surface. The inoculated rice sheath was maintained in moist condition at room temperature for 30 h.

2.4.5 Rice root infection

The root infection assay was performed by dropping 0.2 mL of 1×10^5 mL^{-1}conidial suspension on to two-week old rice roots. The rice roots were initially washed with sterile water and placed on the sterilized wet filter paper. Then the plants were kept at 22℃ for 7 days post inoculation.

2.4.6 Membrane penetration

Membrane penetration of appressorium was conducted by using PUDO-193 cellophane (a kind gift from Marc-Henri Lebrun, France). Twenty microliter of conidial suspension was inoculated on the pre-wetted PUDO membrane

and the penetration was examined at 48 hpi.

2.5 Microscopy

2.5.1 Light microscopy

We used the Leica DMLB microscope and the Optronics DEI-750T cooled CCD camera (Muskogee, OK) and Leica Qwin software. Images were processed and assembled using Fiji (ImageJ) and Adobe Photoshop CS6.

2.5.2 Confocal microscopy

Laser scanning confocal microscopy was performed using a Microlambda spinning disk w/FRAP (with incubator and motorized stage) equipped with a Hamamatsu Orca-Flash 4 camera and a DPSS 491 nm 100 mW and DPSS561 nm 50 mW laser lines under the control of MetaMorph Premier Software (Universal Imaging, USA). CMAC, EGFP and mCherry excitation was performed at 405 nm, 491 nm and 561 nm respectively.

2.5.3 Transmission electron microscopy

Fresh conidia were harvested and washed with sterile water. Conidia (1×10^5) were inoculated on surface sterilized barley leaves for 36 h. The inoculated area of the leaves was cut and fixed in 2.5% glutaraldehyde in 0.1 M phosphate buffer, v/v, pH 7.2. The samples were fixed under vacuum for 15

min at room temperature and incubated overnight at 4 ^{o}C.

The samples were washed three times for 10 min each in 0.1 M phosphate buffer, pH 7.2 and postfixed in osmium tetraoxide (1%, w/v) for three hours. Then wash throughly for three times in 0.1 M phosphate buffer, pH 7.2.

Samples were dehydrated in a graded ethanol series (25%, 50%, 75%, 100%) for 10 min each. Wash twice with propylene oxide for 10 min each time. Infiltrated with propylene oxide-Spurr's resin (1:1) for two hours, and then infiltrated with pure Spurr's resin overnight.

Subsequent embedding and polymerization was carried out in Spurr's resin at 70 ^{o}C overnight in EMS embedded molds (Electron Microscopy Sciences, USA). The samples were sectioned using the Leica Ultracut UCT. The Ultrathin (80nm) sections were mounted on 200 mesh copper grids. Strained with a mixture of 2% uranyl acetate and 2% Reynolds' lead citrate (10 mL for each grid) for 15 min at room temperature and observed under JEM1230 transmission electron microscope (Jeol, Japan) at 120 kV.

2.6 Mass spectrometry

2.6.1 Appressorial extracts and sample preparation

Conidia from WT or the *pks1*-deletion *strain* were harvested and suspended

separately in water to a final concentration of 1×10^5 conidia/ml. Then the individual conidial suspension was inoculated on the 80 x 80 mm glass sheets (100 Deckglaser, Thermo Scientific) for required time. The appressoria and the surrounding fluid/liquid were all collected from the sheets. The suspension was lyophilized and resuspended in methanol. The methanol extract was then filtered and lyophilized again. The extract was then resuspended in methanol.

2.6.2 Mass spectrometry of appressorial extracts

Non-targeted metabolite profiling was conducted by using a Kinetex SB C18 (2.1×100 mm, 1.7 μ) reverse phase column on an Agilent Infinite 1290 UHPLC system (Agilent Technologies) with an ultra-high definition accurate-mass quadrupole time-of-flight (UPLC-QToF) mass spectrometer. The column temperature was set to 45 ℃ and the auto sampler was set to 5 ℃. Solvent A (0.1% formic acid) and solvent B (0.1% formic acid in LC/MS-grade acetonitrile) was used as the mobile phase. The gradient elution was carried out in following steps: 1. 1 min isocratic elution with 1% B; 2. 11-min gradient to 100% B; 3. hold for 13 min in 100% B; 4. 1% B for 16 min for washing and equilibration. The flow rate was kept as 0.3 ml/min, and 5 μl samples were injected. Both positive and negative ESI modes were carried out using the following instrumental parameters: 4000 V capillary

voltage; 20 V and 40 V collision energies; 115 V fragmentor voltage; 350 ℃ sheath gas temperature; 275 ℃ source gas temperature; nebulizer gas flow; 12 l/min sheath gas flow; 40 psi; 12 l/min drying gas flow.

XCMS Online (http://xcmsonline.scripps.edu/) and R package script was used for data alignment, feature extraction.

Chapter III Results

3.1 Background

The filamentous ascomycete *M. oryzae* is the causal agent of rice blast disease, causing 10-40% yield losses worldwide, and has become a model organism to study infection-related morphogenesis and plant-pathogen interaction (Wilson and Talbot, 2009). Conidia of *M. oryzae* differentiate specialized infection structures, termed appressoria, in response to cues from the host surface. The major function of an appressorium is to generate enormous turgor by accumulating high concentrations of compatible solutes, such as glycerol, to physically breach the plant surface (de Jong et al., 1997).

During appressorium development, there is an overall increase in synthesis of several secondary metabolites such as melanin and various families of toxins or effectors of blast disease (Collemare et al., 2008c). Polyketides are predicted to be the major secondary metabolites with various biological functions in pathogenic fungi. However, the functions of such polyketides are still poorly understood in fungi. There are 22 PKSs and 10 PKS-NRPSs (non-ribosomal peptide synthases) hybrids in the *M. oryzae* genome, indicating an abundance of secondary metabolite production therein (Collemare et al., 2008a).

Additional enzymes are required to modify the intermediate compounds that are synthesized by PKSs. Typically, the genes encoding the modifying enzymes and the PKSs are closely localized in the genome, defining a likely co-expressed gene cluster. The polyketide synthase gene cluster sometimes

involves a gene encoding ATP-binding cassette (ABC) transporter with unknown function during the synthesis (Collemare et al., 2008c). One of the ABC transporters in *M. oryzae*, *ABC3*, has been reported to play an essential role for host penetration and *in planta* growth (Sun et al., 2006a). The genomic neighborhood of the *ABC3* locus contains several genes encoding metabolic enzymes including a putative PKS (MGG_04775; which we designated as *PKS1*). The transcription of *PKS1* is highly upregulated during appressorium formation similar to *ABC3* (Soanes et al., 2012). This suggests that Pks1 may be involved in synthesizing an important secondary metabolite required for appressorium development and/or function. It is also likely that Pks1 synthesizes one (or more) of the efflux targets (Patkar et al., 2012) of the Abc3 pump in *M. oryzae*. Therefore, we decided to investigate the role of *PKS1* and the other genes in this important cluster in growth, development and pathogenesis in *M. oryzae*.

3.2 Functional analysis of the PKS1 gene

3.2.1 pks1Δ appressoria are defective in host penetration

Based on primary sequence analysis, we found that Pks1 is an HR-IPKS. Furthermore, gene-deletion analysis, *pks1*Δ mutant, revealed that Pks1 is essential for host penetration during initiation of rice blast.

A PKS encoding gene (*MGG_04775.7*) was found located 4 KB apart from the *ABC3* locus in *M. oryzae*. The coding sequence of *PKS1* in B157 (wild type)

was established by detailed cDNA analysis and 3' RACE based initially on the sequence predicted by the Magnaporthe Comparative Annotation Database at The Broad Institute, USA. The cDNA sequence analysis revealed four introns in the gene and that the ORF encodes a 2258 amino acid polypeptide. The *PKS1* ORF and the deduced protein sequence are shown in Appendix 1. The domain organization of Pks1 (Fig. 3A) revealed the basic PKS domains: AT, KS and ACP, and also the modifying activities: a trio of beta-keto reduction domains (KR, DH, and ER). According to the domain structure, Pks1 can be classified into a PKS subgroup, the Highly-Reducing Iterative PKS (HR-IPKS), which could produce linear and cyclic nonaromatic compounds (Chooi and Tang, 2012b). As an HR-IPKS, Pks1 lacks the releasing domain TE (Fig. 3A). Therefore, an additional releasing enzyme is likely needed for proper Pks1 function.

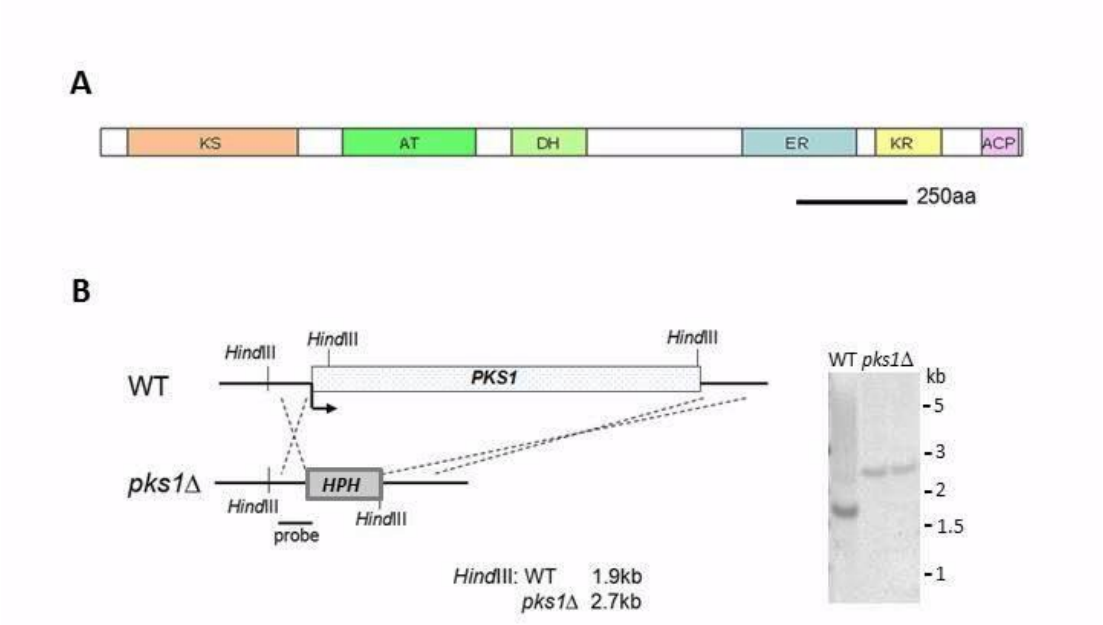

Figure 3 Domain structure of Pks1 and deletion of PKS1 gene. (A) Illustration of the domain structure of Pks1 protein. **(B)** Generation and confirmation of the *pks1*Δ mutant. The schematic shows the generation of *pks1*Δ mutant via replacement of the *PKS1* ORF with the hygromycin resistance cassette *HPH*. The dashed lines indicate the precise sites of homologous recombination that occurred during ATMT. The mutant was confirmed by southern blot analysis, (panel on the right). Genomic DNA from WT or two *pks1*Δ strains was digested by *Hind*III and probed with 1 kb 5'UTR of *PKS1* gene (as shown on the left). Appearance of the 2.7 kb fragment of the mutant and 1.9 kb of the WT indicated that the *HPH* precisely replaced the *PKS1* ORF.

To study the function of *PKS1* during pathogenesis, *pks1*Δ mutant was generated by replacing the entire ORF with the hygromycin resistance cassette in the wild-type B157 strain of *M. oryzae* (Fig. 3B). The deletion was confirmed by southern blot (Fig. 3B) and locus specific PCR. The vegetative growth and colony morphology of the *pks1*Δ mutant were comparable to the wild type on the PA medium (Fig. 4A). As shown in Figure 4B and C, the *pks1*Δ mutant does not have any defects in conidiation and/or appressorium formation.

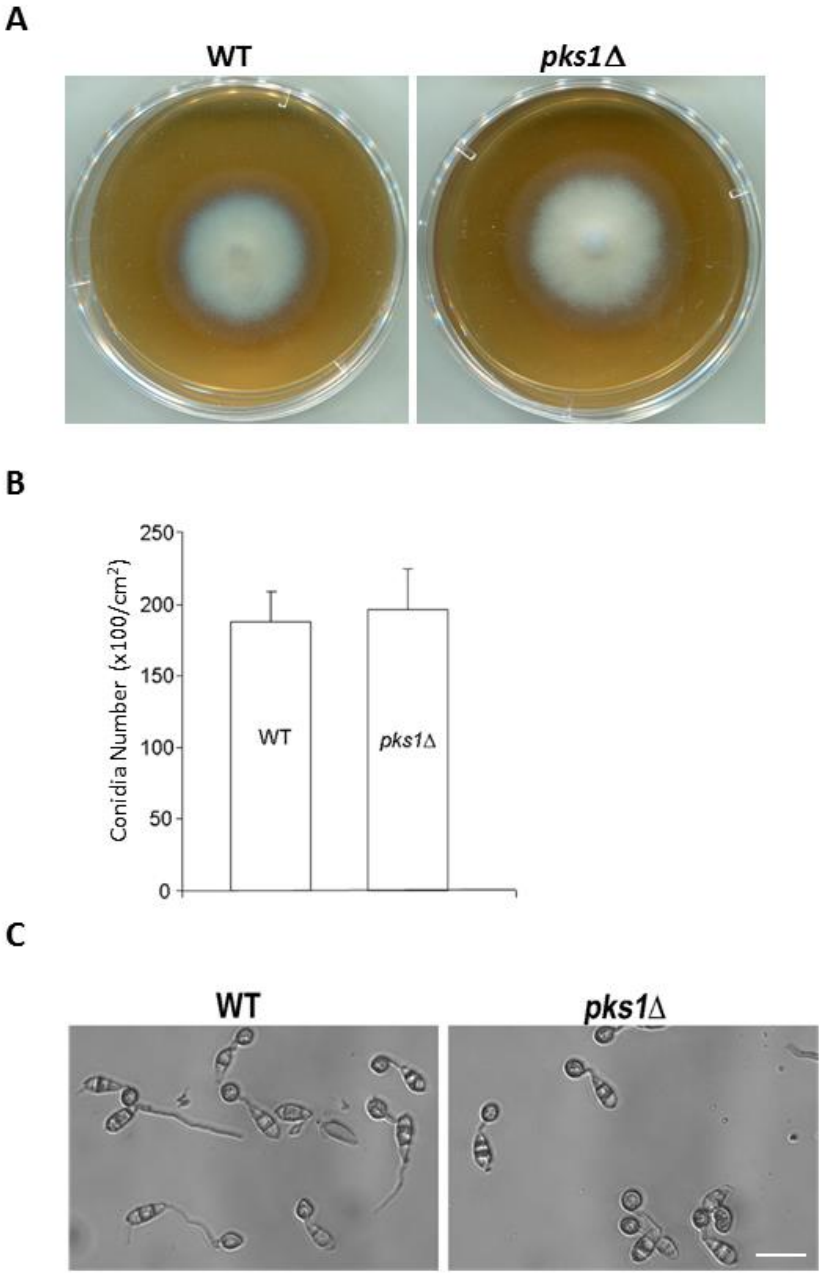

Figure 4 Vegetative growth, conidiation and appressorium formation of *pks1*Δ mutant. (A) Morphology of the WT and *pks1*Δ colonies. The indicated strains were grown on PA medium for 4 days in the dark. **(B)** Bar chart of conidiation assessment. WT and *pks1*Δ mutant were grown on PA medium in the dark for 3 days and exposed to light for 5 days. The error bar represents the standard deviation (SD) of three independent experiments. **(C)** Morphology of the conidia and appressoria of the WT and *pks1*Δ. Images were taken after inoculating conidia on the cover slips for 6 hours. Scale bar = 20μm.

Then we assessed the pathogenicity of the *pks1*Δ mutant. We used conidia to infect rice leaves and barley leaf explants, and the *pks1*Δ mutant showed a complete loss of pathogenesis and failed to cause rice blast disease (Fig. 5A). The non-pathogenic defect of the *pks1*Δ mutant could be suppressed through genetic complementation by expressing the complete *PKS1* locus in *pks1*Δ (Fig. 5A) indicating that the defect is directly associated with the loss of *PKS1* gene. To uncover the reasons for the loss of pathogenicity, we characterized the *pks1*Δ mutant further and found that there were almost no penetration pegs (indicated by aniline blue staining of the callose deposition) formed under the *pks1*Δ appressoria (Fig. 5B) when inoculated on the barley leaves. The penetration ratio of wild type appressoria was 71.0±6.3%, while the ratio of *pks1*Δ mutant was only 0.6±0.6% (Fig. 5C). The *pks1*Δ failed to penetrate the rice sheath or the synthetic PUDO-193 cellophane membrane (Fig. 5D).

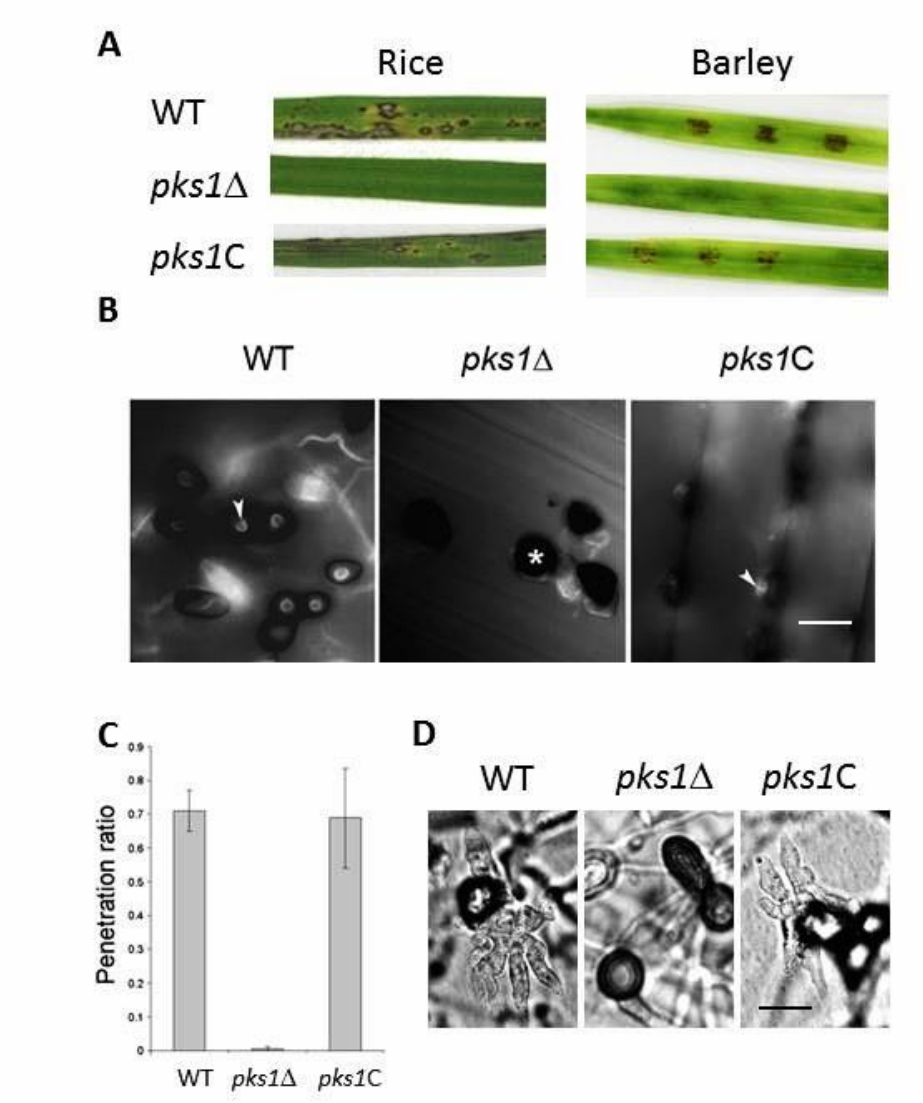

Figure 5 The *pks1*Δ is defective in host penetration. (A) *pks1*Δ mutant is nonpathogenic. Rice seedlings (left) were sprayed with conidial suspension from WT, or *pks1*Δ or the *PKS1* complementary (*pks1*C) strain, and disease symptoms observed after 7 days. Barley leaves were inoculated with 20 μl droplets containing 1000 conidia. Photo was taken 7 dpi. **(B)** Appressorial penetration sites were stained by aniline blue and observed by epifluorescence microscopy. Arrows denote the WT and *pks1*C appressorial penetration sites. Asterisk indicates that *pks1*Δ appressorium failed to penetrate the host. **(C)** Quantitative analysis of the penetration ratios based on the aniline blue staining results. **(D)** Appressorium-based penetration on PUDO membrane. Bulbous invasive hyphae like mycelia were found under WT and *pks1*C appressoria but not *pks1*Δ mutant. Scale bar = 10 μm.

Since the appressoria of *pks1*Δ could not penetrate rice leaves, *in planta* growth of the mutant was investigated by inoculating conidia on rice roots and wounded barley leaves where the appressorium function is not required for the process of root infection or the penetration of wounded/abraded leaves (Sesma and Osbourn, 2004). Interestingly, it seems that the *in planta* growth is not affected by *PKS1* deletion. Both the rice roots and wounded barley leaves displayed blast disease lesions when inoculated with the *pks1*Δ conidia (Fig. 6). This defect differs from the phenotype of *abc3*Δ mutant, which is incapable of host entry and invasive growth. Therefore *ABC3* may not be involved in the Pks1 synthesis pathway, but likely contributes to the transportation of the Pks1 product(s). Taken together, these results suggest that *PKS1* plays an important role in forming a functional appressorium.

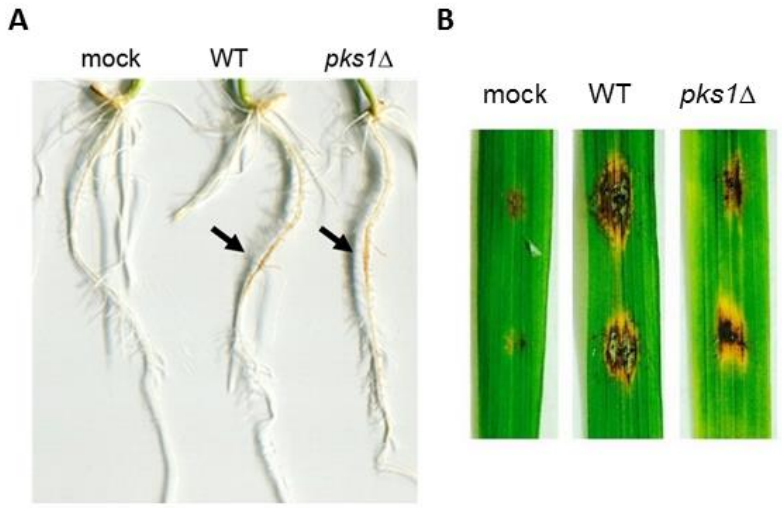

Figure 6 The invasive growth of the *pks1*Δ is normal. (A) Rice roots were inoculated with WT or *pks1*Δ conidia and placed on sterile moist filter paper. Disease lesions were assessed at 7 dpi. Arrows indicate the lesion sites. **(B)** Wounded barley leaves (abraded by needles) were inoculated with the mycelia on PA agar plugs for 7 days.

3.2.2 Pks1-GFP accumulates in the appressorium

We generated a Pks1-GFP strain to investigate the expression and cellular localization of Pks1. The eGFP coding sequence was fused in frame into the C-terminus of the *PKS1* ORF. The strain carrying Pks1-GFP shows no defects in penetration and pathogenesis, indicating that the Pks1-GFP is fully functional. The Pks1-GFP is highly expressed in the appressorium, but has a very low expression level during other growth stages. As shown in Figure 7A, Pks1-GFP mostly localizes to the appressorial cytoplasm at 4 - 8 hours after conidial germination. While in mature appressoria (20 - 30 hpi), the Pks1-GFP signal appeared reduced and a large proportion of the Pks1-GFP was found in the vacuolar compartment. Co-localization of Pks1-GFP and vacuoles was confirmed by CMAC staining (Fig. 7C). Pks1-GFP is likely excluded from the nuclei as judged by the lack of overlap with the histone hH1-RFP (Fig. 7B). The high expression level of *PKS1* in the appressorium is consistent with previous transcriptomic analyses (Oh et al., 2008; Soanes et al., 2012).

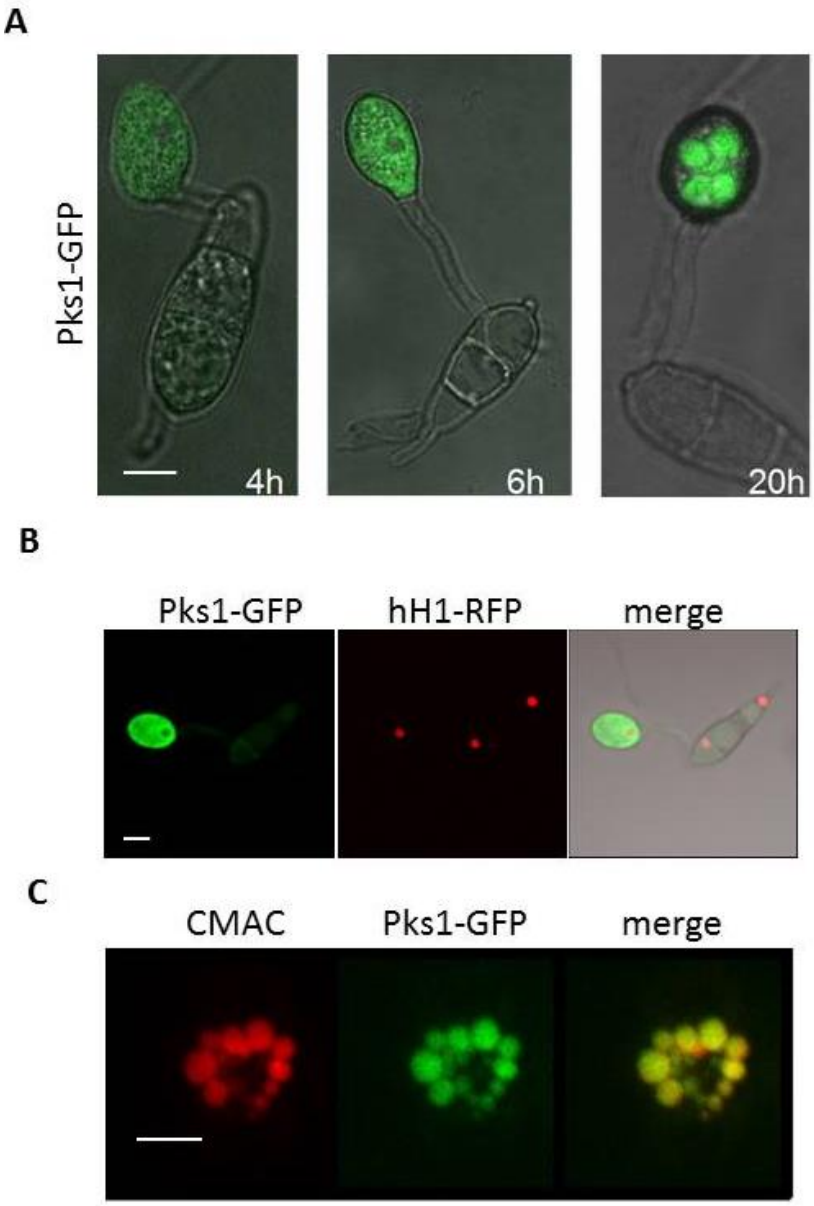

Figure 7 Subcellular localization of Pks1-GFP. (A) Pks1-GFP expresses strongly in the appressorium. Conidia of Pks1-GFP strain were inoculated on the cover slips. Images were taken at different time points post appressorium development. **(B)** Pks1-GFP is excluded from nuclei. hH1-RFP was used as a nuclear marker. Pks1-GFP and hH1-RFP co-expressing strain was observed after 6 hpi. **(C)** Pks1-GFP localizes to the vacuoles in mature appressoria. Vacuoles in the mature appressorium (20 hpi) of the Pks1-GFP strain were stained with CMAC (pseudocolored red). Scale bar = 5 μm.

3.2.2 Melanin deposition is abnormal in *pks1*Δ appressoria

The appressorial turgor was judged indirectly by cytorrhysis assays using exogenously added glycerol (de Jong et al., 1997). As shown in Figure 8A, the ratio of collapsed appressoria in *pks1*Δ is significantly lower than that in wild type, which indicated that the mutant appressoria are more resistant to external glycerol. Transmission electron microscopy (TEM) was used to observe the internal structures of the mature appressoria (36 hpi). In the wild-type strain, an electron dense homogeneous melanin layer (Fig. 8B, arrow head) was evident between the plasma membrane and the cell wall (Fig. 8B, asterisk). However, the melanin layer formed in the *pks1*Δ appressoria was significantly thicker and uneven compared to the wild type (Fig. 8B). The average thickness of the mutant melanin layer (223±4 nm) is almost two fold higher than the wild-type melanin layer (113±17 nm) (Fig. 8C). These data suggest that *PKS1* is essential for proper biosynthesis and deposition of melanin, and for maintaining the appressorial turgor during pathogenic development in *M. oryzae*.

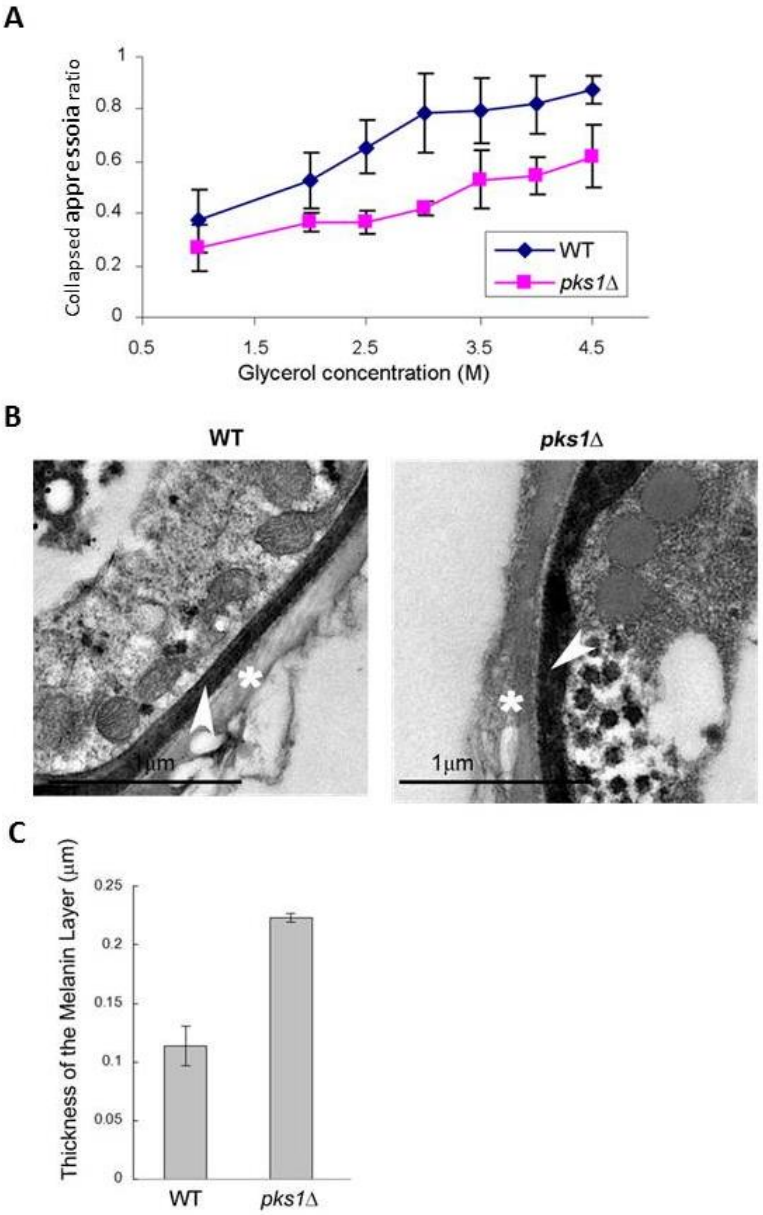

Figure 8 Loss of *PKS1* leads to uneven and aberrant melanization of appressoria in *M. oryzae*. (A) Appressorial cytorrhysis assay was conducted in wild type and *pks1*Δ. Indicated concentration of glycerol was added to the appressoria, which had been formed for 40 h on the inductive surface. The collapsed appressoria were counted strictly within 10 min after glycerol addition. Three tests were carried out independently. Error bar = SD. **(B)** Transmission electron micrographs showing the outer layer of the appressoria which were developed on barley leaf surface at 36 hpi. Asterisks mark cell wall of the appressoria. Arrowheads indicate the position of the melanin layer. **(C)** Average thickness (±SD) of WT and *pks1*Δ melanin layer was quantified based on the TEM images. At least 20 appressoria were measured for each strain. P<0.001.

To gain further insight into the deregulated melanin synthesis/deposition in *pks1*Δ appressoria, the transcription levels of the melanin synthesis genes *ALB1* and *BUF1* was estimated by Real-Time PCR (Fig. 9A). At 6 hpi, the transcript levels of *ABL1* and *BUF1* were comparable between wild type and *pks1*Δ mutant. Whereas, the *ABL1* mRNA level was higher in the mutant appressoria at 22 hpi. We also conducted a semi-quantitative reverse transcription PCR, which further confirmed the aforementioned results. The transcription level of *ALB1* was likewise higher in the mutant compared to the wild type at 22 hpi (Fig. 9B). The deletion of *PKS1* did not affect the expression of two other PKSs, *MGG_08285* and *MGG_15100,* in *M. oryzae* (Fig. 9B) suggesting that *PKS1* specifically affects the *ALB1* transcription but not the other PKSs. In addition, we observed some dark granules clustered in the vicinity of the aberrant melanin layer in the *pks1*Δ appressoria but not in wild type (Fig. 8B). We infer that melanin biosynthesis and deposition is deregulated upon loss of *PKS1* activity during appressorial maturation in *M. oryzae*.

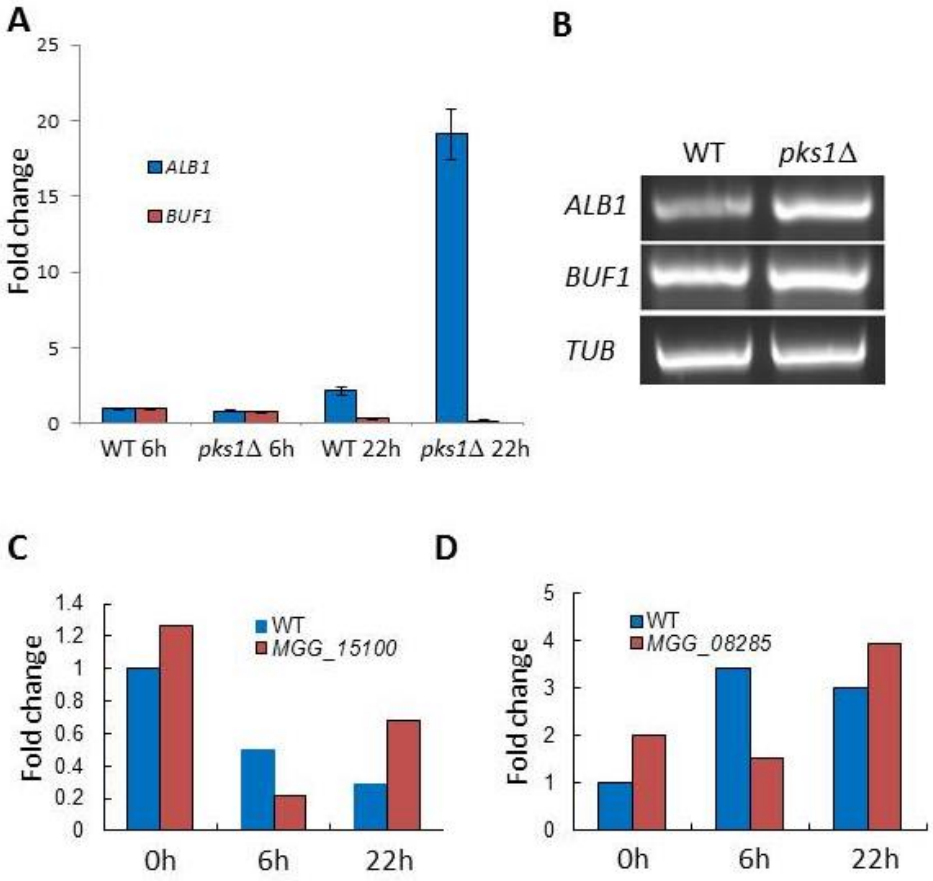

Figure 9 Transcription level of *ALB1* is upregulated in the mature *pks1*Δ appressorium. (A) Real-time RTPCR was carried out using total RNA from wild type or *pks1*Δ appressoria. *TUBULIN* (*MGG_00604.6*) was used as internal reference. Transcription level of *ALB1* and *BUF1* were assessed at 6 hpi and 22 hpi during appressorium development. Error bar = SD **(B)** Semi-quantitative reverse transcriptase PCR was performed by using the same 22 hpi appressoria from WT and *pks1*Δ. **(C-D)** Real time RTPCR was performed to test the transcription level of *MGG_15100* and *MGG_08285* in appressoria at the indicated developmental stages. *TUBULIN* was used as an internal control.

To further investigate whether loss of Pks1 leads to excess DHN melanin accumulation and to test whether reduced melanin levels would suppress pathogenic defects therein, we treated the WT or mutant appressoria with tricyclazole, which is a specific inhibitor of DHN melanin synthesis (Woloshuk et al., 1980). As shown in Figure 10A, tricyclazole treatment significantly reduced the deposition of melanin in wild-type and mutant appressoria. The TEM analysis further revealed that the residual melanin layer in the tricyclazole-treated mutant is thinner than in the wild type (Fig. 10B), suggesting that Pks1 might be involved in the synthesis of one or more of the components in the melanin layer which could not be inhibited by tricyclazole treatment. In addition, simply reducing the melanin deposition via tricyclazole could not suppress the host penetration defects in the *pks1*Δ mutant (Fig. 11). Different concentration of tricyclazole was added to both wild type and *pks1*Δ conidia before inoculating on barley leaves. We tried 100 pg/ml, 10 pg/ml, 1 pg/ml and 0.1 pg/ml tricyclazole, and found that 1 pg/ml is the lowest concentration needed to inhibit the penetration in WT appressoria. As shown in Figure 11, *pks1*Δ could not induce lesion formation even when the concentration of tricyclazole (0.1 pg/ml) was not high enough to inhibit the wild type strain to penetrate. As tricyclazole may affect the other protein functions in the appressoria, a *pks1*Δ *alb1*Δ double deletion strain was generated. The double deletion strain behaved like the *alb1*Δ

mutant and failed to form melanized and functional appressoria (Fig. 11). Therefore, the thickened and aberrant melanin layer in the *pks1*Δ mutant is likely not the direct cause of the non-functional appressoria.

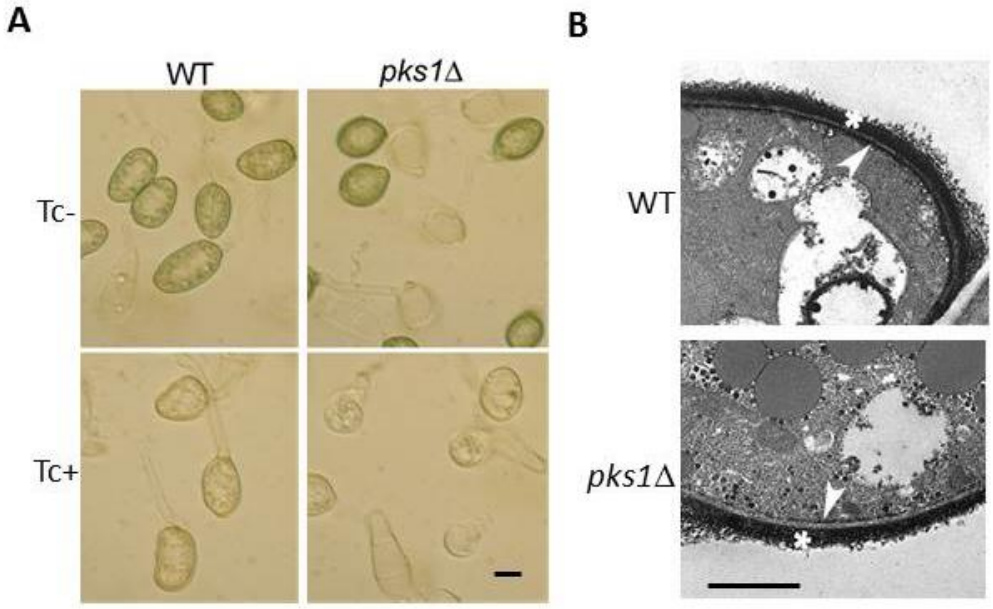

Figure 10 Tricyclazole (Tc) inhibits melanin layer formation in *pks1*Δ appressoria. (A) Morphological changes in the appressoria upon treatment with tricyclazole. Conidia of WT or *pks1*Δ were inoculated with or without 100 pg/ml tricyclazole. The appressoria formed at 24 hpi were transparent when tricyclazole was added. Scale bar = 4 μm. **(B)** TEM images of the Tc-treated appressoria. Arrowheads point to the residual melanin deposits. Asterisks indicate the cell wall in each instance. Scale bar = 1 μm.

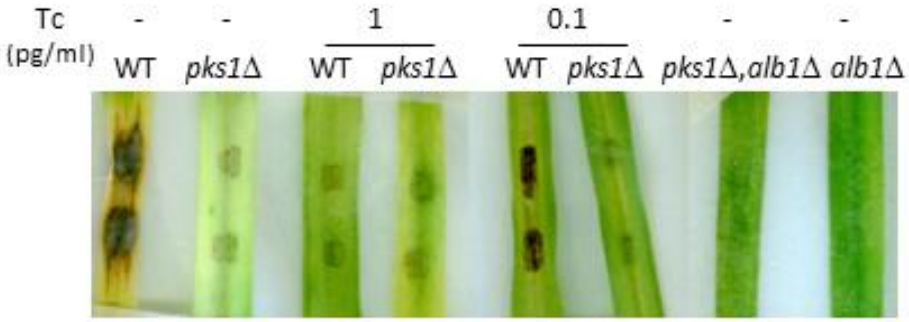

Figure 11 Host penetration and infection related defects in *pks1*Δ mutant could not be suppressed by reducing melanin synthesis. Barley leaves were inoculated with conidia (5000 conidia per droplet) of WT, *pks1*Δ, *pks1*Δ *alb1*Δ double deletion mutant or *alb1*Δ for 7 days. Low concentration of Tc was added to the indicated conidial suspensions. 1 pg/ml Tc inhibited the appressorial penetration in WT, but 0.1 pg/ml Tc could not inhibit the lesion formation in WT. However suboptimal (0.1 pg/ml) levels of Tc could not rescue the *pks1*Δ defect. No trace of fungal material can be seen on the barley leaves inoculated with *pks1*Δ *alb1*Δ double mutant or the *alb1*Δ since such mutants are completely colorless or albino.

3.2.5 Vacuolar localization of Pks1-GFP is affected by melanin synthesis

To find out if melanin synthesis affects Pks1 expression, we deleted *ALB1* and *BUF1* in Pks1-GFP strain. Interestingly, we found out that the vacuolar localization of Pks1-GFP is affected upon disruption of melanin synthesis. When the melanin synthesis inhibitor tricyclazole was added or *ALB1* and *BUF1* were deleted, the Pks1-GFP predominantly localized in the cytosol of the appressorium at 20-30 hpi and the signal was much stronger than in the WT control (Fig. 12). This result suggests that aberrant melanin synthesis or the resultant morphogenesis defects could indirectly affect the Pks1 synthesis/homeostasis and inhibit the Pks1 degradation. Likewise, the trafficking of Pks1 to the vacuoles is important for the function of Pks1 or its downstream modification enzymes.

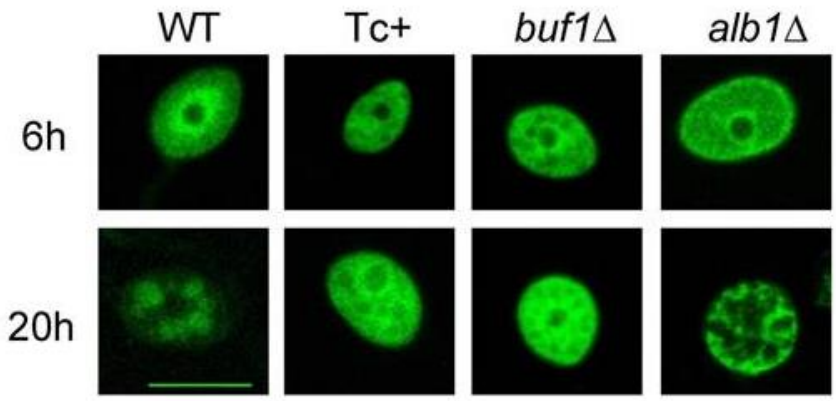

Figure 12 Melanin deficiency or the resultant defects thereof affect Pks1-GFP localization. Pks1-GFP localization was checked in appressoria of WT (untreated), Tc-treated WT, *buf1*Δ or *alb1*Δ. Confocal microscopy analysis was carried out at two time point 6 hpi and 20 hpi. Scale bar = 10 μm.

3.2.5 Deletion of *PKS1* affects pore wall overlay

We also observed the appressorium pore region by TEM (Fig. 13A). In wild-type appressoria, there is a pore wall overlay formed inside the melanin layer (Bourett and Howard, 1990). However, this overlay was not evident in the *pks1*Δ appressoria. Next, we removed the appressoria from the cover slip by sonication and examined the attachment zones/appressorial residues (Bourett and Howard, 1992) using a bright field microscope. The *pks1*Δ mutant appressoria are likely defective in proper attachment and left significantly less residues than the wild type (Fig. 13B). This further suggests that the pore wall overlay is lower or missing underneath the mutant appressoria and the overlay formation either requires the proper and timely deposition of melanin and/or the polyketide product(s) synthesized by Pks1 activity

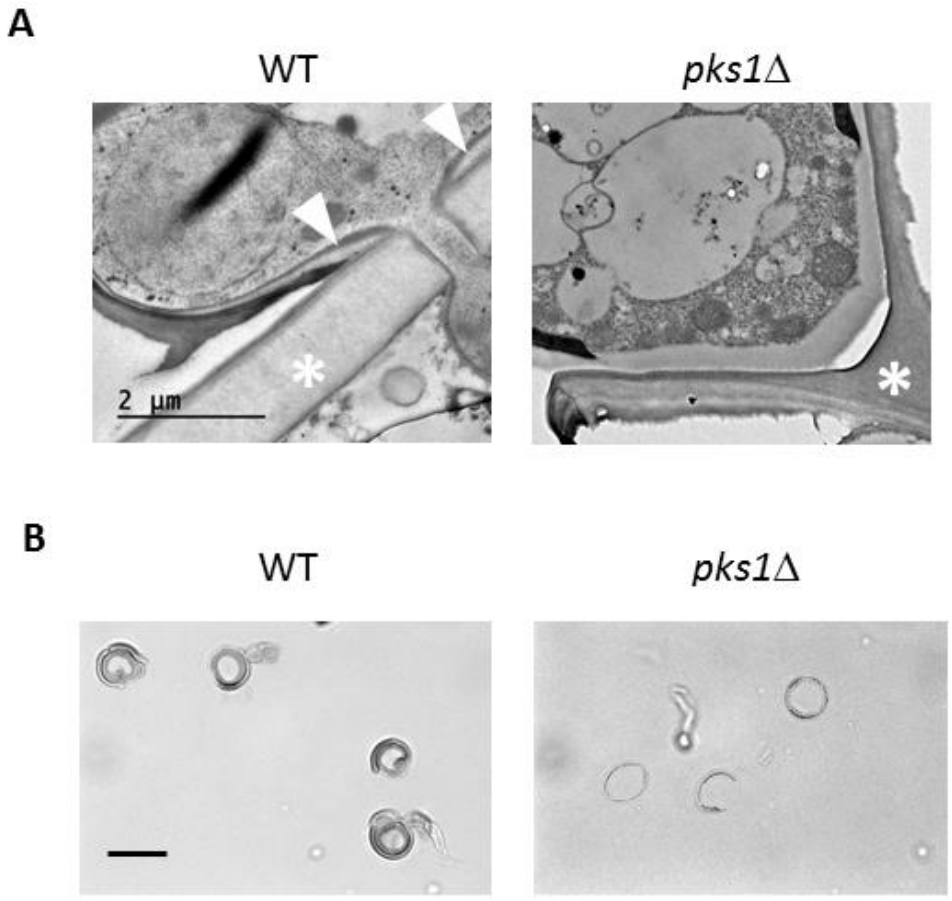

Figure 13 Pore wall overlay is missing in the *pks1*Δ mutant appressorium. (A) TEM images of the base of the appressoria. Pore wall overlay is denoted by arrowheads. Asterisks indicate the plant surface where the appressoria are attached to host cell wall. **(B)** Appressorial residues/remnants on the cover slip post sonication. Conidia were inoculated on the cover slips for 30 h and the cover slips were sonicated in water. Scale bar = 10 µm.

3.2.6 Pks1 function and melanin deposition are essential for proper septin ring assembly in the appressorium

To further understand the role of Pks1 in the organization of penetration zone, we deleted *PKS1* in the Sep5-GFP strain. Septins, including Sep5, regulate penetration peg formation in *M. oryzae* by forming a septin organized torroidal F-actin structure at the appressorium pore position (Dagdas et al., 2012). As shown in Figure 14A, the *pks1*Δ appressoria form aberrant septin structures which lack the central penetration pore structures. Interestingly, inhibition of the melanin synthesis likewise disrupts proper septin ring formation, which suggests that both the Pks1 biosynthetic pathway and/or the proper melanin synthesis are essential for the septin ring assembly and demarcation of penetration zone/pore. Interestingly, the average diameter of the septin disk is significantly larger in the mutant appressoria (6.85 ±0.74 μm) than in the WT appressoria (5.52 ±0.66 μm) (Fig. 14A and B).

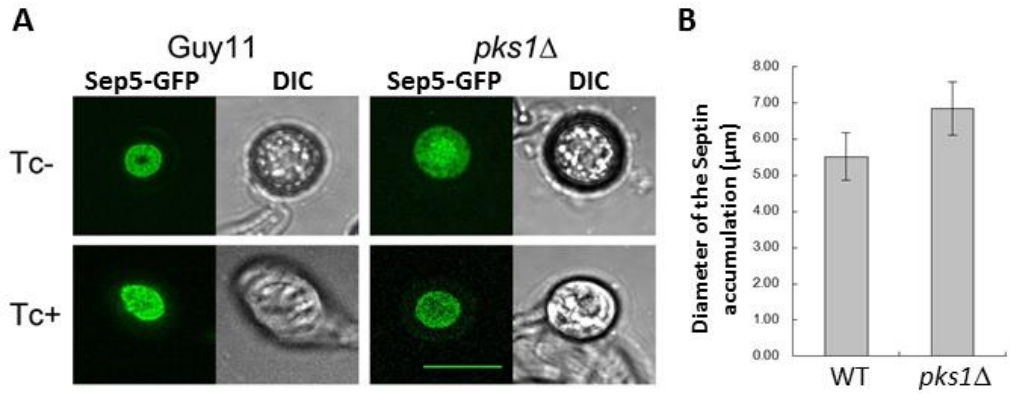

Figure 14 *PKS1* and proper melanization are required for septin ring formation. (A) Sep5-GFP indicates the septin structure in the appressoria. In the wild type, a septin ring structure is formed at the base of the mature appressorium. While in the *pks1*Δ mutant, Sep5-GFP forms a large disorganized structure at the base of the appressorium without a proper pore. When Tc was added to the appressoria (lower panel), neither WT nor the mutant formed the septin ring structures. Scale bar = 10 μm. **(B)** Quantification of the average diameters (±SD) of the septin accumulation. Appressorial diameter was measured using ImageJ and based on the confocal images. More than 50 appressoria were measured for each treatment or experiment ($P<0.001$).

3.2.7 The reducing domains are essential for *PKS1* function

There are three reducing domains, DH, ER and KR, in Pks1. The chain extension of the Pks1 product is likely determined by optional usage of these domains. Deactivation of the reducing domains could probably deactivate the Pks1 protein or lead to different products. We made two Pks1 mutants DH-ERΔ and KRmut that lack functional reducing domains as shown in Figure 15A. DH and ER domains are deleted in the DH-ERΔ. We mutated the KR domain by changing YXXXN catalytic signature to LXXXR (Keatinge-Clay and Stroud, 2006).

These two mutants behaved exactly like the *pks1*Δ mutant as they showed normal vegetative growth, conidiation and appressorium formation but failed to penetrate the host as judged by aniline blue staining of callose deposits (Fig. 15B and C). The mature appressoria of the DH-ERΔ or KRmut appeared to be darker than the WT appressoria, which suggests that the melanin layer was also thickened and aberrant in these two mutants as in *pks1*Δ (Fig. 15C). We conclude that the reducing domains of Pks1 are essential for the proper function of this important polyketide synthase in *M. oryzae*.

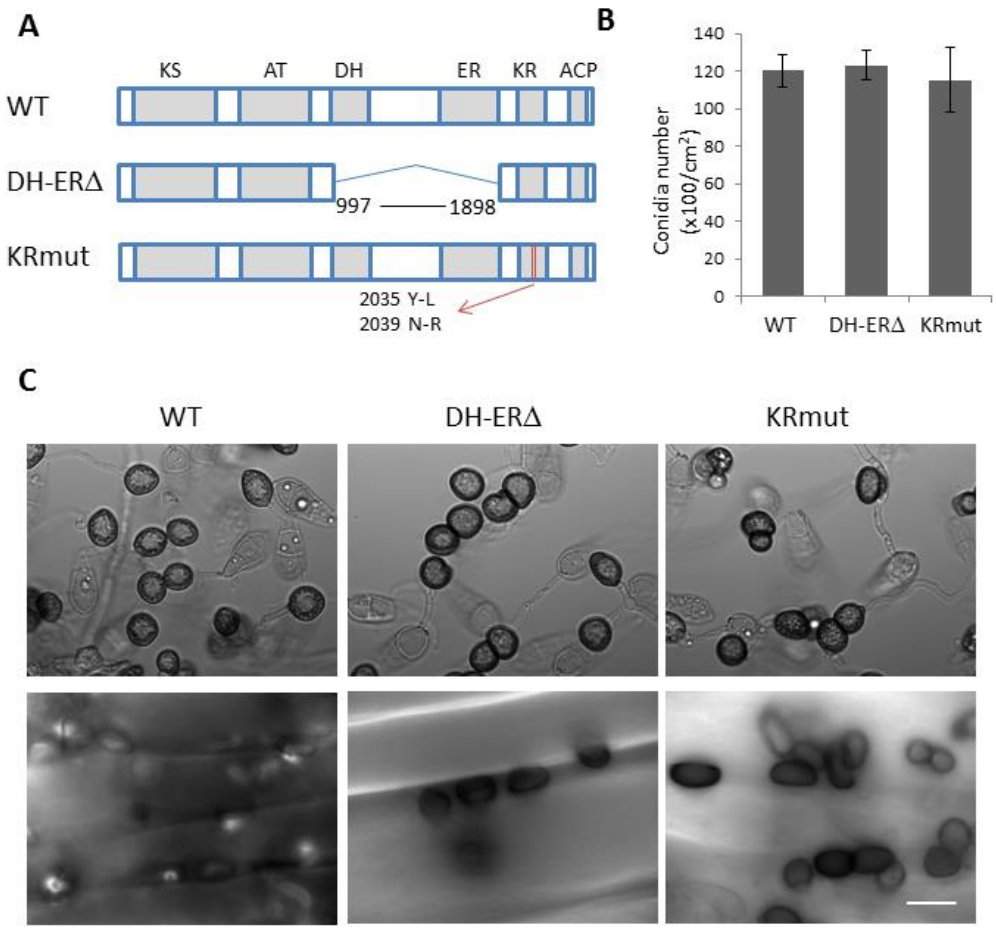

Figure 15 The DH-ER and KR domains are essential for the Pks1 function. (A) Schematic representation of the domain structure of DH-ERΔ and KRmut derivatives of Pks1. Numbers indicate the amino acid sequence. **(B)** Quantification of the conidia produced by the WT, DH-ERΔ and KRmut. There were no significant differences between WT, DH-ERΔ and KRmut. Three independent experiments were conducted. Error bar = SD. **(C)** Appressorial morphology (upper panel) and penetration assessment (lower panel, aniline blue staining assay) of the WT, DH-ERΔ and KRmut. Images were taken at 28 hpi. Scale bar = 10 μm.

3.3 Functional analysis of the cluster of co-expressed genes

The biosynthetic genes are usually clustered in the genome and display the same expression pattern (Keller et al., 2005), so we analyzed the transcription levels of the genes near *PKS1* based on previous genome-wide profiling (Soanes et al., 2012). We found out that only the transcription of *ABC3*, *MGG_04774*, *MGG_04776* and *MGG_13763* are upregulated during appressorium development (Table 3) (Soanes et al., 2012). The co-regulated genes around *PKS1* and *ABM* (*MGG_04777*) (Patkar et al., 2015) are shown in Figure 16. The *ABC3* transporter has been shown to be important for the efflux of steroidal glycoside ATS, and for host penetration (Patkar et al., 2012; Sun et al., 2006b). *MGG_04774* encodes a predicted esterase or serine hydrolase (hereafter referred to as *FSH1*) and *MGG_13763* encodes a predicted glycerate kinase (referred as *GK1*).

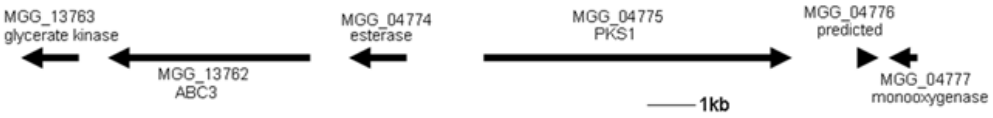

Figure 16 ORFs predicted near the *PKS1* locus in Magnaporthe genome.

Table 3 Transcription levels of the genes during appressorium development*

Gene	Annotation	0h	6h	16h
FSH1	esterase_lipase family	0.65	273	42
PKS1	polyketide synthase	15	12334	2013
MGG_04776	predicted protein	0.46	4	18
ABC3	multidrug resistance protein 3	40	1144	356
GK1	glycerate kinase	0.65	81	63

*Data was collected from http://cogeme.ex.ac.uk/supersage/ (Soanes et al., 2012).

3.3.1 *FSH1* and *ABC3* are functionally related to *PKS1*

To study their Pks1-related functions (if any), gene deletion analysis was carried out for *FSH1* and *GK1*. The *fsh1*Δ mutant showed a nonpathogenic phenotype (Fig. 17A). Similar to *pks1*Δ mutant, *fsh1*Δ could infect the rice root (Fig. 17B), but it was incapable of appressoria-mediated penetration of the host leaves, a defect reminiscent of the *ABC3* or *PKS1* deletion mutant (Fig. 17B). We created a genetic complementation strain (*fsh1*C) by introducing the *FSH1* gene including 1 kb flanks into the *fsh1*Δ mutant. The *fsh1*C strain completely suppressed the host penetration defects of the *fsh1*Δ mutant (Fig. 17 A and C).

The *GK1* deletion mutant shows no such defect and had normal growth and pathogenesis (data not shown). This suggests that *FSH1* and *ABC3*, but not *GK1* may be involved in this Pks1 related biosynthetic pathway, and this gene cluster is very important for appressorium-mediated host penetration in *M. oryzae*.

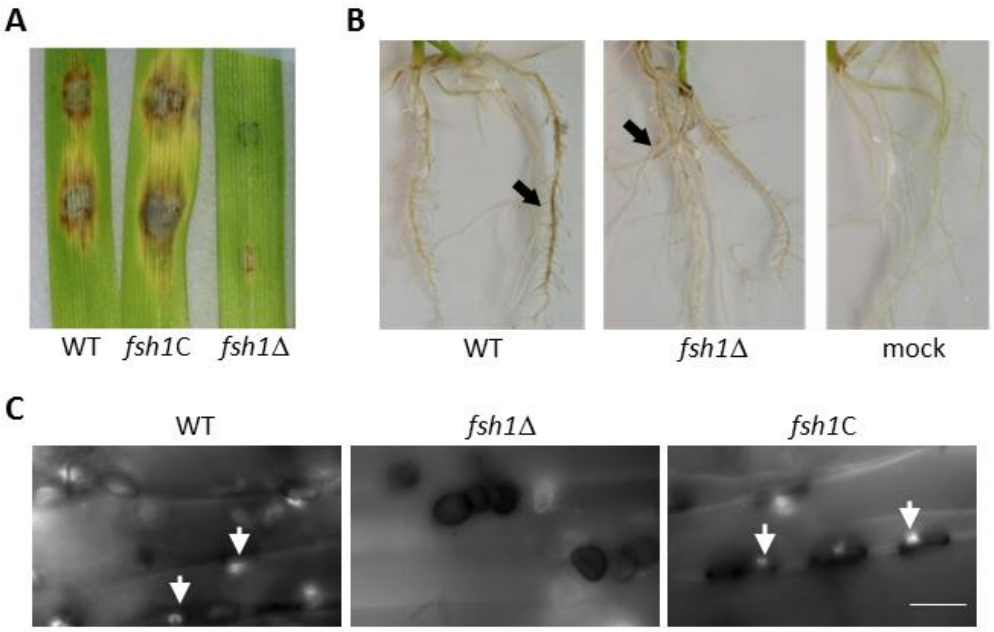

Figure 17 *FSH1* deletion mutant is defective in host penetration and pathogenesis. (A) Barley leaves were inoculated independently with 1000 conidia each of WT, or complemented *fsh1*Δ (*fsh1*C), or *fsh1*Δ. Photo was taken 7 days post inoculation. **(B)** Rice roots were inoculated with WT or *fsh1*Δ conidia on sterile filter paper. Disease lesions were assessed 7 days after inoculation. Arrows indicate the necrosis/lesion sites. **(C)** Appressorial penetration sites were stained by aniline blue and observed by epifluorescence microscope. Arrows denote the host penetration sites in WT and *fsh1*C. Scale bar = 10 μm.

To further confirm their relationship, *ABC3* and *FSH1* were deleted in the Pks1-GFP background. As can be seen in Figure 18, deletion of the *FSH1* and *ABC3* affect the Pks1-GFP expression pattern. At 20 hpi, the Pks1-GFP still accumulated in the cytoplasm of the appressorium in the *fsh1*Δ and *abc3*Δ mutant. The degradation of Pks1-GFP is likely inhibited upon loss of Fsh1 or Abc3, similar to the tricyclazole treatment (loss of melanin) during appressorium formation. As the *abc3*Δ mutant accumulated an excess digoxin-like efflux substrate ATS, we assessed how Pks1-GFP responds to increased accumulation of such cytotoxic moeity. However, addition of a high concentration of digoxin (200 μM) did not affect the translocation of Pks1-GFP, which indicated that accumulation of ATS is likely not the reason why deletion of *ABC3* inhibits the vacuolar localization of Pks1. Thus, Abc3 may be responsible for the transportation/efflux of other compounds in the Pks1 pathway.

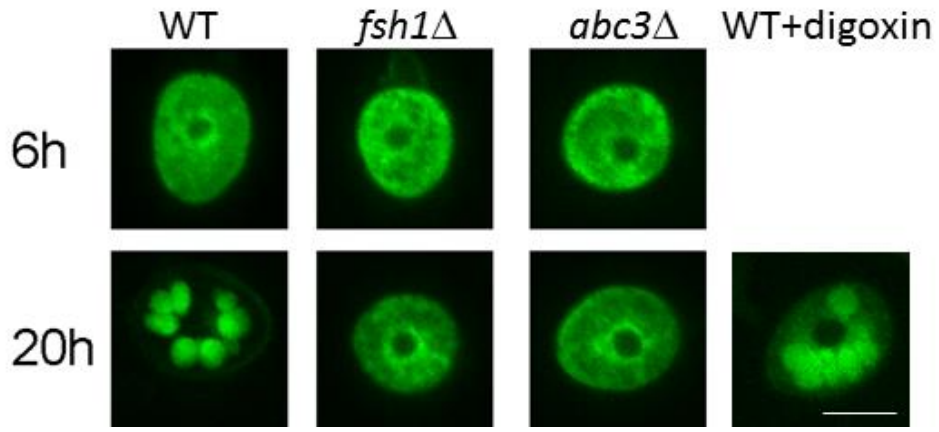

Figure 18 Loss of *FSH1* or *ABC3* affects Pks1-GFP localization. Confocal microscopy of Pks1-GFP in WT, *fsh1*Δ, *abc3*Δ or WT treated with digoxin. Digoxin (200 μM) was added at 5 hpi to Pks1-GFP appressoria. Scale bar = 5 μm.

3.3.2 Phenotypic defects of *fsh1*Δ differ from those shown by *pks1*Δ.

We investigated the defects of the *fsh1*Δ mutant to assess the similarities with *pks1*Δ mutant. Firstly, we observed the melanin layer by TEM. The thickness of the melanin layer in *fsh1*Δ was comparable to the WT, but the mutant layer was not as uniformly distributed as the WT melanin. Like the *pks1*Δ, there was no pore wall overlay in the *fsh1*Δ appressoria (Fig. 19A). The cytorrhysis assay showed that more *fsh1*Δ appressoria collapsed in 1 M glycerol, which suggested the melanin layer in *fsh1*Δ in appressoria may not be as strong as the WT melanin layer (Fig. 19B). This result showed that only deletion of *PKS1* promotes excess melanization, and that proper deposition of the melanin layer requires both Pks1 and Fsh1. Next, we deleted *FSH1* in Sep5-GFP strain and assessed the septin ring formation. Similar to *pks1*Δ mutant, the septin accumulation in *fsh1*Δ was disrupted (Fig. 19C), and the diameter of the mutant disk (6.94±0.63 μm) was comparable to the *pks1*Δ mutant (6.85±0.74 μm) and was significantly larger than in WT (5.52±0.66 μm, $P<0.01$).

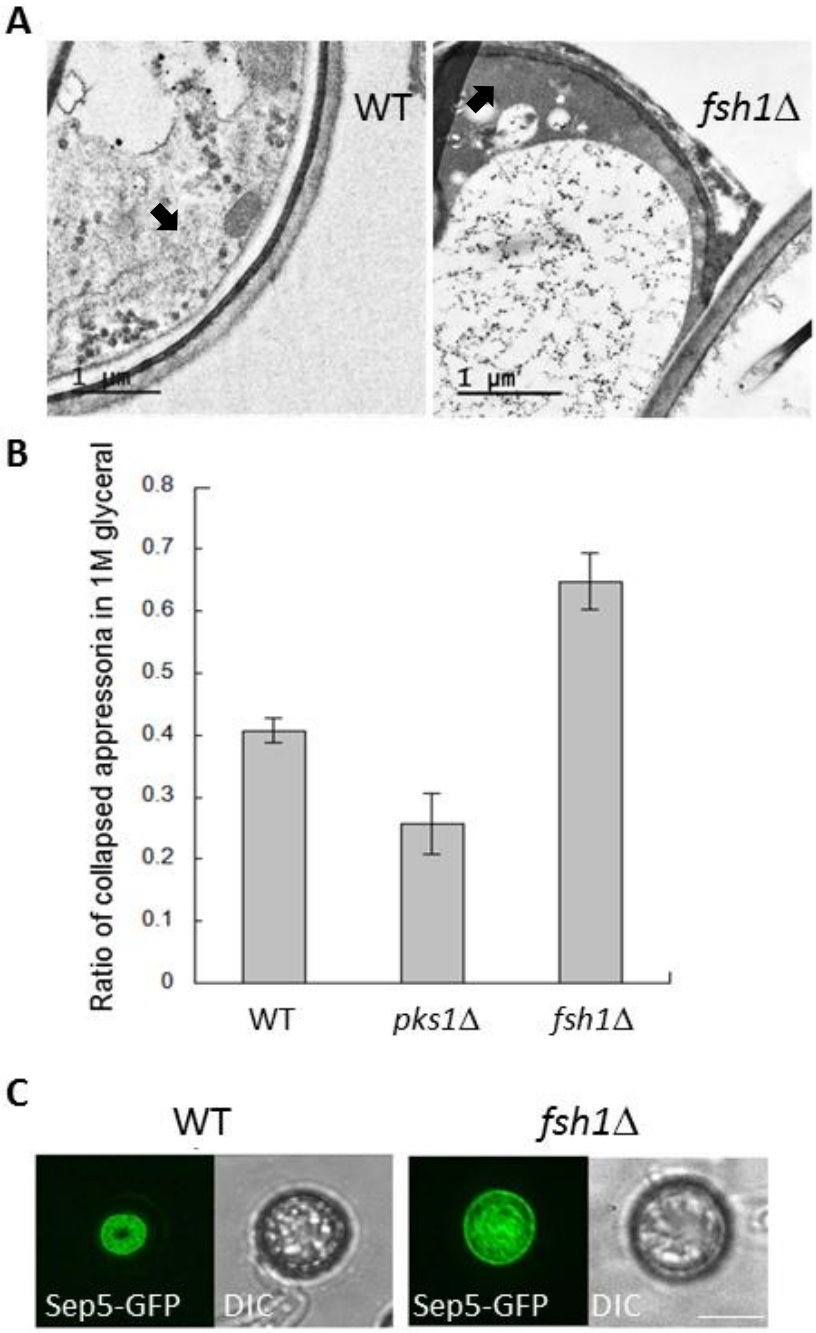

Figure 19 Melanin deposition and septin ring assembly are affected upon *FSH1* deletion. (A) TEM of the WT and *fsh1*Δ appressoria. Arrows indicate the melanin layer. **(B)** Appressorial cytorrhysis assay of the WT, *pks1*Δ or *fsh1*Δ by incubating the appressoria in 1 M external glycerol. 40.7±2.0% WT appressoria, 25.6±5.9% *pks1*Δ appressoria and 64.8±4.5% *fsh1*Δ appressoria collapsed after a 10 min incubation. Error bar = SD. **(C)** Confocal images of the Sep5-GFP in WT and *fsh1*Δ appressoria. Scale bar = 5 μm.

3.3.3 Fsh1 is mainly functional in the appressorium

We also studied the subcellular localization of Fsh1-mCherry in the Pks1-GFP background. Based on the transcription levels, the Fsh1-mCherry is primarily expressed during appressorium differentiation. However, the expression pattern of *FSH1* is different from *PKS1*. The Fsh1-mCherry signal was undetectable until 10-12 hpi, and the protein primarily localized to the vacuolar structures (Fig. 20A). Thus, Fsh1-mCherry co-localizes with Pks1-GFP during or upon translocation to the vacuoles at 20 hpi. Deletion of *PKS1* or inhibition of melanin synthesis could not affect the vacuolar localization of Fsh1-mCherry (Fig. 20B). This suggests that Fsh1 functions in the vacuoles after Pks1 is expressed, and its subcellular localization is independent of the *PKS1* product(s) or of melanin synthesis.

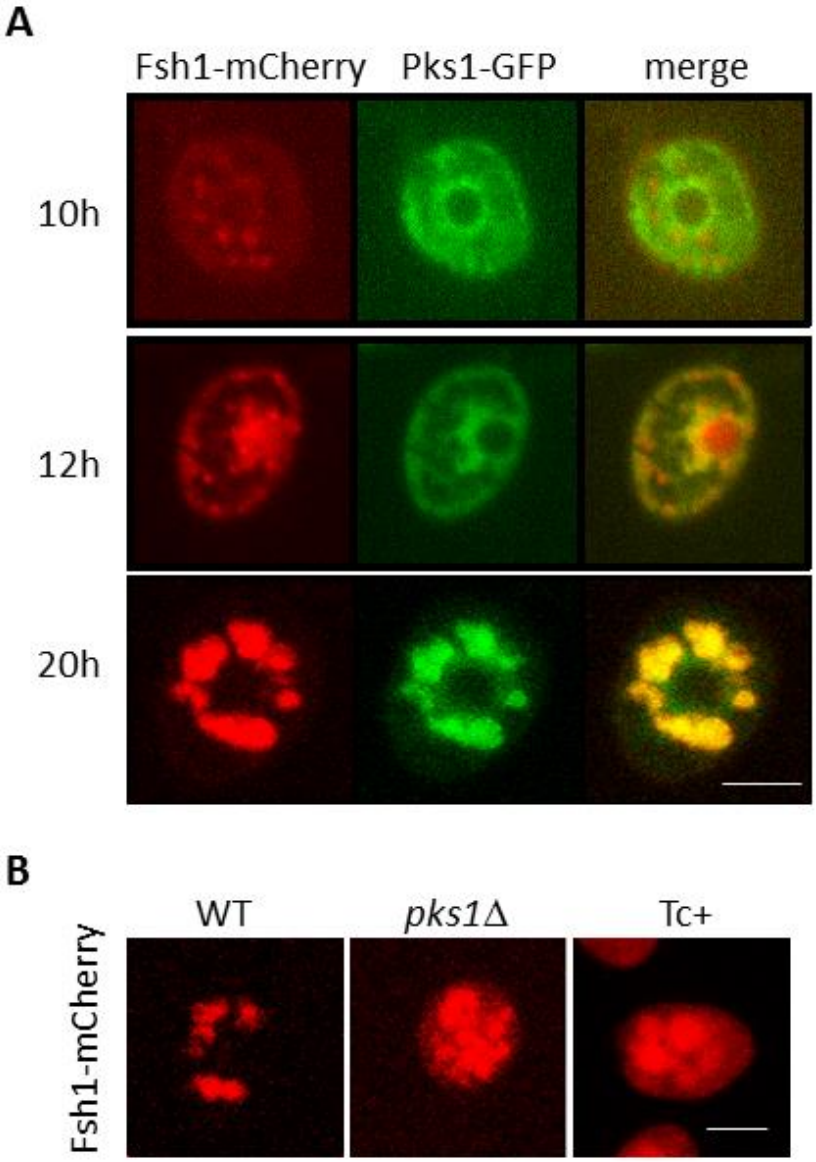

Figure 20 Subcellular localization of Fsh1-mCherry. (A) Confocal microscopy of the Fsh1-mCherry Pks1-GFP dual-tagged strain. Scale bar = 5 μm. **(B)** Confocal microscopy of the Fsh1-mCherry in WT, *pks1*Δ or in WT treated with 100ng/ml tricyclazole. Images were taken at 20 hpi. Scale bar = 5 μm.

To check if Fsh1 interacted with Pks1, Co-IP was conducted using TrpC-pro:Pks1-GFP and TrpC-pro:Fsh1-mCherry co-expressed strain. In this strain, the expression of Pks1-GFP and Fsh1-mCherry fusion protein was driven by the constitutive TrpC promoter in *M. oryzae*. So Pks1-GFP and Fsh1-mCherry proteins were over-expressed in the mycelia. TrpC-pro:Pks1-GFP and TrpC-pro:Fsh1-mCherry co-expressed strain does not have any defects in vegetative growth, but its appressoria failed to penetrate into the host, probably due to the deceased expression levels of Pks1-GFP in the appressoria. We used RFP-Trap (Chromo Tek GmbH, Germany) to pull down the Fsh1-mCherry protein and used α-GFP antibody to detect if any Pks1-GFP was immunoprecipitated together with Fsh1-mCherry. As shown in Figure 21B, we could not detect any Pks1-GFP protein, which indicates that Pks1-GFP and Fsh1-mCherry likely do not interact physically with each other.

Interestingly, we observed an abnormal vacuolar morphology and aggregation in the *pks1*Δ and *fsh1*Δ mutant (Fig. 22). The vacuoles are small and tend to aggregate together in the mutant appressoria. However, other organelles, including peroxisomes, mitochondria and lipid bodies, do not have any morphology changes in the *pks1*Δ mutant (data not shown), which implicated the importance of vacuoles for Pks1 mediated biosynthesis or trafficking.

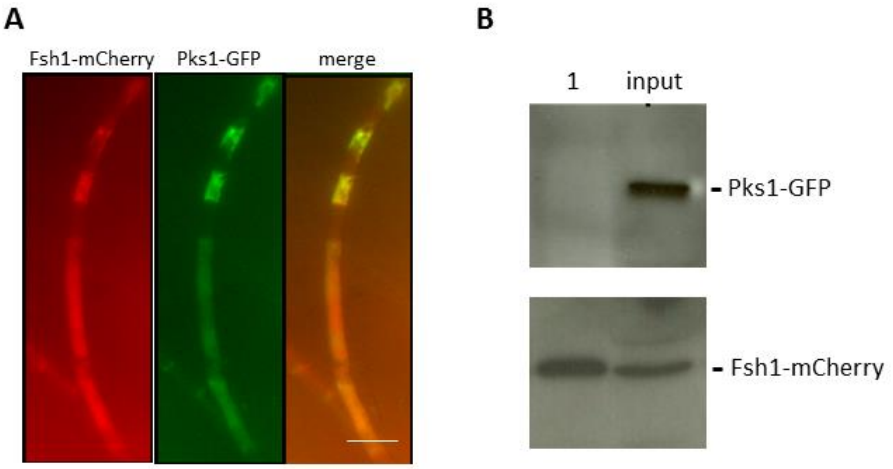

Figure 21 Pks1 does not interact with Fsh1 in mycelia. (A) Epifluorescence microscopy of TrpC-pro:Pks1-GFP and TrpC-pro:Fsh1-mCherry co-expressed strain. The fungus was grown on PA medium in dark for 4 days and mycelia were picked up from the medium for observation. Scale bar = 10 μm. **(B)** Co-immunoprecipitation of the Pks1-GFP and Fsh1-mCherry. The total protein lysate from the TrpC-pro:Pks1-GFP and TrpC-pro:Fsh1-mCherry co-expressed mycelia served as a control. The proteins pulled down by RFP-Trap were run in lane 1. Anti-GFP antibody probed the Pks1-GFP protein in the input lane (upper panal). Anti-RFP antibody probed the Fsh1-mCherry protein (lower panal).

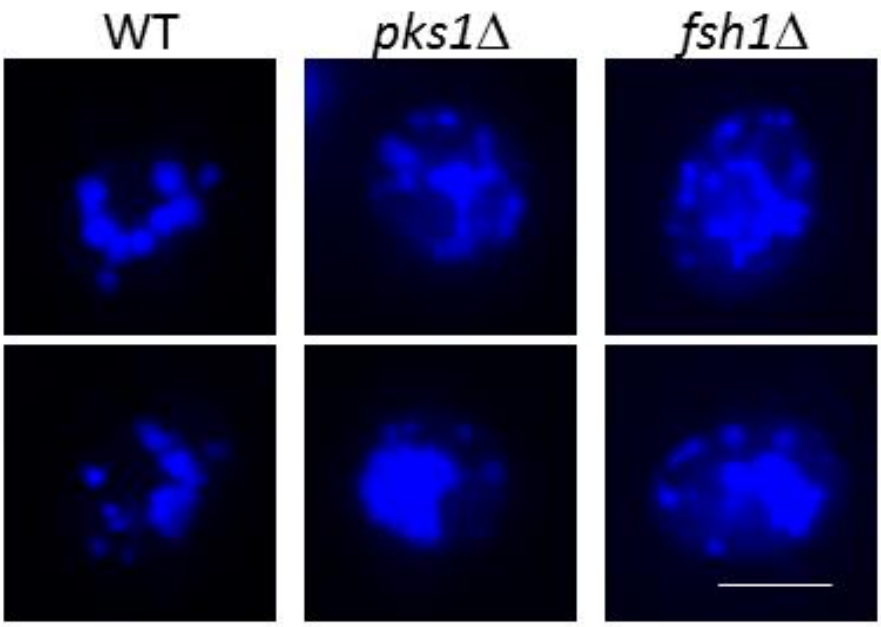

Figure 22 Pks1 and Fsh1 are involved in vacuolar morphology in appressoria. Confocal microscopy of the CMAC stained appressoria of WT, *pks1*Δ and *fsh1*Δ. Images were taken at 20 hpi and two appressoria are shown for each strain. Scale bar = 5 μm.

3.4 Regulation of the PKS1 gene cluster

We examined the genomic loci around *PKS1* since the regulatory genes are often clustered with the biosynthetic genes. However, transcription factor-encoding genes were absent in the *PKS1* cluster. Therefore, the *PKS1* gene cluster is likely regulated by elements that are elsewhere on the genome. We deleted several known regulators including *MoVEA, MST12, MSTU1* or *CSN7* (Kim et al., 2014; Nishimura et al., 2009; Park et al., 2002; Wei et al., 2008), which are related to secondary metabolism or appressorial penetration to investigate their relationship with *PKS1*.

VeA is a global secondary metabolism transcription factor in fungus (Myung et al., 2012). We deleted the *veA* homolog *MoVEA* in the Pks1-GFP strain. The *MoveA*Δ mutant produced less melanin during vegetative growth, but formed melanized appressoria (Fig. 23). The Pks1-GFP expression level was normal in the *MoveA*Δ mutant (Fig. 24).

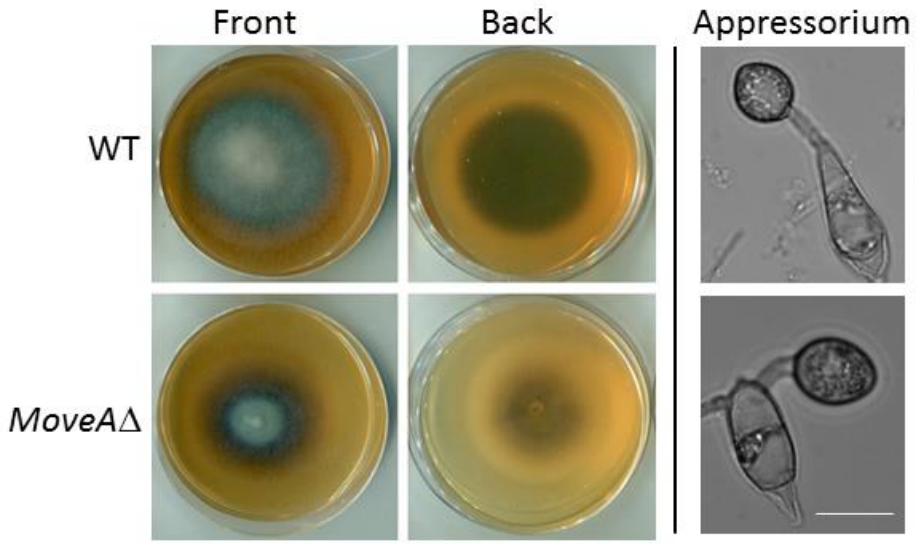

Figure 23 *MoVEA* regulates melanin synthesis in mycelia but not in appressoria. Left panels show the vegetative growth of WT and *MoveA*Δ on PA medium. Plates were cultured in dark for 3 days and exposed to light for 4 days. Right panels show the melanized appressoria of WT and *MoveA*Δ. Scale bar = 10 μm.

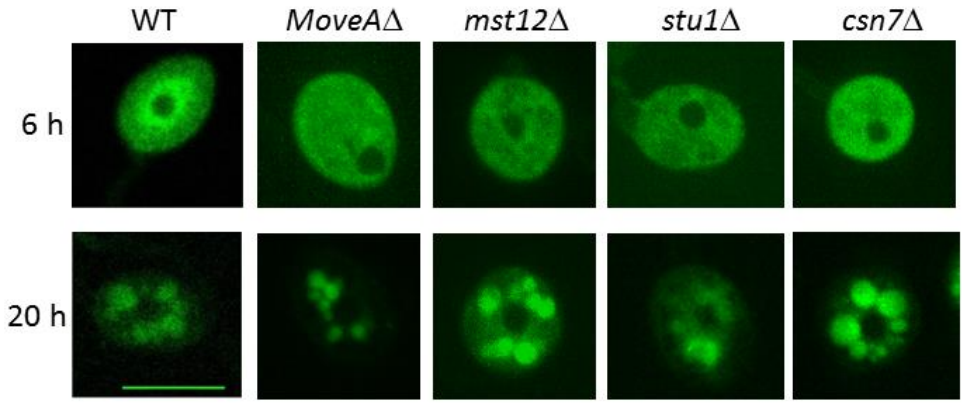

Figure 24 Confocal microscopy of Pks1-GFP in WT, *MoveA*Δ, *mst12*Δ, *stu1*Δor *csn7*Δ. Scale bar = 10 μm.

MST12 and *MSTU1* are two transcription factors that regulate appressorium-mediated host penetration (Nishimura et al., 2009; Park et al., 2002). However, deletion of these genes did not affect the Pks1-GFP expression and localization (Fig. 24). Therefore, the induction of Pks1 in the appressorium is not regulated by *MST12* and *MSTU1*.

Deactivation of the COP9 signalosome activates some silenced secondary metabolism gene clusters in *A. nidulans* (Gerke et al., 2012). We deleted one of the COP9 subunit *CSN7* in Pks1-GFP strain. The *csn7*Δ mutant grew slower and produced less conidia compared to the WT, but it developed melanized functional appressoria capable of host penetration (Fig. 25). In addition, Pks1 was not upregulated in the *csn7*Δ mycelia, and the expression pattern of Pks1-GFP in the mutant is the same as in the WT (Fig. 24). Accordingly, Csn7 could not regulate the Pks1 expression.

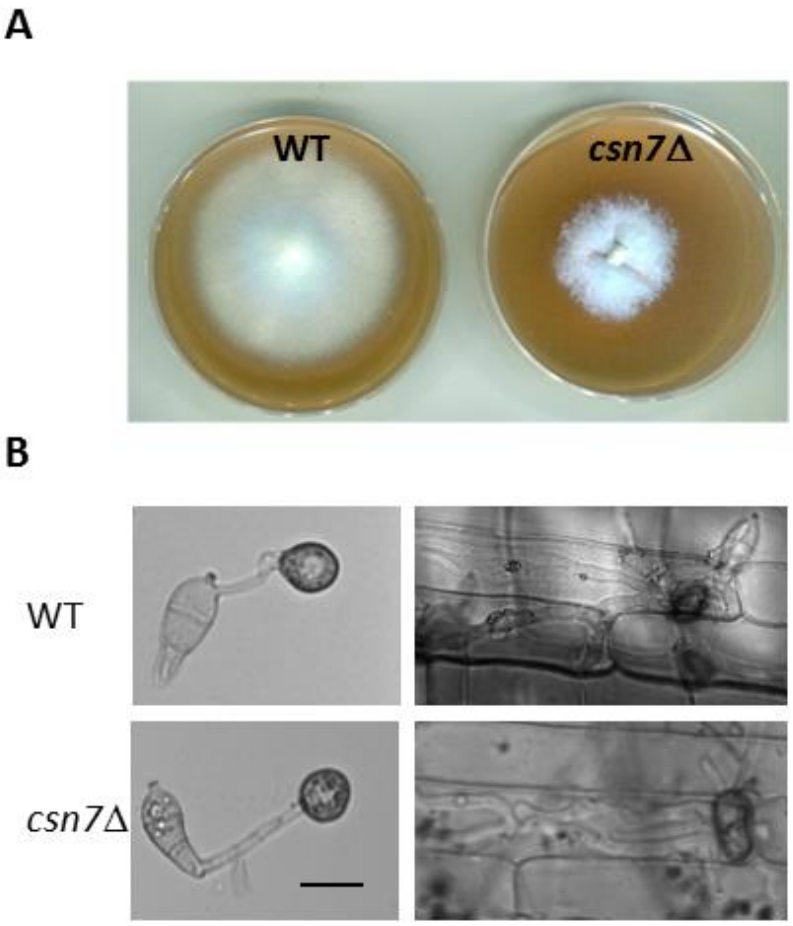

Figure 25 Phenotype of *csn7*Δ mutant. (A) Vegetative growth of *csn7*Δ is highly reduced. WT and *csn7*Δ were grown on PA medium in the dark for 7 days. **(B)** *csn7*Δ develops functional and melanized appressorium. Left panel shows the appressoria of WT and *csn7*Δ at 20 hpi. Right panel shows the penetration of WT and *csn7*Δ appressoria at 48 hpi.

3.5 Metabolomic profiling of the WT and pks1Δ

To identify the possible Pks1 product and substrate, total metabolites at different developmental stages (6 hpi and 24 hpi) were extracted from the *pks1*Δ mutant and WT appressoria, and were subjected to non-targeted metabolite profiling by LC/MS. Unfortunately, we could not identify a single polyketide, differentially present in the WT appressorial samples when compared to that of the *pks1*Δ. Therefore the metabolomics changes between WT and *pks1*Δ appressorial samples were assessed at 6 hpi and 24 hpi. A total of 481 and 391 metabolite features were differentially accumulated between WT and *pks1*Δ samples at 6 hpi and 24 hpi (fold change ≥ 2, P-value ≤ 0.05; Figure 26 A and B), suggesting a remarkable change in the metabolic activities and/or biosynthesis of a number of metabolites in the absence of Pks1 function during appressorial development in *M. oryzae*. At 6 hpi, there are 58 upregulated features in the *pks1*Δ and 423 upregulated features in the WT samples. At 24 hpi, there are 70 upregulated features in the *pks1*Δ and 321 upregulated features in the WT samples. Moreover there are total 221 features have fold change larger than 20 and all these 221 features are upregulated in the WT samples (Figure 26C). These results indicate that deletion of PKS1 leads to reduced metabolite synthesis in the appressoria and the reduction is more significant at 6 hpi when the appressoria are immature.

A

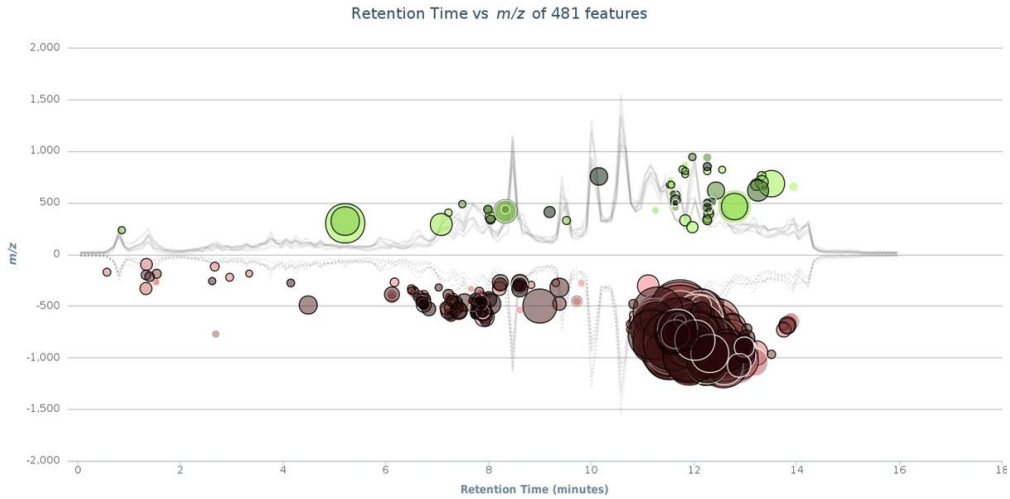

Upregulated features *pks1Δ* (58)

Downregulated features *pks1Δ* (423)

B

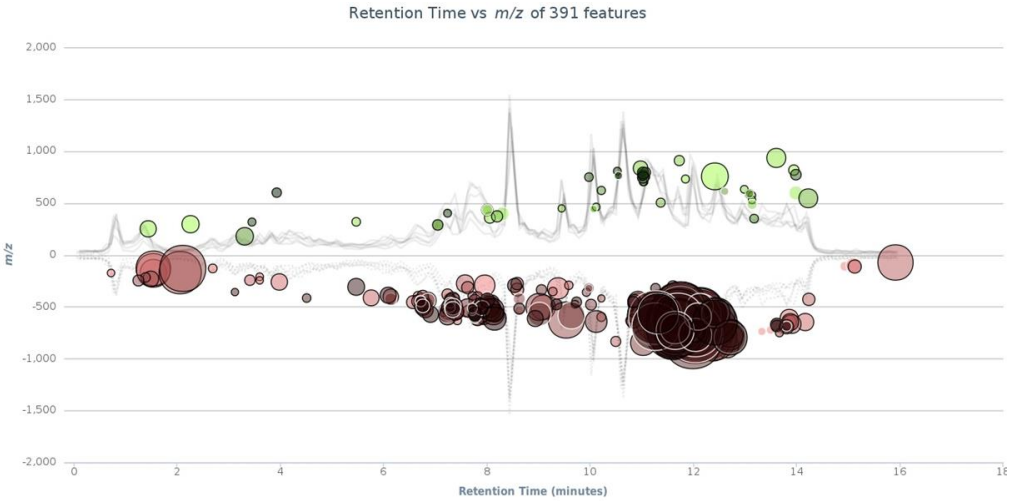

Upregulated features *pks1Δ* (70)

Downregulated features *pks1Δ* (321)

C

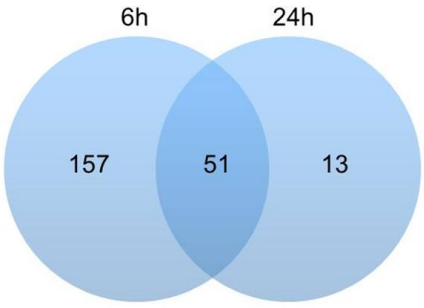

Fold change > 20

Figure 26 Differential metabolite features of the *pks1*Δ and WT appressoria. The methanol extraction of *pks1*Δ and WT appressoria at 6 hpi and 24 hpi were analyzed by LC/MS and features were extracted by XCMS Online (http://xcmsonline.scripps.edu/). **(A and B)** Significant features between WT and *pks1*Δ samples at 6 hpi **(A)** and 24 hpi **(B)**. Features are chosen if fold change ≥ 2 and P-value ≤ 0.05. P-value is represented by color intensity (more intense means lower P-value). Fold change is represented by feature radius. Upregulated feature means it is higher in *pks1*Δ and downregulated feature is higher in WT. **(C)** Number of features who have a fold change larger than 20.

Chapter IV General Discussion

In recent years, our knowledge of the pathology of rice blast disease and *M. oryzae* has been broadened dramatically. Many factors or pathways that are involved in pathogenesis and virulence have been discovered. However, there are limited studies about how secondary metabolism affects pathogenicity or virulence in *M. oryzae*. Since the *M. oryzae* genome is rich in secondary metabolism genes (Collemare et al., 2008a), we believe that *M. oryzae* produces necessary secondary metabolites that help it to efficiently infect the host plants.

This study explored the role of Pks1-mediated secondary metabolism during pathogenic growth of *M. oryzae*. A PKS gene cluster, which contains Pks1, Fsh1 and Abc3 was found to be essential for host penetration and appressorium function. Pks1 and Fsh1 are responsible for polyketide biosynthesis therefore the polyketide catalyzed by Pks1 and/or Fsh1 is a key factor for the normal appressorial penetration function.

PKS1 and melanin biosynthesis

We noticed that the Pks1 biosynthesis pathway is associated with melanin biosynthesis pathway during appressorium formation. Deletion of *PKS1* leads to the thicker melanin layer and increased transcription of the *ALB1*

gene (Fig. 8 and 9). It came as no surprise because: Firstly, the PKS protein Alb1 catalyzes the initial step of melanin synthesis in *M. oryzae*, which means that Alb1 and Pks1 probably share the same precursor or substrate and the unbalanced usage of the precursor or substrate affects melanin synthesis. Secondly, melanin is formed by highly cross-linked complex heteropolymers (Gómez and Nosanchuk, 2003), and the exact structure of melanin is unknown yet, hence polyketide(s) generated by Pks1 might be involved in the heteropolymer complex and affects the melanin layer formation. This melanin synthesis-related function of Pks1 is of importance since the study of melanin is very limited due to its insolubility (Gómez and Nosanchuk, 2003), and the Pks1 function should help further explore the structure and components of melanin biogenesis and transport in fungi.

We have ruled out the possibility that the aberrant melanin layer is the direct cause of the penetration defects of *pks1*Δ since reducing the melanin synthesis could not suppress the said defects (Fig. 11). Second, the *fsh1*Δ mutant showed similar host penetration defects but it did not produce thick melanin layer in the appressorium (Fig. 19A). So we tend to believe that the thickened melanin layer is caused by secondary metabolism disorders.

As shown in Figure 13 and 19, deletion of *PKS1* or *FSH1* disrupted the pore wall overlay formation. Although the composition or function of the pore

wall overlay is not known yet. However, the emergence of the penetration peg from within the pore wall overlay region indicates an important function in proper host penetration (Bourett and Howard, 1990). The failure of the mutants to generate the penetration peg might be due to the lack of pore wall overlays. Furthermore, the lack of pore wall overlay could also be the cause of the enlarged zone of septin accumulation and the lack of septin ring in the *pks1*Δ and *fsh1*Δ appressoria. However, this remains a hypothesis, as there are limited studies of the pore wall overlay and temporal dynamics of appressorial melanization during *M. oryzae* pathogenesis. We failed to suppress the penetration defects by reducing the melanin synthesis, adding WT or *fsh1*Δ mutant appressorial extracts or by feeding the appressoria with additional malonyl-CoA.

PKS1 gene cluster

The secondary metabolite synthesis genes are usually co-regulated and clustered (Keller and Hohn, 1997). In this study, only three genes were found involved in the polyketide synthesis in the *PKS1* gene cluster: *PKS1*, *FSH1* and *ABC3*. These genes were highly expressed in the appressorium and were found to be essential for the host penetration step of pathogenesis. *PKS1* encodes a HR-PKS which contains three reducing domains DH, ER and KR. Some of the PKSs with the same domain structure have been studied:

ACTTS3 is responsible for the ACT-toxin synthesis in *A. alternata* (Miyamoto et al., 2010); PSS (prosolanapyrone synthase) encoded by Sol1 produces solanapyrone in *Alternaria solani* (Kasahara et al., 2010); Hpm8 is involved in the biosynthesis hypothemycin in *Hypomyces subiculosus* (Reeves et al., 2008). Therefore, it is evident that by different modifications and/or by using various reducing domains, the HR-PKSs are capable of producing diverse and complex polyketide products.

Compared to other well studied PKS gene clusters, like the fumonisin gene cluster in *G. fujikuroi*, which contains 16 genes, or the aflatoxin gene cluster in *Aspergillus parasiticus* which consists of 24 genes (Ehrlich et al., 2005), the *PKS1* gene cluster is relatively small. It is probable that most of the modification enzymes are not involved in this gene cluster. However, *PKS1* cluster is not the only PKS gene cluster that has only two synthesis genes. It has been recently reported that the fusaric acid gene cluster in *F. fujikuroi* also contains two similar proteins: one is an HR-IPKS (Fub1) and the other is a serine hydrolase (Fub4) which is highly related to Fsh1 (Niehaus et al., 2014). Although there are 5 genes coregulated (*FUB1-FUB5*) in the *FUB* gene cluster (Brown et al., 2012), only *FUB1* and *FUB4* are essential for fusaric acid biosynthesis. Based on these two studies, we suggest that the study of fusaric acid and Pks1 synthesis pathway should provide valuable information since there might be a conserved novel polyketide synthesis

mechanism shared by these two or more gene clusters.

Fsh1 is predicted to be a serine hydrolase or an esterase lipase. We found that orthologs of *FSH1* are mainly present in fungi except one ortholog in the Arabidopsis genome based on BLink at the NCBI database. Fsh1 is a fungus specific enzyme. Interestingly, there is a paralog of *FSH1*, MGG_05593, which is located near MGG_05589, an HR-PKS with domain structure similar to Pks1. However, its transcription level is not upregulated in the appressorium. MGG_05589 and MGG_05593 are likely not required for normal growth, and their function(s) could be analyzed in future studies.

Abc3 has been studied in our lab previously (Patkar et al., 2012; Sun et al., 2006a) and is involved in the efflux of the cytotoxic ATS in the appressoria. It remains to be seen whether the high concentration of ATS is the real cause of the penetration defects shown by *abc3*Δ. Deletion of the mycH, an ABC transporter in *M. aeruginosa* PCC 7806, results in the lack of expression of other biosynthesis genes (Pearson et al., 2004) and led to the loss of microcystin production. While *FUM19*, an ABC transporter in *FUM* gene cluster in *G. moniliformis*, could only cause subtle changes in fumonisin production (Proctor et al., 2003). However, the exact function of Abc3 in the PKS gene cluster still remains elusive.

In this study, we showed that Abc3 is involved in the Pks1-mediated

polyketide synthesis as loss of *ABC3* affects proper Pks1-GFP localization. The *abc3*Δ mutant has different phenotypes compared to the *pks1*Δ and *fsh1*Δ mutant, as it has defects in invasive growth and cellular stress, but it could form proper pore wall overlay and is able to penetrate the PUDO-193 membrane. This suggests that the Abc3 is not directly involved in the efflux of polyketide product(s) *per se*, but affects the transportation of a precursor and/or an intermediate product in this pathway.

Vacuoles and Pks1 mediated biosynthesis

Vacuoles are known to separate or compartmentalize the toxic secondary metabolites to protect the host cell. Many enzymes localize in the vacuoles to synthesize the secondary metabolites. For instance, the biosynthesis of aflatoxin occurs in the cytosol and vacuoles in *A. parasiticus* (Chanda et al., 2009; Hong and Linz, 2008, 2009; Lee et al., 2004). The aflatoxin synthase Nor-1, Ver-1 and OmtA are first expressed in the cytosol and later transferred to the vacuoles and vesicles. In addition, blocking the vacuolar fusion in *A. parasiticus* affects the aflatoxin synthase accumulation and aflatoxin production (Chanda et al., 2009). Pks1 shows a similar pattern of cellular localization as the aflatoxin synthase, but Fsh1 only localizes to the vacuoles. This suggested that the synthesis likely starts in the cytosol but shifts to the vacuoles at the late stages. Thus, Fsh1 likely modifies the Pks1 product in

the vacuoles. And the translocalization of Pks1 is probably required for such synthesis. However whether Pks1 as well as Fsh1 remains stable and functional in the vacuoles still needs to be studied in the future. Interestingly, vacuoles in the *pks1*Δ and *fsh1*Δ appressoria are small and aggregated, which indicates that increased accumulation of precursor/intermediate of the Pks1 pathway affects the fusion of vacuoles in *M. oryzae*.

Regulation of the *PKS1* gene cluster

Our study failed to identify any regulators that would control the Pks1 gene cluster. This is probably because the Pks1 gene cluster is associated with appressorium formation. Therefore, the Pks1 gene cluster is controlled by a global regulator such as the Pmk1 MAP kinase. The melanin synthesis is also specifically regulated in the appressorium. As the Pks1 pathway is related to the melanin synthesis, we would like to believe that the induction of melanin synthesis in appressoria is associated with *PKS1* expression, and that this process is triggered by upstream regulators of appressorium formation. How initiation of appressorium development triggers Pks1-associated secondary metabolism is an interesting question that will be addressed in the future.

Identification of Pks1 substrate and product

The prediction of the Pks1 product is not available with our current knowledge of HR-IPKS. Researchers have tried to find out the PKS products

by heterologous expression of the PKSs, mining the secondary metabolites or biosynthesis of the products *in vitro* (cell free system). However, heterologous expression or in vitro assays do not always produce the exact compounds synthesized *in vivo* (Punya et al., 2013; Song et al., 2015). We compared the metabolism of WT and *pks1*Δ appressoria. The globally changed metabolism made it very difficult to figure out the specific products of Pks1 pathway. As we do not have any method to identify the specific compounds, *in vitro* assay should be conducted to get better understanding of the Pks1 mediated synthesis.

Chapter V Conclusions and Future Directions

We found a new PKS gene cluster, which includes at least three important genes, *PKS1*, *FSH1* and *ABC3*, essential for the appressorium-assisted host penetration. This gene cluster is upregulated during appressorium formation. Pks1 and Fsh1 are required for proper biogenesis and deposition of melanin; in pore wall overlay formation and proper assembly of the septin ring in *M. oryzae*. The detailed study of the cellular localization of Pks1 and Fsh1 indicates that the Pks1 mediated biosynthesis starts in the cytosol and then transfers to the vacuoles. Interestingly, septin dynamics and regulation is under control via the *PKS1*. In addition, we found out that global metabolism is disrupted in the *pks1*Δ mutant. Our study provides a new direction to the mechanistic studies underlying host entry and colonization. A new PKS gene cluster was also characterized, which adds to the previous work on NRPS/PKS in *M. oryzae* (Chumley and Valent, 1990; Collemare et al., 2008b; Song et al., 2015; Yun et al., 2015). In addition, Pks1 would serve as a new target for developing antifungals against -rice blast and/or other fungal diseases of importance to agriculture.

Due to time and technological limitations, we have not finished all the Pks1 function studies yet, and several interesting directions could be investigated in the future:

The most important future direction would be the proper identification of Pks1 substrate and product(s) relevant to the host penetration stage of *M. oryzae*. Since the appressorial extract of the WT could not suppress the penetration defects in the *pks1*Δ, we failed to identify such active compound/polyketide produced by Pks1. However, the heterologous expression and *in vitro* assay showed promising results in preliminary experiments and would be followed up in future to identify the product(s) of Pks1 activity. The function of Fsh1 would likewise be further studied if the *in vitro* assay is successful. In addition, metabolomic profiling of the other two mutants, *fsh1*Δ and *abc3*Δ, could also give us more information of the intermediate or product in this synthesis pathway, and would further reveal the relationship between *PKS1*, *FSH1* and *ABC3*.

As the metabolic profiles differ a lot between *pks1*Δ mutant and WT, it is interesting to investigate if any other synthesis enzymes were affected in the mutant. Therefore RNA sequencing could be performed to compare the *pks1*Δ and WT transcriptome.

The studies on secondary metabolism are still very limited in *M. oryzae*. As only two PKSs have been investigated thus far in *M. oryzae*, the functions of the other PKSs remain to be explored as part of future studies in the rice blast pathosystem.

References

Alspaugh, J.A., Perfect, J.R., and Heitman, J. (1998). Signal Transduction Pathways Regulating Differentiation and Pathogenicity ofCryptococcus neoformans. Fungal Genetics and Biology *25*, 1-14.

Andersen, M.R., Nielsen, J.B., Klitgaard, A., Petersen, L.M., Zachariasen, M., Hansen, T.J., Blicher, L.H., Gotfredsen, C.H., Larsen, T.O., and Nielsen, K.F. (2013). Accurate prediction of secondary metabolite gene clusters in filamentous fungi. Proceedings of the National Academy of Sciences *110*, E99-E107.

Arunachalam, C., and Doohan, F.M. (2013). Trichothecene toxicity in eukaryotes: Cellular and molecular mechanisms in plants and animals. Toxicology letters *217*, 149-158.

Bayram, Ö., Krappmann, S., Ni, M., Bok, J.W., Helmstaedt, K., Valerius, O., Braus-Stromeyer, S., Kwon, N.-J., Keller, N.P., and Yu, J.-H. (2008). VelB/VeA/LaeA complex coordinates light signal with fungal development and secondary metabolism. Science *320*, 1504-1506.

Bell, A.A., and Wheeler, M.H. (1986). Biosynthesis and functions of fungal melanins. Annual review of phytopathology *24*, 411-451.

Bhatnagar, D., Cary, J.W., Ehrlich, K., Yu, J., and Cleveland, T.E. (2006). Understanding the genetics of regulation of aflatoxin production and Aspergillus flavus development. Mycopathologia *162*, 155-166.

Birch, A., and Donovan, F. (1953). Studies in relation to biosynthesis. I. Some possible routes to derivatives of orcinol and phloroglucinol. Australian Journal of Chemistry *6*, 360-368.

Böhnert, H.U., Fudal, I., Dioh, W., Tharreau, D., Notteghem, J.-L., and Lebrun, M.-H. (2004). A putative polyketide synthase/peptide synthetase from Magnaporthe grisea signals pathogen attack to resistant rice. The Plant cell *16*, 2499-2513.

Bok, J.W., Hoffmeister, D., Maggio-Hall, L.A., Murillo, R., Glasner, J.D., and Keller, N.P. (2006). Genomic mining for Aspergillus natural products. Chemistry & biology *13*, 31-37.

Bok, J.W., and Keller, N.P. (2004). LaeA, a regulator of secondary metabolism in Aspergillus spp. Eukaryotic cell *3*, 527-535.

Bourett, T., and Howard, R. (1992). Actin in penetration pegs of the fungal rice blast pathogen, Magnaporthe grisea. Protoplasma *168*, 20-26.

Bourett, T.M., and Howard, R.J. (1990). In vitro development of penetration structures in the rice blast fungus Magnaporthe grisea. Canadian Journal of Botany *68*, 329-342.

Brakhage, A.A., and Schroeckh, V. (2011). Fungal secondary metabolites–strategies to activate silent gene clusters. Fungal Genetics and Biology *48*, 15-22.

Brown, D.W., Butchko, R.A., Busman, M., and Proctor, R.H. (2012). Identification of gene clusters associated with fusaric acid, fusarin, and perithecial pigment production in Fusarium verticillioides. Fungal Genetics and Biology *49*, 521-532.

Butler, M., and Day, A. (1998). Fungal melanins: a review. Canadian Journal of Microbiology *44*, 1115-1136.

Calvo, A.M., Wilson, R.A., Bok, J.W., and Keller, N.P. (2002). Relationship between secondary metabolism and fungal development. Microbiology and Molecular Biology Reviews *66*, 447-459.

Chanda, A., Roze, L.V., Kang, S., Artymovich, K.A., Hicks, G.R., Raikhel, N.V., Calvo, A.M., and Linz, J.E. (2009). A key role for vesicles in fungal secondary metabolism. Proceedings of the National Academy of Sciences *106*, 19533-19538.

Choi, W., and Dean, R.A. (1997). The adenylate cyclase gene MAC1 of Magnaporthe grisea controls appressorium formation and other aspects of growth and development. The Plant cell *9*, 1973-1983.

Chooi, Y.-H., and Tang, Y. (2012a). Navigating the Fungal Polyketide Chemical Space: From Genes to Molecules. The Journal of organic chemistry *77*, 9933-9953.

Chooi, Y.H., and Tang, Y. (2012b). Navigating the fungal polyketide chemical space: from genes to molecules. The Journal of organic chemistry *77*, 9933-9953.

Chumley, F.G., and Valent, B. (1990). Genetic analysis of melanin-deficient, nonpathogenic mutants of Magnaporthe grisea. Mol Plant-Microbe Interact *3*, 135-143.

Collemare, J., Billard, A., Böhnert, H.U., and Lebrun, M.-H. (2008a). Biosynthesis of secondary metabolites in the rice blast fungus Magnaporthe grisea: the role of hybrid PKS-NRPS in pathogenicity. Mycological research *112*, 207-215.

Collemare, J., Billard, A., Bohnert, H.U., and Lebrun, M.H. (2008b). Biosynthesis of secondary metabolites in the rice blast fungus Magnaporthe grisea: the role of hybrid PKS-NRPS in pathogenicity. Mycological research *112*, 207-215.

Collemare, J., Pianfetti, M., Houlle, A.E., Morin, D., Camborde, L., Gagey, M.J., Barbisan, C., Fudal, I., Lebrun, M.H., and Böhnert, H.U. (2008c). Magnaporthe grisea avirulence gene ACE1 belongs to an infection‐specific gene cluster involved in secondary metabolism. New Phytologist *179*, 196-208.

Collie, J.N. (1893). XXIII.—The production of naphthalene derivatives from dehydracetic acid. Journal of the Chemical Society, Transactions *63*, 329-337.

Couch, B.C., Fudal, I., Lebrun, M.-H., Tharreau, D., Valent, B., van Kim, P., Nottéghem, J.-L., and Kohn, L.M. (2005). Origins of host-specific populations of the blast pathogen Magnaporthe oryzae in crop domestication with subsequent expansion of pandemic clones on rice and weeds of rice. Genetics *170*, 613-630.

Cox, R.J. (2007). Polyketides, proteins and genes in fungi: programmed nano-machines begin to reveal their secrets. Organic & biomolecular chemistry *5*, 2010-2026.

Cox, R.J., Glod, F., Hurley, D., Lazarus, C.M., Nicholson, T.P., Rudd, B.A., Simpson, T.J., Wilkinson, B., and Zhang, Y. (2004). Rapid cloning and expression of a fungal polyketide synthase gene involved in squalestatin biosynthesis. Chemical communications, 2260-2261.

Dagdas, Y.F., Yoshino, K., Dagdas, G., Ryder, L.S., Bielska, E., Steinberg, G., and Talbot, N.J. (2012). Septin-mediated plant cell invasion by the rice blast fungus, Magnaporthe oryzae. Science *336*, 1590-1595.

de Jong, J.C., McCormack, B.J., Smirnoff, N., and Talbot, N.J. (1997). Glycerol generates turgor in rice blast. Nature *389*, 244-244.

Dean, R., Van Kan, J.A., Pretorius, Z.A., Hammond‐Kosack, K.E., Di Pietro, A., Spanu,

P.D., Rudd, J.J., Dickman, M., Kahmann, R., and Ellis, J. (2012). The Top 10 fungal pathogens in molecular plant pathology. Molecular plant pathology *13*, 414-430.

Dean, R.A., Talbot, N.J., Ebbole, D.J., Farman, M.L., Mitchell, T.K., Orbach, M.J., Thon, M., Kulkarni, R., Xu, J.-R., and Pan, H. (2005). The genome sequence of the rice blast fungus Magnaporthe grisea. Nature *434*, 980-986.

DeZwaan, T.M., Carroll, A.M., Valent, B., and Sweigard, J.A. (1999). Magnaporthe grisea pth11p is a novel plasma membrane protein that mediates appressorium differentiation in response to inductive substrate cues. The Plant cell *11*, 2013-2030.

Ebbole, D.J. (2007). Magnaporthe as a model for understanding host-pathogen interactions. Annu Rev Phytopathol *45*, 437-456.

Ehrlich, K., Yu, J., and Cotty, P. (2005). Aflatoxin biosynthesis gene clusters and flanking regions. Journal of Applied Microbiology *99*, 518-527.

Foster, A.J., Jenkinson, J.M., and Talbot, N.J. (2003). Trehalose synthesis and metabolism are required at different stages of plant infection by Magnaporthe grisea. The EMBO Journal *22*, 225-235.

Fudal, I., Collemare, J., Böhnert, H.U., Melayah, D., and Lebrun, M.-H. (2007). Expression of Magnaporthe grisea avirulence gene ACE1 is connected to the initiation of appressorium-mediated penetration. Eukaryotic cell *6*, 546-554.

Fujii, I., Mori, Y., Watanabe, A., Kubo, Y., Tsuji, G., and Ebizuka, Y. (2000). Enzymatic synthesis of 1, 3, 6, 8-tetrahydroxynaphthalene solely from malonyl coenzyme A by a fungal iterative type I polyketide synthase PKS1. Biochemistry *39*, 8853-8858.

Geis, P.A., Wheeler, M.H., and Szaniszlo, P.J. (1984). Pentaketide metabolites of melanin synthesis in the dematiaceous fungus Wangiella dermatitidis. Archives of microbiology *137*, 324-328.

Gerke, J., Bayram, Ö., Feussner, K., Landesfeind, M., Shelest, E., Feussner, I., and Braus, G.H. (2012). Breaking the silence: protein stabilization uncovers silenced biosynthetic gene clusters in the fungus Aspergillus nidulans. Applied and environmental microbiology *78*, 8234-8244.

Gómez, B.L., and Nosanchuk, J.D. (2003). Melanin and fungi. Current opinion in infectious diseases *16*, 91-96.

Gowda, M., Venu, R., Raghupathy, M.B., Nobuta, K., Li, H., Wing, R., Stahlberg, E., Couglan, S., Haudenschild, C.D., and Dean, R. (2006). Deep and comparative analysis of the mycelium and appressorium transcriptomes of Magnaporthe grisea using MPSS, RL-SAGE, and oligoarray methods. BMC genomics *7*, 310.

Hamer, J.E., Howard, R.J., Chumley, F.G., and Valent, B. (1988). A mechanism for surface attachment in spores of a plant pathogenic fungus. Science *239*, 288-290.

Hendrickson, L., Davis, C.R., Roach, C., Aldrich, T., McAda, P.C., and Reeves, C.D. (1999). Lovastatin biosynthesis in Aspergillus terreus: characterization of blocked mutants, enzyme activities and a multifunctional polyketide synthase gene. Chemistry & biology *6*, 429-439.

Hertweck, C. (2009). The biosynthetic logic of polyketide diversity. Angewandte Chemie International Edition *48*, 4688-4716.

Hicks, J.K., Yu, J.H., Keller, N.P., and Adams, T.H. (1997). Aspergillus sporulation and

mycotoxin production both require inactivation of the FadA Gα protein-dependent signaling pathway. The EMBO Journal *16*, 4916-4923.

Hong, S.-Y., and Linz, J.E. (2008). Functional expression and subcellular localization of the aflatoxin pathway enzyme Ver-1 fused to enhanced green fluorescent protein. Applied and environmental microbiology *74*, 6385-6396.

Hong, S.-Y., and Linz, J.E. (2009). Functional expression and sub-cellular localization of the early aflatoxin pathway enzyme Nor-1 in Aspergillus parasiticus. Mycological research *113*, 591-601.

Horbach, R., Graf, A., Weihmann, F., Antelo, L., Mathea, S., Liermann, J.C., Opatz, T., Thines, E., Aguirre, J., and Deising, H.B. (2009). Sfp-type 4′-phosphopantetheinyl transferase is indispensable for fungal pathogenicity. The Plant cell *21*, 3379-3396.

Hosaka, T., Ohnishi-Kameyama, M., Muramatsu, H., Murakami, K., Tsurumi, Y., Kodani, S., Yoshida, M., Fujie, A., and Ochi, K. (2009). Antibacterial discovery in actinomycetes strains with mutations in RNA polymerase or ribosomal protein S12. Nature biotechnology *27*, 462-464.

Howard, R.J., Ferrari, M.A., Roach, D.H., and Money, N.P. (1991). Penetration of hard substrates by a fungus employing enormous turgor pressures. Proceedings of the National Academy of Sciences *88*, 11281-11284.

Howard, R.J., and Valent, B. (1996). Breaking and entering: host penetration by the fungal rice blast pathogen Magnaporthe grisea. Annual Reviews in Microbiology *50*, 491-512.

Jelitto, T.C., Page, H.A., and Read, N.D. (1994). Role of external signals in regulating the pre-penetration phase of infection by the rice blast fungus, Magnaporthe grisea. Planta *194*, 471-477.

Jeon, J., Park, S.-Y., Chi, M.-H., Choi, J., Park, J., Rho, H.-S., Kim, S., Goh, J., Yoo, S., and Choi, J. (2007). Genome-wide functional analysis of pathogenicity genes in the rice blast fungus. Nature genetics *39*, 561-565.

Kale, S.P., Cary, J.W., Baker, C., Walker, D., Bhatnagar, D., and Bennett, J.W. (2003). Genetic analysis of morphological variants of Aspergillus parasiticus deficient in secondary metabolite production. Mycological research *107*, 831-840.

Kale, S.P., Cary, J.W., Bhatnagar, D., and Bennett, J. (1996). Characterization of experimentally induced, nonaflatoxigenic variant strains of Aspergillus parasiticus. Applied and environmental microbiology *62*, 3399-3404.

Kasahara, K., Miyamoto, T., Fujimoto, T., Oguri, H., Tokiwano, T., Oikawa, H., Ebizuka, Y., and Fujii, I. (2010). Solanapyrone synthase, a possible Diels–Alderase and iterative type I polyketide synthase encoded in a biosynthetic gene cluster from Alternaria solani. ChemBioChem *11*, 1245-1252.

Kato, N., Brooks, W., and Calvo, A.M. (2003). The expression of sterigmatocystin and penicillin genes in Aspergillus nidulans is controlled by veA, a gene required for sexual development. Eukaryotic cell *2*, 1178-1186.

Kawamura, C., Tsujimoto, T., and Tsuge, T. (1999). Targeted disruption of a melanin biosynthesis gene affects conidial development and UV tolerance in the Japanese pear pathotype of Alternaria alternata. Molecular Plant-Microbe Interactions *12*, 59-63.

Keatinge-Clay, A.T., and Stroud, R.M. (2006). The structure of a ketoreductase determines the organization of the β-carbon processing enzymes of modular polyketide synthases. Structure *14*, 737-748.

Keller, N.P., and Hohn, T.M. (1997). Metabolic pathway gene clusters in filamentous fungi. Fungal Genetics and Biology *21*, 17-29.

Keller, N.P., Turner, G., and Bennett, J.W. (2005). Fungal secondary metabolism—from biochemistry to genomics. Nature Reviews Microbiology *3*, 937-947.

Kim, H.-J., Han, J.-H., Kim, K.S., and Lee, Y.-H. (2014). Comparative functional analysis of the velvet gene family reveals unique roles in fungal development and pathogenicity in Magnaporthe oryzae. Fungal Genetics and Biology *66*, 33-43.

Kim, H.-S., Han, K.-Y., Kim, K.-J., Han, D.-M., Jahng, K.-Y., and Chae, K.-S. (2002). The veA gene activates sexual development in Aspergillus nidulans. Fungal Genetics and Biology *37*, 72-80.

Kim, Y.T., Lee, Y.R., Jin, J., Han, K.H., Kim, H., Kim, J.C., Lee, T., Yun, S.H., and Lee, Y.W. (2005). Two different polyketide synthase genes are required for synthesis of zearalenone in Gibberella zeae. Molecular microbiology *58*, 1102-1113.

Lai, J.R., Koglin, A., and Walsh, C.T. (2006). Carrier protein structure and recognition in polyketide and nonribosomal peptide biosynthesis. Biochemistry *45*, 14869-14879.

Langfelder, K., Streibel, M., Jahn, B., Haase, G., and Brakhage, A.A. (2003). Biosynthesis of fungal melanins and their importance for human pathogenic fungi. Fungal Genetics and Biology *38*, 143-158.

Lee, L.-W., Chiou, C.-H., Klomparens, K.L., Cary, J.W., and Linz, J.E. (2004). Subcellular localization of aflatoxin biosynthetic enzymes Nor-1, Ver-1, and OmtA in time-dependent fractionated colonies of Aspergillus parasiticus. Archives of microbiology *181*, 204-214.

Lee, Y.-H., and Dean, R.A. (1993). cAMP regulates infection structure formation in the plant pathogenic fungus Magnaporthe grisea. The Plant cell *5*, 693-700.

Liu, H., Suresh, A., Willard, F.S., Siderovski, D.P., Lu, S., and Naqvi, N.I. (2007). Rgs1 regulates multiple Gα subunits in Magnaporthe pathogenesis, asexual growth and thigmotropism. The EMBO journal *26*, 690-700.

Malz, S., Grell, M.N., Thrane, C., Maier, F.J., Rosager, P., Felk, A., Albertsen, K.S., Salomon, S., Bohn, L., and Schäfer, W. (2005). Identification of a gene cluster responsible for the biosynthesis of aurofusarin in the Fusarium graminearum species complex. Fungal Genetics and Biology *42*, 420-433.

Meier, J.L., and Burkart, M.D. (2009). The chemical biology of modular biosynthetic enzymes. Chemical Society Reviews *38*, 2012-2045.

Mitchell, T.K., and Dean, R.A. (1995). The cAMP-dependent protein kinase catalytic subunit is required for appressorium formation and pathogenesis by the rice blast pathogen Magnaporthe grisea. The Plant cell *7*, 1869-1878.

Miyamoto, Y., Masunaka, A., Tsuge, T., Yamamoto, M., Ohtani, K., Fukumoto, T., Gomi, K., Peever, T., Tada, Y., and Ichimura, K. (2010). ACTTS3 encoding a polyketide synthase is essential for the biosynthesis of ACT-toxin and pathogenicity in the tangerine pathotype of Alternaria alternata. Molecular plant-microbe interactions *23*, 406-414.

Monaghan, R.L., and Tkacz, J.S. (1990). Bioactive microbial products: focus upon mechanism of action. Annual Reviews in Microbiology *44*, 271-331.

Myung, K., Zitomer, N., Duvall, M., Glenn, A., Riley, R., and Calvo, A. (2012). The conserved global regulator VeA is necessary for symptom production and mycotoxin synthesis in maize seedlings by Fusarium verticillioides. Plant pathology *61*, 152-160.

Nicolaus, R.A., Piattelli, M., and Fattorusso, E. (1964). The structure of melanins and melanogenesis—IV: On some natural melanins. Tetrahedron *20*, 1163-1172.

Niehaus, E.-M., von Bargen, K.W., Espino, J.J., Pfannmüller, A., Humpf, H.-U., and Tudzynski, B. (2014). Characterization of the fusaric acid gene cluster in Fusarium fujikuroi. Applied microbiology and biotechnology *98*, 1749-1762.

Nishimura, M., Fukada, J., Moriwaki, A., Fujikawa, T., Ohashi, M., Hibi, T., and Hayashi, N. (2009). Mstu1, an APSES transcription factor, is required for appressorium-mediated infection in Magnaporthe grisea. Bioscience, biotechnology, and biochemistry *73*, 1779-1786.

Nishimura, M., Park, G., and Xu, J.R. (2003). The G‐beta subunit MGB1 is involved in regulating multiple steps of infection‐related morphogenesis in Magnaporthe grisea. Molecular microbiology *50*, 231-243.

Nunes, C.C., Gowda, M., Sailsbery, J., Xue, M., Chen, F., Brown, D.E., Oh, Y., Mitchell, T.K., and Dean, R.A. (2011). Diverse and tissue-enriched small RNAs in the plant pathogenic fungus, Magnaporthe oryzae. BMC genomics *12*, 288.

Ochi, K., Okamoto, S., Tozawa, Y., Inaoka, T., Hosaka, T., Xu, J., and Kurosawa, K. (2004). Ribosome engineering and secondary metabolite production. Advances in applied microbiology *56*, 155-184.

Oh, Y., Donofrio, N., Pan, H., Coughlan, S., Brown, D.E., Meng, S., Mitchell, T., and Dean, R.A. (2008). Transcriptome analysis reveals new insight into appressorium formation and function in the rice blast fungus Magnaporthe oryzae. Genome biology *9*, R85.

Ou, S. (1980). Pathogen variability and host resistance in rice blast disease. Annual review of phytopathology *18*, 167-187.

Park, A.R., Son, H., Min, K., Park, J., Goo, J.H., Rhee, S., Chae, S.K., and Lee, Y.W. (2015). Autoregulation of ZEB2 expression for zearalenone production in Fusarium graminearum. Molecular microbiology *97*, 942-956.

Park, G., Xue, C., Zheng, L., Lam, S., and Xu, J.-R. (2002). MST12 regulates infectious growth but not appressorium formation in the rice blast fungus Magnaporthe grisea. Molecular plant-microbe interactions *15*, 183-192.

Patkar, R.N., Benke, P.I., Qu, Z., Chen, Y.Y.C., Yang, F., Swarup, S., and Naqvi, N.I. (2015). A fungal monooxygenase-derived jasmonate attenuates host innate immunity. Nature chemical biology *11*, 733-740.

Patkar, R.N., Xue, Y.K., Shui, G., Wenk, M.R., and Naqvi, N.I. (2012). Abc3-mediated efflux of an endogenous digoxin-like steroidal glycoside by Magnaporthe oryzae is necessary for host invasion during blast disease.

Pearson, L.A., Hisbergues, M., Börner, T., Dittmann, E., and Neilan, B.A. (2004). Inactivation of an ABC transporter gene, mcyH, results in loss of microcystin production in

the cyanobacterium Microcystis aeruginosa PCC 7806. Applied and Environmental Microbiology *70*, 6370-6378.

Proctor, R.H., Brown, D.W., Plattner, R.D., and Desjardins, A.E. (2003). Co-expression of 15 contiguous genes delineates a fumonisin biosynthetic gene cluster in Gibberella moniliformis. Fungal Genetics and Biology *38*, 237-249.

Proctor, R.H., Desjardins, A.E., Plattner, R.D., and Hohn, T.M. (1999). A polyketide synthase gene required for biosynthesis of fumonisin mycotoxins in Gibberella fujikuroi mating population A. Fungal Genetics and Biology *27*, 100-112.

Prota, G., d'Ischia, M., and Napolitano, A. (1998). The chemistry of melanins and related metabolites. The pigmentary system, 307-332.

Punya, J., Tachaleat, A., Wattanachaisaereekul, S., Haritakun, R., Boonlarppradab, C., and Cheevadhanarak, S. (2013). Functional expression of a foreign gene in Aspergillus oryzae producing new pyrone compounds. Fungal Genetics and Biology *50*, 55-62.

Ramanujam, R., Calvert, M.E., Selvaraj, P., and Naqvi, N.I. (2013). The Late Endosomal HOPS Complex Anchors Active G-Protein Signaling Essential for Pathogenesis in Magnaporthe oryzae. PLoS pathogens *9*, e1003527.

Ramanujam, R., and Naqvi, N.I. (2010). PdeH, a high-affinity cAMP phosphodiesterase, is a key regulator of asexual and pathogenic differentiation in Magnaporthe oryzae. PLoS pathogens *6*, e1000897-e1000897.

Ramos‐Pamplona, M., and Naqvi, N.I. (2006). Host invasion during rice‐blast disease requires carnitine‐dependent transport of peroxisomal acetyl‐CoA. Molecular microbiology *61*, 61-75.

Reeves, C.D., Hu, Z., Reid, R., and Kealey, J.T. (2008). Genes for the biosynthesis of the fungal polyketides hypothemycin from Hypomyces subiculosus and radicicol from Pochonia chlamydosporia. Applied and environmental microbiology *74*, 5121-5129.

Reyes‐Dominguez, Y., Bok, J.W., Berger, H., Shwab, E.K., Basheer, A., Gallmetzer, A., Scazzocchio, C., Keller, N., and Strauss, J. (2010). Heterochromatic marks are associated with the repression of secondary metabolism clusters in Aspergillus nidulans. Molecular microbiology *76*, 1376-1386.

Roze, L.V., Arthur, A.E., Hong, S.Y., Chanda, A., and Linz, J.E. (2007). The initiation and pattern of spread of histone H4 acetylation parallel the order of transcriptional activation of genes in the aflatoxin cluster. Molecular microbiology *66*, 713-726.

Roze, L.V., Beaudry, R.M., Keller, N.P., and Linz, J.E. (2004). Regulation of aflatoxin synthesis by FadA/cAMP/protein kinase A signaling in Aspergillus parasiticus. Mycopathologia *158*, 219-232.

RUDD, B.A., and HOPWOOD, D.A. (1979). Genetics of actinorhodin biosynthesis by Streptomyces coelicolor A3 (2). Journal of general microbiology *114*, 35-43.

Ryder, L.S., Dagdas, Y.F., Mentlak, T.A., Kershaw, M.J., Thornton, C.R., Schuster, M., Chen, J., Wang, Z., and Talbot, N.J. (2013). NADPH oxidases regulate septin-mediated cytoskeletal remodeling during plant infection by the rice blast fungus. Proceedings of the National Academy of Sciences *110*, 3179-3184.

Sambrook, J., Fritsch, E.F., and Maniatis, T. (1989). Molecular cloning, Vol 2 (Cold spring

harbor laboratory press New York).

Scherlach, K., Nützmann, H.W., Schroeckh, V., Dahse, H.M., Brakhage, A.A., and Hertweck, C. (2011). Cytotoxic pheofungins from an engineered fungus impaired in posttranslational protein modification. Angewandte Chemie International Edition *50*, 9843-9847.

Sesma, A., and Osbourn, A.E. (2004). The rice leaf blast pathogen undergoes developmental processes typical of root-infecting fungi. Nature *431*, 582-586.

Shen, B. (2003). Polyketide biosynthesis beyond the type I, II and III polyketide synthase paradigms. Current opinion in chemical biology *7*, 285-295.

Shimizu, K., Hicks, J.K., Huang, T.-P., and Keller, N.P. (2003). Pka, Ras and RGS protein interactions regulate activity of AflR, a Zn (II) 2Cys6 transcription factor in Aspergillus nidulans. Genetics *165*, 1095-1104.

Shwab, E.K., Bok, J.W., Tribus, M., Galehr, J., Graessle, S., and Keller, N.P. (2007). Histone deacetylase activity regulates chemical diversity in Aspergillus. Eukaryotic cell *6*, 1656-1664.

Soanes, D.M., Chakrabarti, A., Paszkiewicz, K.H., Dawe, A.L., and Talbot, N.J. (2012). Genome-wide transcriptional profiling of appressorium development by the rice blast fungus Magnaporthe oryzae. PLoS pathogens *8*, e1002514.

Song, Z., Bakeer, W., Marshall, J.W., Yakasai, A.A., Khalid, R.M., Collemare, J., Skellam, E., Tharreau, D., Lebrun, M.-H., and Lazarus, C.M. (2015). Heterologous expression of the avirulence gene ACE1 from the fungal rice pathogen Magnaporthe oryzae. Chemical Science *6*, 4837-4845.

Spatafora, J.W., and Bushley, K.E. (2015). Phylogenomics and evolution of secondary metabolism in plant-associated fungi. Current opinion in plant biology *26*, 37-44.

Staunton, J., and Weissman, K.J. (2001). Polyketide biosynthesis: a millennium review. Natural product reports *18*, 380-416.

Sun, C.B., Suresh, A., Deng, Y.Z., and Naqvi, N.I. (2006a). A multidrug resistance transporter in Magnaporthe is required for host penetration and for survival during oxidative stress. The Plant cell *18*, 3686-3705.

Sun, C.B., Suresh, A., Deng, Y.Z., and Naqvi, N.I. (2006b). A multidrug resistance transporter in Magnaporthe is required for host penetration and for survival during oxidative stress. The Plant cell *18*, 3686-3705.

Talbot, N.J. (2003). On the trail of a cereal killer: exploring the biology of Magnaporthe grisea. Annual Reviews in Microbiology *57*, 177-202.

Thines, E., Weber, R.W., and Talbot, N.J. (2000). MAP kinase and protein kinase A–dependent mobilization of triacylglycerol and glycogen during appressorium turgor generation by Magnaporthe grisea. The Plant cell *12*, 1703-1718.

Thompson, J.E., Fahnestock, S., Farrall, L., Liao, D.-I., Valent, B., and Jordan, D.B. (2000). The Second Naphthol Reductase of Fungal Melanin Biosynthesis inMagnaporthe grisea TETRAHYDROXYNAPHTHALENE REDUCTASE. Journal of Biological Chemistry *275*, 34867-34872.

Tokousbalides, M.C., and Sisler, H. (1979). Site of inhibition by tricyclazole in the melanin biosynthetic pathway of Verticillium dahliae. Pesticide Biochemistry and Physiology *11*,

64-73.

Tsai, H.-F., Washburn, R.G., Chang, Y.C., and Kwon-Chung, K. (1997). Aspergillus fumigatus arp1 modulates conidial pigmentation and complement deposition. Molecular microbiology *26*, 175-183.

Tsai, H.-F., Wheeler, M.H., Chang, Y.C., and Kwon-Chung, K. (1999). A developmentally regulated gene cluster involved in conidial pigment biosynthesis in Aspergillus fumigatus. Journal of Bacteriology *181*, 6469-6477.

Tsuji, G., Kenmochi, Y., Takano, Y., Sweigard, J., Farrall, L., Furusawa, I., Horino, O., and Kubo, Y. (2000). Novel fungal transcriptional activators, Cmr1p of Colletotrichum lagenarium and Pig1p of Magnaporthe grisea, contain Cys2His2 zinc finger and Zn (II) 2Cys6 binuclear cluster DNA‐binding motifs and regulate transcription of melanin biosynthesis genes in a developmentally specific manner. Molecular microbiology *38*, 940-954.

Umetsu, N., Kaji, J., and Tamari, K. (1972). Investigation on the toxin production by several blast fungus strains and isolation of tenuazonic acid as a novel toxin. Agricultural and Biological Chemistry *36*, 859-866.

Valent, B., and Chumley, F.G. (1991). Molecular genetic analysis of the rice blast fungus, Magnaporthe grisea. Annual review of phytopathology *29*, 443-467.

Wang, Z., Soanes, D., Kershaw, M., and Talbot, N. (2007). Functional analysis of lipid metabolism in the rice blast fungus Magnaporthe grisea reveals a role for peroxisomal boxidation in appressorium-mediated plant infection. Molec Plant–Microbe Interact *20*, 475-491.

Wei, N., Serino, G., and Deng, X.-W. (2008). The COP9 signalosome: more than a protease. Trends in biochemical sciences *33*, 592-600.

Weissman, K.J. (2009). Introduction to polyketide biosynthesis. Methods in enzymology *459*, 3-16.

Wheeler, M.H., and Bell, A.A. (1988). Melanins and their importance in pathogenic fungi. In Current topics in medical mycology (Springer), pp. 338-387.

Wilson, R.A., and Talbot, N.J. (2009). Under pressure: investigating the biology of plant infection by Magnaporthe oryzae. Nature reviews Microbiology *7*, 185-195.

Woloshuk, C.P., Sisler, H.D., Tokousbalides, M.C., and Dutky, S.R. (1980). Melanin biosynthesis in Pyricularia oryzae: site of tricyclazole inhibition and pathogenicity of melanin-deficient mutants. Pesticide Biochemistry and Physiology *14*, 256-264.

Wu, D., Oide, S., Zhang, N., Choi, M.Y., and Turgeon, B.G. (2012). ChLae1 and ChVel1 regulate T-toxin production, virulence, oxidative stress response, and development of the maize pathogen Cochliobolus heterostrophus. PLoS pathogens *8*, e1002542-e1002542.

Xiao, J.-Z., Watanabe, T., Kamakura, T., Ohshima, A., and Yamaguchi, I. (1994). Studies on cellular differentiation of Magnaporthe grisea. Physicochemical aspects of substratum surfaces in relation to appressorium formation. Physiological and Molecular Plant Pathology *44*, 227-236.

Xu, J.-R., and Hamer, J.E. (1996). MAP kinase and cAMP signaling regulate infection structure formation and pathogenic growth in the rice blast fungus Magnaporthe grisea.

Genes & development *10*, 2696-2706.
Yun, C.-S., Motoyama, T., and Osada, H. (2015). Biosynthesis of the mycotoxin tenuazonic acid by a fungal NRPS-PKS hybrid enzyme. Nature communications *6*.
Zeigler, R.S., Leong, S.A., and Teng, P.S. (1994). Rice blast disease (Int. Rice Res. Inst.).

Appendices

Appendix 1. PKS1 gene and protein sequences

PKS1 ORF (introns highlighted in grey)

ATGGCGCCGTCGAGACTCTACAACTTTTCATCGTCGGGCACGTCA
CCGACATCAAGCTCCGCCTTTACGGTTCCCTCCGTTGCCAACTCCG
AGACCGACTCGGCCGCCGACATGCATCCGCCAATGAACGGCCACC
GTCAGTTTGACGGCTTCTCAGACCCGGGCATGACGCCTCGCGCTC
CGATGCCTATAGCCATCGTGGGAATGGCCTGTCGCATGCCCGGCA
GCGTTGCGACTCCGGCAGAGTTTTGGGAGCTTTGCTCTCGTGCAC
GAAGCGGCTATACCAAGGTGCCAAAGGAGCGGTTCAACCACGAT
CTCTTTTACCATCCCAATCCGGGAAAGACTGGAGCATACCACGCT
CAGGGAGGCAACTTTCTGGATGTCGACCTGGCCGCTTTCGATGCT
CCCTTTTTCGGCCTCACCGAGAAGGAGGCCATATCAATGGACCCT
CAGCAAAGGCTTCTGCTCGAGTGCACCTTTGAGGCGCTGGAAAAC
GCCGGTGTACCAAAGCATTCCATAGTCGGAAAGGACGTTGGTGTG
TTTGTCGGTGGCAGCTTTGCCGAGTATGAAAGTCATTTGTTTCGTG
ATAGCGACACGATTCCGATGCACCAGGCCACAGGTAAGCTTGTTT
GTGTTTGCTATTCTTGGCTTCTGCTAACGAATCAGGCTGCGCACAT
GCTATGCAGTCCAACAGGCTATCCCACTTTTTCGATCTCCGAGGCC
CCAGCTTCACCGCCGATACCGCATGCTCCGCCAGTTTGGTGGCTCT
ACATCTTGCTTGCCAGAGTTTACGGTCTGGCGAATCCTCATCCGCC
ATCGTTGGTAGCTGTCATCTGAACATGCTGCCCGAGTTCTTTGTTT
CATTCTCTACATGTCGATTGCTTTCGGACACTGGTCGTTCGATCGC
TTTTGACGAGCGTGGAACGGGTTTCGGGCGTGGTGAAGGATGTGG
CATTATTATTCTGAAGCCTCTAGACCAGGCTGTGCGGGATAATGA
TACCATCCGGGCTGTTATCATGGGTACAGGTATCAACCAGGACGG
CAAGACGCCTGGTATCACCATGCCCAGTGGCGAGGCACAAGGTAT
GTTTTACGGCATCGATATGGAGAAGTTCAAGGAGCTAACATCTTG
CAGAGAAACTCATCAACCAGGTTTACAACAACTTTGGCCTAGACC
CTATGGACTGTGGCTACGTCGAGGCCCACGGTACCGGAACCAAGG
TCGGTGATCCGATCGAGGCCACCGCTCTACACAACGCTCTCGGTC

AGGGCAGGACGGCAGCTGATCCTCTCTTTATCGGATCGGTCAAAT
CGAACATTGGCCATTTGGAGGCTGCGTCAGGTTTGGCTGGTGTCA
TCAAGGCTGCGCTCATGCTTGAGCGTGGTTTCATTCTTCCCAACCA
CGACTTCAAAAAGCCAAACCCAAAGATTCCCTGGAAGCAATGGC
ACATGACGGTGGCTAGAAGCCAAAGGCCTTGGCCCCGTGGCAAG
AAATACATCTCGGTCAACAACTTTGGTTTTGGTGGTACCAATGCC
CACGTCGTCCTCGCCAAGGCTCCTTTCACCGCCGATACTACAGTTG
CAGCACAGCTTCAAAATAATGACTCGCGAAAACCCAAGCAGACC
AAGAAGCTGATTGTTCTTACGGCCAACGACAAAGATTCCCTCGCC
GGTGTCATGAAGAAGCTGGTCATCTACCTGGAGCAACGGCCCGAA
GTCTTCCAGGCCGACTTGATGAGAAACGTCGCTTACACCCTTGGC
CAAAGGCGCTCGCATCTGCAATGGAGGCTTGCGGTTCCCGTGTCA
ACCTCATTCGAGCTTGTTGATACGCTAAACTCGGGCAAGGTTGTA
TCGGCCAAGATGCAGCCAGAGGCCCCCAGGATAGGATTCGTGTTT
ACAGGTCAAGGCGCTCAGTGGCACGGTATGGGCCGTGAGCTCTAT
GACTCTTACCCGGTCTATGCGGCCGCCATGGACCGTGCCGATGCT
AAACTCAAGGAGCTCGGTGCTACATGGTCGTTGCTGGAGGAGCTG
AGCAAAGATGGCAAGACTTCCAAGGTGTCCGAGGCACACATCAG
TCAGCCCGCATGCACAGCCGTGCAGTTGGCCATCACGGACCTTCT
CAAATCCTGGGGCGTGGTACCCGTCGCCGTCGCCGGCCACTCGTC
TGGTGAGATTTGCGCCGCCTATGCCGCCGGCATCATCAACTTTGA
CTCGGCCGTCGCCATTGCTTACCACAGGGGTCGGCTGATTCCCGT
GCTCAAGTCCCGGCACCCCGACCTTGCCGGTGGTATGATGGCCGT
CGGTGGGTCCGAATCCGATATGCAGCCCATGATCGATGCTGTCAA
GCGCAAGCAGCAAGAGGTTCGCATCGCCTGCTTCAACAGCCCTTC
CAGTCTGACCATCTCTGGTGATGCCTCCGTCCTGAATGACCTCGA
GCGCGTCATCGAGGAGGAGCAACCTGAAATGTTCCGCCGCAAGCT
GCAGGTTGACGTTGCCTACCACTCGCACCACATGAACCTCGTGGC
CGATGAGTACCGTGATTCGATTGAGCACCTTTCCAAGCCGAGGAA
CACGGACGTGCAATTCCACTCTTCTCTGTTTGGCAAGCGTGTCGA
GGGCTACAAGTGTACTGCTTCATACTGGGTTGAGAATCTGACCTG
CCCCGTCCGCTTCTCCGAGGCCCTCAGCGGCATGCTCGAGGCCAA
GCCCGAGGACGGTGTCAGCACCCTTATCGAGATTGGTCCTCACTC
GGCTCTTCAAGGTCCCATCAAGCAGATCCTCGCCGCTGCTGGTCG
CCCCAAGCTCCCCTACGCTTCGGCTTTGGTCCGCAACAAGGATGC
CGTCGACACGGCCCTTGACCTGGCTGGTAACCTCTTCATGAAGGG
TGCATTCCTCAACATGGATGCTGTCAACTTCCCCAGCCACCTCCAC
GCCCCGGCTACTTCGACCATTCCGTTGAACCTGCACACTTCGGCC
GCCAAGCAGCCCACACTGCTCACCGATCTCCCGCGCTATGTGTGG
AACCATTCGTCCAAATACTGGCACGAGTCGCGCATGACTGAGATG
CACAAGTTCCGCAAGTTCCCGCGCAACGATCTCATTGGTGTCGAG
GCCATCTACTCTACCGATGTCGAGCCTACATGGCGCAACATTGTG

GCTCTCGATGACCTGCCGTGGCTGAGGCACCACCGCATCCAGTCT
CTGACCATCTTTCCCTTTTCCGGCTTCGTGGCCATGGCCCTCGAGG
CTGCAGCCCAACAGGCTCTGAAGAGAGAGGCCAAGTACGACAGG
TTCGAGCTGCGCCGAGTTGTCGTCTCCAAGCCGTTGGCCATGGGA
GACGGCGACGTTGAGATGGACATCAGCCTCAGGCCACACTCCGAC
TCCCAGAAGCACCAGGCCGGATGGAGGCAGTTCCGCATTGCCAGC
TGGACCAAGAACGGTGGCTGGGCCGAGCACTGCACTGGAGAGGT
TGCCGCCTTGTCAGACGACGACAACGAAGTTGACGGCGAGCGTCA
AAAGCAGGCTATTCGCCGCAGGGTAGAAGCTGCTTCCACCATGGG
CGAGGATGCCGTCGACGTTGCCGAGGTCGACATGTACAACTGTCT
GGAAGAGCTGGGCGTGACATTTGGTGCTGCCTTCCAGGGCGTCAA
GGCATGCAAGGCTTCCAACACAAAGGCATCTGCCGATATCGTTGC
CACCGACATTGCTGTCGATATGCCAAACCACTACATGACCGAGTC
GGTGTTGCACCCCAGTGTGCTCGAGTCTCTGGTCCAGATGTACTG
GCCCATTCTTGGCGCCGGTCGCACATCTCCCGACACCGTCTACCTG
CCATCCTCTGTTGGCAAGGTCTCCATCTCGCGCGAGGTGACAGCG
CACACCAACGCTCCTGGCAAGACGATTCGCGCTTTTGGCAAGGCA
GAGTTCGCCCAGCCCTGCGAGGAGCCCCGTGCCACCAGCGTCTCT
GTCATGGCCACCACCCAGGACGGCCAGCTCCTCGTCGAGATTGAG
GACCTCAAGGTTGCGCCCATCATCGACGGTGAGGGTGAGACCGAC
TCTAGCACCCCGCGTGAGCTTTGCTACAAGCTCGAGTGGGAGCAG
GTTCTGAAGCCCGCCCTCGTCAACGGTACCCCTGCCGACTCCAAC
ACGCTGCCCGAGGCCGAGATTGTCATTGTACATGGTGACACCGCC
TTCCAACACACCCTTGCCCGCGCACTGGCCGATATTATCGAAAAG
GCCACATCTACTTCGCCTGTGGCAATGGGCACACTTGGCCACATC
GAGACCGAGGGCAAGGTCTGCATCGTCTTGACCGAGATTGACATG
CCTTTCCTTGCCGACCCTACGGAGCAGCAGTTTGAAGCCGTGCAG
AAGCTCATCGGCTCTGTTCAGGGTCTCCTCTGGGTTGTGCGTGGG
GCTTACGACAAGGCAACCTCTCCCGACTCCAACATGGTCTGTGGT
CTTTCTCGTTCGGTCAGGTCAGAGACTCTGCTGCCGTTTGCGACAC
TCGACCTGGATTCCATCGAGGCTTCCACCGCCCACGTTTCCAAGTC
CATCCTGGACGTGTTCAAGATCGCCTTCAATGGTGGTTTGAGCGC
AACCAAGGAGATGGAGTTTATGGAGCGTGGAGGCAAGCTCTTCA
CCCCCAGGATCCTGGATGATGCAGAGACGAACGCCTACGTGCACA
AGCGCACCAACCCCGACATCCTCGAGAAGCAGCCGTTTGCCCAAG
AGGGTCGCCAGCTGAAGATGGTTGGTGGCAAGACGCTGCACTTTG
TCGACGCCACGATCGACACTCTCGGCGCTGACGAGGTCGAGATTG
AGGTCAAGGCTGTGGGTGTCAACGCCAGTGATGCTCAGCAACTGG
CCAAGAGCACTGCCGAGTCGCCTGCTCCTGTTGGATCCGAGGCAG
CTGGCATTGTCACCCGGGTCGGCGCCAATGTCACCTCCATCAAGA
AGGGTGATCGCGTTGCCGCACTGACCCTCTCCAGCGGTGCTTACT
CGACCGTCACACGAGCCTCTGCCGCCAACACCATCCCGATCCCTC

AGGCTATGGACTTTTCCCAGGCTGCGACGTTGCCCTTTGCCTATGT
GACCGCCCACCACGCTCTTGAGCAGGCTAGGCTTTCATCGGGCCA
GAGCGTCCTCATCCACTCTGCTGCCAGTGCTGTTGGCCAAGCTGC
CGTCTGCCTCGCCCAGCTCCGCGACGCCGAGGTGTTTGTCACCGT
GTCCTCTGCTGCCGAGAAGAAGCTGATCATGACCAAGTTCTCCGT
GTCTGAGGACCGCATCTTTTACAACCGCGGCGTAGGCTTTGGATC
AGCTATCCGAGAAGCAACTGCCGGTGAGGGTGTAGATGTTGTCAT
TTCCATCCGATCAGACGCCGAGGTTGTTCGTGAGAGCTGGGACTG
CCTGGATCGATTCGGCTGTCTTGTCAACGTCTCTGAAGGATCGTCT
CGTCTCGATCTGAGCACTGATGGTCGACCAAGCAACGCATCGTTT
GTCAACGTTGACATTCAATGCCTTGCTGCCGAGCGCCCTGCCATTC
TCAAGAGGCTGGTTGACAGTGTTGCCAAGTTGGTTGGTCAGGGCC
AGGCTACTCCTGTAGAGGCCACCGTCTTTGCTGTGTCTGAGGTTCA
AGATGCTCTCAAGAGCGCCAGCAAGACATCCTGTGGAAAGTCGGT
GGTTGTTCTGGGCGCTGACGACATGGTAATGGTAAGTTATCAGCA
TCCACTCCATACTCGCATCCCTGCTAACTCCTTCCAGGCCACACCC
TCCAAGGTCACCAAGAAGATTCTCCGCTCCGACGGCACCTACCTG
CTCATCGGTGGAACTGGTGGTCTCGGTCGCAGCATGGCCAAGTGG
ATGGTCGACAACGGTGCCGGCAATGTCGTCCTTCTCTCCCGTAGC
GGTTCGGCCACCGGACAAGTCAAGCAGCTGATCGATGCCGCAAG
CGAGGCCGGATCCCAGGTGATTGTCAAGCGCTGCGATGTTGCCAA
CAAGGCTAGCGTCGACGAGCTGTTCAAGGGACTGAGTGATCTGCC
TCCAGTCCGAGGTATTGTTCACGGAGCCATGGTTTTGAGGGTAAG
TTACAGCGCCCATCAGCCTCGTATCAACACTCACTAACACTCCAC
AGGATGTCCTCTTTGAGAAAATGGCATACACCGATTACACCACCG
TCATCGAGTCCAAGGTCGCTGGCGCCTGGAACTTCCACCACGCCC
TGGCTGCCAACTCTTGCCCCGTCGACTTCTTCATCGCCATCTCATC
CGCAGCCGGTGCCGTCGGCAACAGAGGTCAGGCCGCATATGCGG
CCGCCAACACGTTCCTCAACGCCTTGGTGCAGCACCGCCTTGCCG
CAGGTCTGCCCGCCGCGTCTTTGGACCTGACTGCCGTTTCGGATGC
TGGATACCTCGCCGACGGTGACGCCGAGCGTGCTGCAGAGGTGGC
CAAGAACCTGGGTGCCGACAGTACAATCTGCGAGGCCGAGGTCTT
GGCTCTCATCGGGGCTTGCATCGAGGGCAAGACGAACGTCTGCAA
CGGTCACGTCATCACTGGTATGCGCATCCCGCCCACGCCTACCAA
GCCTTTCTGGGCCACGGATGCCAAGTTCAAGACGCTGCGGTTGAC
CGCCGAGGCGGCCGAGCTGGCGGCAAACGGAGGCGACTCTGCCA
CGGCGTCGCTATCGCCAGGTGCAGCAGTCAAGGCCGCAACGTCGC
TGGCCGAGGCGGAGGAGGCGGTCTGCGCAGGCCTGGTCGACAAG
ATCTCGTCGGTGCTCATGATGGAGGCGGACGAGATTGACGTGACC
AGGAGCTTGACGCACTACCCGCTCGACTCGCTGGTGGCCATTGAG
ATTCGCAACTTTATCACGCGGGAGTTCGAGGCCAACATGCAAGTG

TTGGAGCTGTTGAGCAGTGGAAGCGTGCAGACGCTGACCAAGGC
AGTCTGCAAGAAGAGCAAGCTTTGTGTTGGGTTGAGCTAG

Pks1 protein sequence

MAPSRLYNFSSSGTSPTSSSAFTVPSVANSETDSAADMHPPMNGHRQ
FDGFSDPGMTPRAPMPIAIVGMACRMPGSVATPAEFWELCSRARSG
YTKVPKERFNHDLFYHPNPGKTGAYHAQGGNFLDVDLAAFDAPFFG
LTEKEAISMDPQQRLLLECTFEALENAGVPKHSIVGKDVGVFVGGSF
AEYESHLFRDSDTIPMHQATGCAHAMQSNRLSHFFDLRGPSFTADTA
CSASLVALHLACQSLRSGESSSAIVGSCHLNMLPEFFVSFSTCRLLSD
TGRSIAFDERGTGFGRGEGCGIIILKPLDQAVRDNDTIRAVIMGTGINQ
DGKTPGITMPSGEAQEKLINQVYNNFGLDPMDCGYVEAHGTGTKVG
DPIEATALHNALGQGRTAADPLFIGSVKSNIGHLEAASGLAGVIKAAL
MLERGFILPNHDFKKPNPKIPWKQWHMTVARSQRPWPRGKKYISVN
NFGFGGTNAHVVLAKAPFTADTTVAAQLQNNDSRKPKQTKKLIVLT
ANDKDSLAGVMKKLVIYLEQRPEVFQADLMRNVAYTLGQRRSHLQ
WRLAVPVSTSFELVDTLNSGKVVSAKMQPEAPRIGFVFTGQGAQWH
GMGRELYDSYPVYAAAMDRADAKLKELGATWSLLEELSKDGKTSK
VSEAHISQPACTAVQLAITDLLKSWGVVPVAVAGHSSGEICAAYAAG
IINFDSAVAIAYHRGRLIPVLKSRHPDLAGGMMAVGGSESDMQPMID
AVKRKQQEVRIACFNSPSSLTISGDASVLNDLERVIEEEQPEMFRRKL
QVDVAYHSHHMNLVADEYRDSIEHLSKPRNTDVQFHSSLFGKRVEG
YKCTASYWVENLTCPVRFSEALSGMLEAKPEDGVSTLIEIGPHSALQ
GPIKQILAAAGRPKLPYASALVRNKDAVDTALDLAGNLFMKGAFLN
MDAVNFPSHLHAPATSTIPLNLHTSAAKQPTLLTDLPRYVWNHSSKY
WHESRMTEMHKFRKFPRNDLIGVEAIYSTDVEPTWRNIVALDDLPW
LRHHRIQSLTIFPFSGFVAMALEAAAQQALKREAKYDRFELRRVVVS
KPLAMGDGDVEMDISLRPHSDSQKHQAGWRQFRIASWTKNGGWAE
HCTGEVAALSDDDNEVDGERQKQAIRRRVEAASTMGEDAVDVAEV
DMYNCLEELGVTFGAAFQGVKACKASNTKASADIVATDIAVDMPN
HYMTESVLHPSVLESLVQMYWPILGAGRTSPDTVYLPSSVGKVSISR
EVTAHTNAPGKTIRAFGKAEFAQPCEEPRATSVSVMATTQDGQLLVE
IEDLKVAPIIDGEGETDSSTPRELCYKLEWEQVLKPALVNGTPADSNT
LPEAEIVIVHGDTAFQHTLARALADIIEKATSTSPVAMGTLGHIETEG
KVCIVLTEIDMPFLADPTEQQFEAVQKLIGSVQGLLWVVRGAYDKAT
SPDSNMVCGLSRSVRSETLLPFATLDLDSIEASTAHVSKSILDVFKIAF
NGGLSATKEMEFMERGGKLFTPRILDDAETNAYVHKRTNPDILEKQP
FAQEGRQLKMVGGKTLHFVDATIDTLGADEVEIEVKAVGVNASDAQ
QLAKSTAESPAPVGSEAAGIVTRVGANVTSIKKGDRVAALTLSSGAY
STVTRASAANTIPIPQAMDFSQAATLPFAYVTAHHALEQARLSSGQS

VLIHSAASAVGQAAVCLAQLRDAEVFVTVSSAAEKKLIMTKFSVSED
RIFYNRGVGFGSAIREATAGEGVDVVISIRSDAEVVRESWDCLDRFG
CLVNVSEGSSRLDLSTDGRPSNASFVNVDIQCLAAERPAILKRLVDSV
AKLVGQGQATPVEATVFAVSEVQDALKSASKTSCGKSVVVLGADD
MVMATPSKVTKKILRSDGTYLLIGGTGGLGRSMAKWMVDNGAGNV
VLLSRSGSATGQVKQLIDAASEAGSQVIVKRCDVANKASVDELFKGL
SDLPPVRGIVHGAMVLRDVLFEKMAYTDYTTVIESKVAGAWNFHHA
LAANSCPVDFFIAISSAAGAVGNRGQAAYAAANTFLNALVQHRLAA
GLPAASLDLTAVSDAGYLADGDAERAAEVAKNLGADSTICEAEVLA
LIGACIEGKTNVCNGHVITGMRIPPTPTKPFWATDAKFKTLRLTAEAA
ELAANGGDSATASLSPGAAVKAATSLAEAEEAVCAGLVDKISSVLM
MEADEIDVTRSLTHYPLDSLVAIEIRNFITREFEANMQVLELLSSGSVQ
TLTKAVCKKSKLCVGLS

Appendix 2. List of Publications

(1) Deng Y*, **Qu Z***, Naqvi NI. (2015). Twilight, a Novel Circadian -Regulated Gene, Integrates Phototropism with Nutrient and Redox Homeostasis during Fungal Development. *PLOS Pathogens.* 11(6): e1004972. [*Co-first author].

(2) Patkar RN, Benke PI, **Qu Z**, Constance Chen YY, Yang F, Swarup S, Naqvi NI. (2015) A fungal monooxygenase-derived jasmonate attenuates host innate immunity. *Nature Chemical Biology* 11(9): 733-740.

(3) Deng Y, **Qu Z**, Naqvi NI. (2013) The role of Snx41-based pexophagy in Magnaporthe development. *PLOS One.* 8(11): e79128.

(4) Deng Y, **Qu Z**, He Y, Naqvi NI. (2012) Sorting nexin Snx41 is essential for conidiation and mediates glutathione-based antioxidant defense during invasive growth in *Magnaporthe oryzae*. *Autophagy.* 8(7): 1058-1070.

(5) Deng Y, **Qu Z**, Naqvi NI. (2012) Role of macroautophagy in nutrient homeostasis during fungal development and pathogenesis. *Cells.* 1(3): 449-463.